

The variety of progenitors and afterglows: analysis of three *Swift* Gamma-Ray Bursts

Dissertation
zur Erlangung des akademischen Grades
Dr. rer. nat.

vorgelegt dem Rat der Physikalisch-Astronomischen Fakultät
der Friedrich-Schiller-Universität Jena

eingereicht von Dott.ssa Magistrale Patrizia Ferrero
geboren am 29.06.1975 in Asti (Italien)

Gutachter

1. **Prof. Dr. Artie P. Hatzes (Jena University)**
2. **Prof. Dr. Ulrich Heber (Erlangen-Nürnberg University)**
3. **Prof. Dr. Giampaolo Piotto (Padova University)**

Tag der letzten Rigorosumsprüfung: **18.05.2009**

Tag der öffentlichen Verteidigung: **09.06.2009**

Zusammenfassung

Gammastrahlungsausbrüche (engl. Gamma-ray bursts, kurz: GRBs) sind kurz andauernde Ereignisse im Gammastrahlungsband, die sich im Mittel nur wenige Male am Tag ereignen. Wenn sie auftreten, dann überstrahlen sie jede andere kosmische Quelle in diesem Spektralbereich. Tatsächlich sind sie sogar die leuchtkräftigsten elektromagnetischen Erscheinungen im Universum.

Noch bis vor 11 Jahren wurden GRBs in keinem anderen Spektralbereich als dem Gamma-band detektiert, was ihre Lokalisierung enorm erschwerte und keinen direkten Schluss auf die Art ihres Ursprungs zuließ. Heutzutage wird die immense Energiefreisetzung durch den gravitativen Kollaps des Kerns eines massereichen Sterns oder durch die Verschmelzung zweier kompakter Objekte erklärt, wobei in beiden Fällen grosse Energiemengen in kurzer Zeit (Sekunden oder weniger) erzeugt werden können. Die plötzliche Energiefreisetzung führt zu einem ultra-relativistisch expandierenden Feuerball, in dem aufgrund innerer dissipativer Prozesse die Gammastrahlung generiert wird. Der Einfall des Feuerballs in das die Burstquelle umgebende interstellare Medium bewirkt das Auftreten einer ultra-relativistisch expandierenden Schockwelle. Dabei wird ein kontinuierlich schwächer werdendes “Nachglühen” der Materie am Ort der Explosion (engl. Afterglow) erzeugt, welches vom Röntgen- bis hin zum Radiobereich sichtbar ist. Mit Hilfe der Afterglows können Informationen über die Vorläuferobjekte und die bei der Explosion auftretenden physikalischen Prozesse erlangt werden.

In dieser Doktorarbeit werden drei verschiedene GRBs untersucht, für welche umfangreiche Nachfolgebeobachtungen gewonnen werden konnten. Dabei liegt der Schwerpunkt auf der Natur der Vorläuferobjekte, der Phänomenologie der Afterglows und auf den Muttergalaxien.

In Kapitel 1 wird eine kurze Einführung in die Geschichte der GRB-Forschung gegeben. Daran anschließend wird die Gliederung der Doktorarbeit vorgestellt. Kapitel 2 ist dem gegenwärtigen Stand der Beobachtungsergebnisse und den am meisten akzeptierten Modellvorstellungen gewidmet. Kapitel 3 gibt einen Überblick über die Datengewinnung an verschiedenen, über die ganze Erde verteilten Teleskopen. Kapitel 4 bis 6 konzentrieren sich auf bestimmte Aspekte der Nachfolgebeobachtungen wie die Suche nach Hinweisen auf die Natur der Vorläuferobjekte, die Phänomenologie und physikalische Interpretation der Afterglows sowie die Eigenschaften der GRB-Muttergalaxien. Kapitel 7 fasst die Doktorarbeit und deren Ergebnisse zusammen.

Abstract

Gamma-Ray Bursts (GRBs) are brief events in the gamma-ray sky occurring at an average rate of a few per day. While they are on, they outshine every source of gamma-rays in the sky. In fact, they are the brightest electromagnetic explosions in the Universe. Until 11 years ago, they were undetected at any wavelengths other than gamma-rays, which provided poor directional information and hence no direct clues about their site of origin.

The current interpretation of how this prodigious energy release is produced is that a large amount of energy is released in a short time (seconds or less) by the collapse of the core of a massive star or the merger of two compact stellar objects. This sudden energy liberation results in a fireball expanding at highly relativistic speed, which undergoes internal dissipation leading to gamma-rays, and later develops into a blast wave as it decelerates against the external medium, producing an *afterglow* which gets progressively weaker.

The afterglows provide information about the nature of the GRB progenitor and the physical processes involved in these explosions. In this Thesis three GRBs are discussed where extensive follow-up observations could be performed. Thereby, this Thesis concentrates on the nature of the GRB progenitors, the phenomenology of the afterglows and the host galaxies.

In Chapter 1 a brief historical introduction is given about this research field, followed by an overview of the Thesis. In Chapter 2 a broader summary is presented about the observational status of the field, including the most popular theoretical models. Chapter 3 contains information about the data gathering at various telescopes worldwide. Chapters 4 to 6 are then devoted to certain aspects of GRB follow-up observations, namely the search for signatures of the nature of the GRB progenitors, the phenomenology and physical interpretation of the observed afterglow light as well as the nature of the GRB host galaxies. Chapter 7 finally summarizes the main work and results of the Thesis.

Contents

1	What are Gamma-Ray Bursts?	1
1.1	A bit of history	1
1.2	Overview of the Thesis	4
2	Gamma-Ray Bursts: a short review	7
2.1	GRB light curves and spectra	7
2.2	Classes of GRBs	8
2.2.1	Long and short	8
2.2.2	X-ray flashes and X-ray rich gamma-ray bursts	9
2.3	Physics of Gamma-ray Bursts	10
2.3.1	The compactness problem	10
2.3.2	The fireball model	11
2.3.3	Afterglow spectral energy distribution and light curves	13
2.3.4	Dark GRBs	17
2.3.5	Jets and energetics	18
2.4	The progenitors	22
2.4.1	Long bursts, collapsars, and supernova bumps	22
2.4.2	Short bursts and neutron star mergers	25
2.5	Host galaxies	25
2.5.1	Host galaxies of long GRBs	25
2.5.2	Host galaxies of short GRBs	26
2.6	Redshift distribution	28
3	The bursts: observational data	29
3.1	The short burst GRB 050813	29
3.1.1	The event	29
3.1.2	OSN, CAHA and VLT data	30
3.2	The GRB-SN event GRB 060218	32
3.2.1	The burst	32
3.2.2	VLT data	32
3.2.3	Liverpool Telescope data and KAIT data	33
3.2.4	The magnitudes of the host galaxy	37
3.2.5	The extinction correction	37
3.3	The long burst GRB 060605	37
3.3.1	Swift BAT data: the burst	37

3.3.2	Swift XRT data	38
3.3.3	Swift UVOT data	38
3.3.4	Spectroscopic data	39
4	Identifying the GRB progenitors	43
4.1	GRB 060218 – a collapsar	43
4.1.1	The supernova light curve	43
4.1.2	Comparison to other GRB-supernovae	46
4.1.3	Comparison to other local stripped-envelope supernovae	48
4.1.4	The stretch factor	50
4.2	GRB 050813 – favouring a NS-NS merger	51
4.2.1	What is a short burst?	51
4.2.2	Upper limits on a rising supernova component	53
4.3	The high- z GRB 060605	54
5	Analysis of the afterglows	55
5.1	GRB 060605: a detailed afterglow analysis	55
5.1.1	The X-ray afterglow	55
5.1.2	The UV/optical light curve and its SED	56
5.1.3	The issue of the jet break	59
5.1.4	The broad-band spectrum	61
5.1.5	The X-ray vs. the optical light curve: a joint fit	63
5.1.6	Energetics of the burst and of the afterglow	66
5.2	GRB 050813: searching for a fading optical afterglow component	69
6	The host galaxies	71
6.1	Searching for the host galaxy of GRB 050813	71
6.2	A compact host galaxy of GRB 060218	72
6.3	The high- z host galaxy of 060605	73
6.3.1	ISM signatures of the host galaxy	73
6.3.2	Global parameters of the host galaxy	75
7	Summary	77
	Appendix	80
A	Integral Field Spectroscopy	I
A.1	Why using Integral Field Spectroscopy?	I
A.2	IFS vs. Long-Slit Spectroscopy	II
A.3	Basic techniques	II
A.4	Reduction and visualization of 3D data	IV
	Bibliography	VI
	Acknowledgements	XXIII

Chapter 1

What are Gamma-Ray Bursts?

Gamma-Ray Bursts (GRBs) are flashes of high-energy radiation which appear in the sky at random times from random directions. Briefly, from a few milliseconds to a few minutes, they outshine every other source of gamma-rays in the sky and then they fade away.

1.1 A bit of history

Since the announcement of their discovery in 1973 (Klebesadel et al. 1973), GRBs have been one of the greatest mysteries of modern astrophysics. They were first observed more than 40 years ago by the U.S. *Vela* satellites, which were launched to verify the compliance with the Limited Nuclear Test Ban Treaty. However, the elusiveness of these events has prevented the detection of longer-wavelength counterparts for almost three decades, until 1997, when the first afterglow was detected.

The original discovery of the bursts was followed by numerous theories attempting to explain these cosmic explosions and fix their position in the Universe (Nemiroff 1994). Of course, a distance determination was needed to decide between a cosmological or a galactic origin of the objects. After *Vela*, other high-energy satellites also detected GRBs, but none of them carried out a systematic analysis of these phenomena.

On April 5, 1991, the *Compton Gamma-Ray Observatory* (CGRO) was launched, carrying the Burst And Transient Source Experiment (BATSE, 25-300 keV; Fishman et al. 1985) among the four on-board instruments. During its lifetime (till June 2000) it observed 2704 GRBs and determined their position with an accuracy of some degrees (Fig. 1.1, left panel). The sky distribution was found to be isotropic (Meegan et al. 1992). This was in disagreement with what the majority of the GRB community was expecting, i.e. a disk-like distribution correlated to a source population in the Galactic disk. This, in combination with the $\text{Log}N - \text{Log}P$ (N = number, P =peak flux) distribution of the bursts, which shows a presence of weak bursts lower than what predicted for a static Euclidean space (Fig. 1.1, right panel), strongly suggested a cosmological distance scale. However, the poor localization accuracy did not allow an easy search of counterparts at lower energies and no source at higher wavelength was identified. Consequently, no redshift was measured.

The great breakthrough came in April 1996 with the launch of the Italian-Dutch high energy satellite *BeppoSAX* (Boella et al. 1997a), named “Beppo” after the Italian physicist

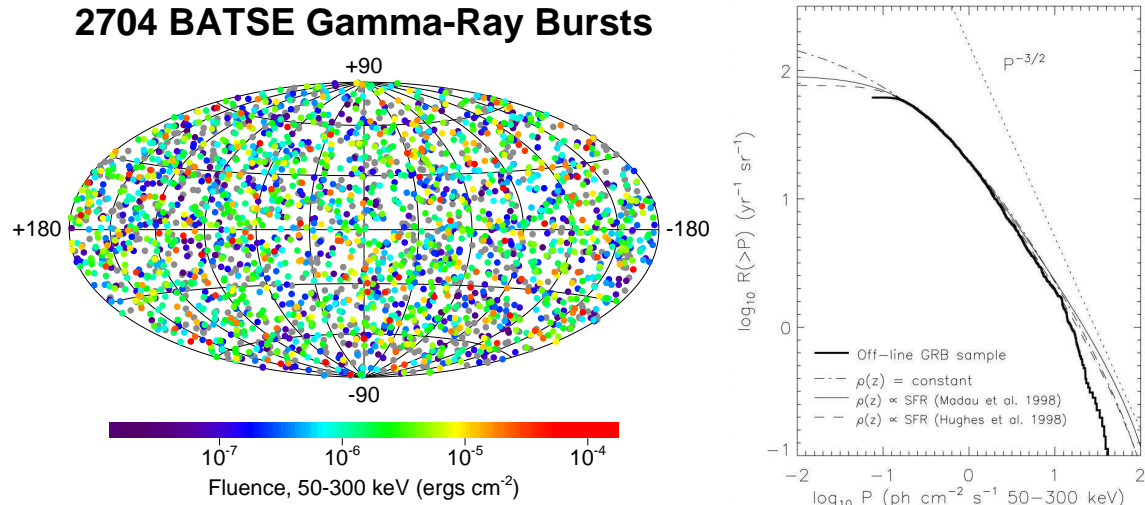


Figure 1.1: *Left: Final sky map of the 2704 BATSE GRBs detected during its nine-years mission. The projection is in galactic coordinates; the plane of the Milky Way is along the horizontal line at the middle of the Figure. The burst locations are colored based on the fluence, which is the energy flux of the burst integrated over the total duration of the event. Red colored are the GRBs with lowest fluence, blue with the highest. Gray colors refers to GRBs for which it was not possible to calculate the fluence due to the incomplete data. Source: <http://www.batse.msfc.nasa.gov/batse/grb/skymap/>. Right: Cumulative peak flux distribution of BATSE bursts, showing a lack of faint bursts and in this way indicating a cosmological origin (Kommers et al. 2000).*

Giuseppe Occhialini (1907-1993).

BeppoSAX carried several instruments to cover the range from 0.1 up to 700 keV. The Gamma-Ray Burst Monitor (GRBM; Frontera et al. 1997) was able to roughly determine the coordinates of a GRB in the energy range 40-700 keV, while the two Wide Field Cameras (WFC, 2-28 keV; Jager et al. 1997) could give a localization of an X-ray source with an uncertainty of about 5 arcminutes. In addition, four Narrow Field Instruments (NFIs; Boella et al. 1997b; Frontera et al. 1997; Manzo et al. 1997; Parmar et al. 1997) were used to repoint the detected GRBs within a few hours, providing an error-box of 1 arcmin accuracy.

Thanks to the precise and rapid localizations, it was possible to begin the follow-up with ground-based telescopes to search for optical/IR or radio counterparts.

After the WFCs detection of a GRB on February 28, 1997 (GRB 970228¹), the first X-ray afterglow was found by Costa et al. (1997) (Fig. 1.2, top pannel) and the optical counterpart by van Paradijs et al. (1997) (Fig. 1.2, bottom pannel). The optical and soft X-ray light curves showed a steep power-law decay, with flux $\propto t^{-1.1}$ (Costa et al. 1997; Galama et al. 1997). This immediately pointed out another request in the search of GRB afterglows in addition to a small error box: the observations had to be performed very quickly.

The following burst was GRB 970508 and it was a decisive event, as observers obtained spectra of its optical afterglow (Fig. 1.3) with one of the Keck telescopes and measured a redshift of 0.835 (Metzger et al. 1997a,b). Thus, the distance issue was finally settled after 30

¹The nomenclature for GRBs is GRB YYMMDD, where YY=year, MM=month, DD=day. An additional letter is added if there are more than one GRB on a certain day.

years of debate: GRBs originate at cosmological distances, making them the most powerful photon emitters in the Universe. This burst was also the first observed in the radio band: Frail et al. (1997) were able to detect the afterglow in the 3.5, 6 and 21 cm bands. They observed also fluctuations in the light curve, even from day to day, that were explained as caused by interstellar scintillation due to the very small angular size of the emitting source. The scintillation stopped one month later, meaning that the angular size of the source had increased over 3 microarcseconds, implying a shell expanding at nearly the speed of light (see also end of Sec. 2.3.1).

After *BeppoSAX*, other satellites have been employed to detect GRB. The *High Energy Transient Explorer (HETE-2)*; Vanderspek et al. 1999) launched in 2000 was able thanks to its Soft X-ray Cameras (SXC), to provide localizations with an accuracy of some arcminutes. While *HETE-2* is a GRB dedicated mission, *INTEGRAL (International Gamma-Ray Astrophysics Laboratory)*; Winkler et al. 2003), was launched in October 2002 to study celestial gamma-ray emission, in particular along the Galactic Plane, and this task includes also the detection of GRBs with error-boxes of few arcminutes.

In November 2004 *Swift*, a new satellite dedicated to GRB science started its operations. On-board *Swift* there are three co-aligned instruments (Gehrels et al. 2004): the Burst Alert Telescope (BAT, 15-150 keV; Barthelmy et al. 2005), the X-ray Telescope (XRT, 0.2-10 keV; Burrows et al. 2005), and the Ultra-Violet/Optical Telescope (UVOT, 170-650 nm; Roming

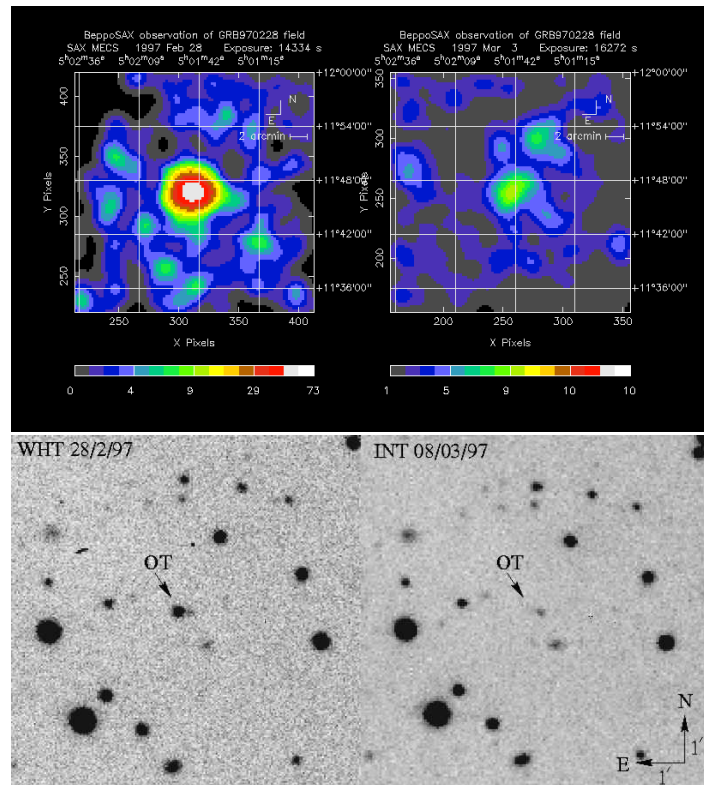


Figure 1.2: *Top*: X-ray counterpart of GRB 970228 detected by WFC/BeppoSAX (Costa et al. 1997). *Bottom*: Observation of the optical counterpart at the William Herschel Telescope (WHT) and the Isaac Newton Telescope (INT) on La Palma (van Paradijs et al. 1997).

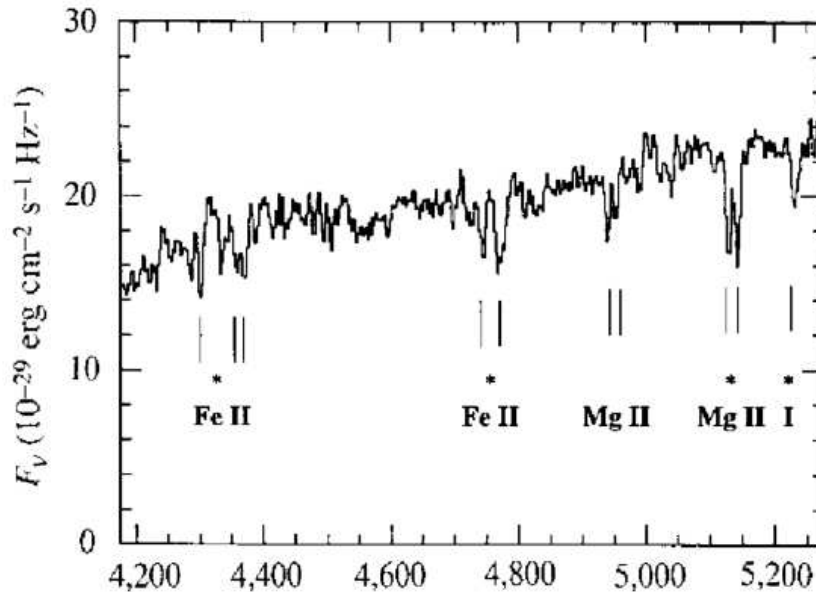


Figure 1.3: *The first spectrum of an optical afterglow ever (In the figure the x-axis is in units of \AA . GRB 970508; adapted from Metzger et al. 1997b).*

et al. 2005). Within seconds from the detection of a burst, the spacecraft autonomously repoints the XRT and UVOT instruments to allow high-precision localizations (few arcseconds of accuracy).

Recently two new satellites were launched: in April 2007 the *Astrorivelatore Gamma ad Immagini ultra LEggero* (*AGILE*, 30 MeV - 50 GeV; Mereghetti et al. 2001) and in June 2008 the *Gamma-Ray Large Area Space Telescope* (*GLAST*, 10 keV - 300 GeV; McEnery & GLAST Mission Team 2006). They will study high-energy transients, including GRBs, and they will extend the gamma-ray observations of the prompt emission to very high energies, up to 300 GeV, allowing to test the prompt emission mechanisms in that energy range.

1.2 Overview of the Thesis

In general, the light of the optical transient (OT) following a GRB is the sum of three components: light from the afterglow (AG), light from an underlying supernova (SN) component and light from the underlying host galaxy. $OT(t) = AG(t) + SN(t) + \text{host}$. This picture might be modified from burst to burst in the sense that, e.g., for short bursts no standard SN light is expected to be seen and that, potentially, a short burst could be offset by many kpc from his host galaxy, which might make it impossible to identify its host at all.

In this Thesis, I am discussing three very different bursts that were detected by the *Swift* satellite in recent years and that were in detail investigated by our group, under my leadership. GRB 060218 allowed us a detailed investigation of the underlying SN light related to the GRB progenitor, but it did not allow for a study of the afterglow since the latter was completely outshined by the luminous SN component. On the other hand, GRB 060605 was

at such high redshift that any underlying SN component was not expected to be seen at all; the light of the optical transient was clean afterglow light, the host galaxy was (naturally, given the redshift) very faint. Finally, GRB 050813 was a short burst, neither an afterglow nor a SN component was detected by us with certainty, and the potential host galaxy is basically only identified by the revised *Swift* XRT error circle in combination with our deep VLT imaging. Table 1.1 summarizes the observational situation for these three bursts.

Table 1.1:

GRB	afterglow detection	supernova detection	host detection
GRB 050813	no	no	yes(?)
GRB 060218	no(?)	yes	yes
GRB 060605	yes	no	yes

In Chapter 2 I will start with a resume of the main observational features accompanying these high-energy events, then I will present the physical processes behind the GRB phenomenon, and at the end a description of their host galaxies.

The data set, on which this Thesis is based, is introduced in Chapter 3: images acquired at ESO (Paranal, Chile), at Calar Alto, Observatorio Sierra Nevada and La Palma (Spain), and at Lick Observatory (California, U.S.) have been reduced and analysed in the standard way, while the Integral Field Unit spectrum acquired with PMAS/PPak at Calar Alto needed a different procedure. More information about the Integral Field Spectroscopy technique are summarized in the Appendix.

The following three Chapters are dedicated to the results obtained from the analysis of the data and to the discussion of their implications in the present understanding of GRBs.

In particular, in Chapter 4 a study on the nature of the possible progenitors of the three GRBs is done. While in case of GRB 060218/SN 2006aj ($z = 0.033$), the presence of a supernova component allowed us to compare this source to other supernovae related to GRB events and to other local stripped-envelope supernovae, the high redshift of GRB 060605 ($z = 3.78$) prevented us to see a possible SN component. In the case of the short GRB 050813 ($z = 0.7$) it was possible to put constraints on any SN light following this event and the non-detection of a SN component is in agreement with one of the strongest criteria to identify the nature of the progenitor of short bursts.

In Chapter 5 the analysis of the GRB afterglows is given. The detection of GRB 060605 afterglow has triggered a deep study of this event, providing hints on the circumburst medium. In the case of GRB 050813 only an upper limit on the magnitude of a possible optical afterglow component has been derived, while the brightness of SN 2006aj outshined a possible afterglow and only an excess of blue light has been found in the early light curve, but unlikely related to the afterglow (see Sect. 4.1.1).

In Chapter 6 the possible host galaxies of these three events are discussed. For GRB 060218 the host galaxy was already securely identified on pre-burst archived data; in the case of 060605 the host is only barely detected on our deep VLT images, and finally only a host

galaxy candidate could be identified for the short burst 050813. However, interesting information on the chemical composition of the interstellar medium of the host of GRB 060605 could be obtained via the bright GRB afterglow.

Chapter 7 includes a summary of the results of this Thesis.

Chapter 2

Gamma-Ray Bursts: a short review

After the discovery of the GRBs afterglows, thanks to a rapid follow-up of the satellite alerts by ground-based telescopes, it has become possible to trace very precise light curves, to check the reliability of the proposed models and to have a guess of the possible progenitors of GRBs.

2.1 GRB light curves and spectra

The light curves of the GRB prompt event show a wide diversity in structure, ranging from smooth, fast-rise and quasi-exponential decay, through curves with several peaks, to highly variable curves (see Fig. 2.1).

The duration of a γ -ray burst is usually given as T_{90} , which is the time in which a burst emits from 5% to 95% of its total measured counts, accumulating 90% of the counts. In agreement with this definition, their duration has been found to last from 10^{-3} s to about 10^3 s.

The γ -ray spectra of GRBs are non-thermal (see Fig. 2.2), with photons observed at energies ranging from a few keV up to several GeV. They can generally be well fitted with an empirical function consisting of two power-laws, smoothly connected by an exponential function, with a break energy in the 0.1 - 2 MeV range (Band et al. 1993).

A measure of the γ -ray spectral properties is given by the GRB hardness, usually designated as HR, that is for BATSE bursts defined as the ratio between the fluence (i.e. the energy flux of the burst integrated over the total duration of the event) in two energy ranges, namely 100-300 keV and 50-100 keV. Thus, the hardness is a measure of the slope of the spectrum: the harder the burst, the larger the portion of energy emitted at high frequencies.

Investigating the evolution of the peak energy for long and bright GRBs, Ford et al. (1995) found that it decreases with time, while Liang & Kargatis (1996) added that it is also decreasing exponentially with the photon fluence. This behaviour is named “hard to soft” spectral evolution (Norris et al. 1986) and it also characterizes the individual pulses of GRBs (Ford et al. 1995).

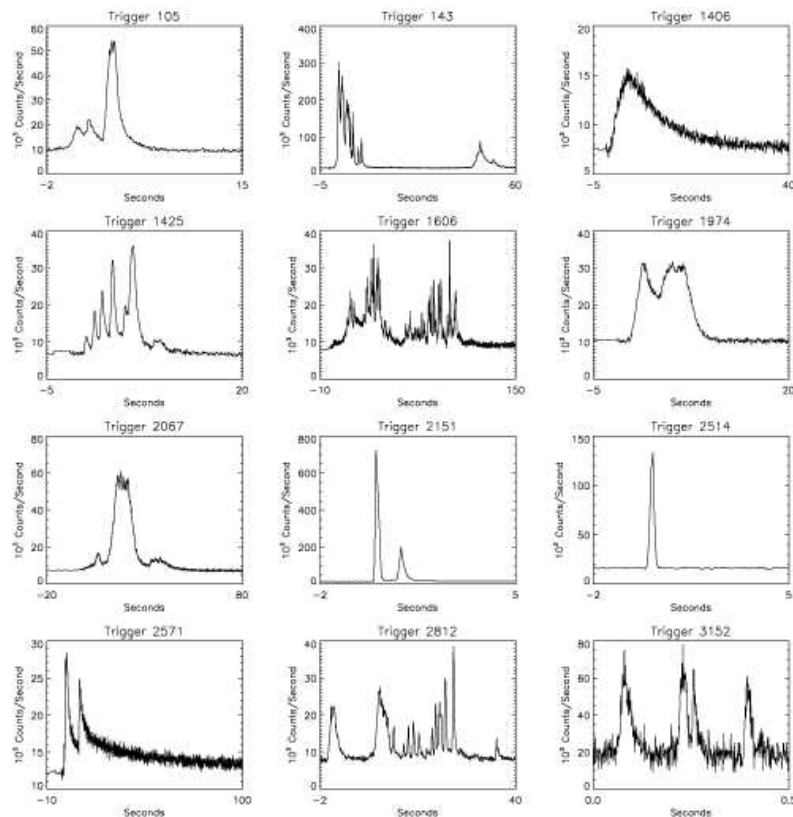


Figure 2.1: A sample of BATSE GRB light curves (from the BATSE page: <http://www.batse.msfc.nasa.gov/batse/grb/lightcurve/>).

2.2 Classes of GRBs

2.2.1 Long and short

Besides the important role that BATSE played in the distance debate (Chapter 1), the large sample of GRBs that BATSE observed was also crucial in the debate on the nature of the GRB progenitors. In fact, this instrument showed that the distribution of GRBs in temporal and spectral properties is bimodal (Kouveliotou et al. 1993). The total population of GRBs can be divided into two classes: long-soft and short-hard bursts (see Fig. 2.3). According to Kouveliotou et al. (1993), the first group has a typical duration larger than 2 seconds, while the second group includes events that last less than that. Donaghy et al. (2006) suggest 5 seconds as a more realistic dividing line. The short GRBs show a higher peak energy in their spectrum than long GRBs: they are harder.

Both classes show an isotropic sky distribution, but their different temporal and spectral properties could indicate that they have different progenitors (see Sects. 2.4.1 and 2.4.2).

Based on the duration distribution, a possible third class of GRBs of intermediate duration, between 2 and 10 s, has been proposed (Horváth 1998; Mukherjee et al. 1998; Horváth et al. 2006), but it is still under debate.

Figure 2.2: A gamma-ray burst spectrum. Shown is the specific flux as a function of energy measured in keV; the line is a fit with two smoothly joined laws. Figure from Bromm & Schaefer (1999).

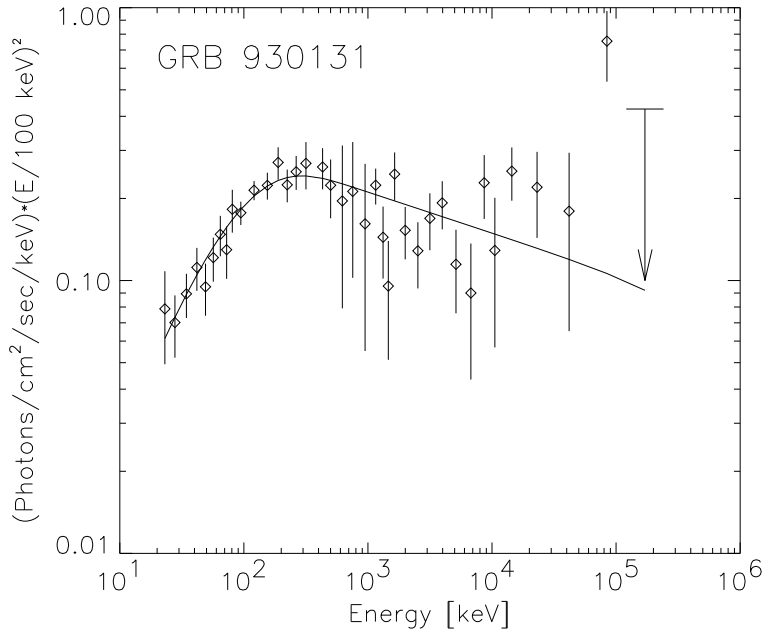
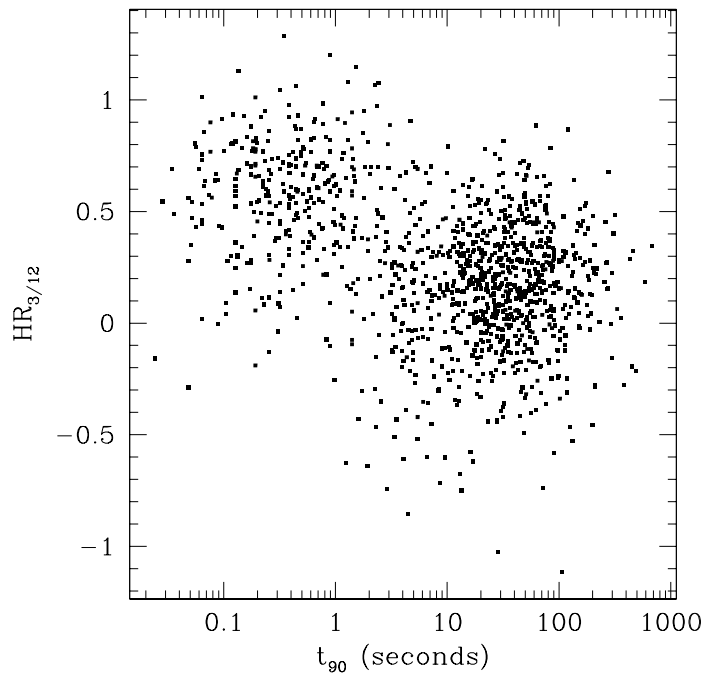


Figure 2.3: The bimodality in hardness ratio and T_{90} (Kouveliotou et al. 1993) suggests the presence of two classes of GRBs.



2.2.2 X-ray flashes and X-ray rich gamma-ray bursts

X-ray flashes (XRFs) are transient sources, similar to long GRBs, but with a softer spectrum. They were first identified with *BeppoSAX* as those bursts that were detected by the X-ray WFCs but not by the GRBM (Heise et al. 2001). They were then extensively studied by *HETE-2*, resulting in a more general classification scheme (Sakamoto et al. 2004) and leading to the expansion of the definition to include an intermediate class, the X-ray rich bursts

(XRR).

This classification is based on the ratio of the fluence S in the X-ray band to the γ -ray one, $S_X/S_\gamma = \log [S_X (2 - 30\text{keV}) / S_\gamma (30 - 400\text{keV})]$. XRFs, XRRs and classical GRBs would be those bursts with $S_X/S_\gamma < -0.5$, $-0.5 < S_X/S_\gamma < 0$ and $0 < S_X/S_\gamma$, respectively. While the three groups have a different definition, they seem to form a continuum of events rather than distinctive distributions.

After their detection, many attempts to explain these differences have been performed. They can be either due to the way in which we are seeing them (extrinsic feature) or to the physics involved in the explosion (intrinsic feature). An extensive treatment of the subject is presented in Zhang (2007).

2.3 Physics of Gamma-ray Bursts

2.3.1 The compactness problem

After the solution of the distance scale problem (Sec. 1.1), a new question had to be addressed: if GRBs have a cosmological origin, the amount of released energy would be enormous. The size of the source that is generating this energy has to be, however, very small if we consider the millisecond fluctuations observed in the gamma-ray light curves. According to this variability it was inferred that the size of the engine generating the GRB has to be smaller than a few hundred kilometres. This means a large amount of energy in a small volume of space: this leads to the *compactness problem*.

The γ -rays prompt emission spectrum is non-thermal in most cases which indicates that the observed emission emerges from an optically thin region. The large distances for cosmological GRBs imply that the bursts release a large amount of energy in gamma-rays of the order of $\sim 10^{52}$ erg. In addition, given the finite speed of light, the millisecond variability observed in the prompt emission implies a compact source with a radius of the order of 1000 km. These two observational facts show that the source of radiation must be optically thick for gamma-rays due to the formation of a large number of electron-positron pairs via $\gamma - \gamma$ interaction. Such a source should emit a blackbody radiation, contrary to what is observed at high energy.

A simple way to see the compactness problem is to estimate the average opacity of the high-energy gamma-ray to pair production (Piran 1997).

The optical depth for pair creation is given by

$$\tau_{\gamma\gamma} = n_\gamma \sigma_{\gamma\gamma} D \quad (2.1)$$

where $\sigma_{\gamma\gamma} \approx \sigma_T$, with the Thomson cross section $\sigma_T = 6.65 \times 10^{-25}$ cm², n_γ the number density of photons, and D the size of the source. Given a characteristic variability time scale Δt the source size can be estimated as

$$D \leq c \cdot \Delta t. \quad (2.2)$$

If we denote the observed fluence of the GRB by f , the luminosity distance of the burst d_L , and assume that the emission is isotropic, the released energy in gamma-rays is

$$E_{iso} \sim 4\pi d_L^2 f. \quad (2.3)$$

For a photon energy $\bar{E}_\gamma \sim 1$ MeV, the photon number density at the source is

$$n_\gamma \sim \frac{3d_L^2 f}{E_\gamma D^3}. \quad (2.4)$$

As the observed photon energy is very high, a fraction of photons is energetic enough to produce electron-positron pairs in collisions.

A photon with energy E_1 can interact with a lower energy photon with energy E_2 and produce electron-positron pairs if $(E_1 E_2)^{1/2} > m_e c^2$. Let A_γ be a numerical factor denoting the average probability that one photon will collide with another photon whose energy is sufficient for pair creation, and fix $D = c \cdot \Delta t$. The optical depth for pair creation then is

$$\tau_{\gamma\gamma} = n_\gamma \cdot \sigma_T \cdot D \sim \frac{d_L^2 f}{\bar{E}_\gamma c^2 \Delta t^2} A_\gamma \sigma_T, \quad (2.5)$$

or, according to Piran (1997),

$$\tau_{\gamma\gamma} \sim 10^{13} A_\gamma \left(\frac{f}{10^{-7} \text{erg/cm}^2} \right) \left(\frac{d_L}{3000 \text{Mpc}} \right)^2 \left(\frac{\Delta t}{10 \text{ms}} \right)^{-2}, \quad (2.6)$$

were typical values and cosmological distances are inserted. The resulting optical depth is extremely large. If this were true, the photons would produce a large amount of e^+e^- pairs, then equilibrate with the latter, and produce a thermal spectrum. This is contrast to what is observed, namely a non-thermal spectrum at high energies.

The problem can be solved assuming a relativistic motion towards us, which leads to two modifications. The first one is related to the spatial dimension of the source: it can be larger by a factor Γ^2 , where Γ is the Lorentz factor of the outflow. The second one is connected to the energy of the photons: as they are blueshifted, their energy in the relativistic outflow frame is lower by a factor Γ . As a consequence, for an observed spectrum of the form $N(\nu)d\nu \sim \nu^{-\alpha}d\nu$, where $N(\nu)$ is the number of photons in the frequency range $[\nu, \nu + d\nu]$ in the fireball which have enough energy to produce electron-positron pairs, the optical depth is smaller by a factor $\Gamma^{2(1+\alpha)}$ (Lithwick & Sari 2001).

The value of this fraction depends on the shape of the spectrum. For a typical spectrum with $\alpha = 2$ (where α is the photon index of the observed γ rays; Preece et al. 2000) τ (Eq. 2.5) has to be corrected by a factor Γ^{-6} . For a non-thermal spectrum $\tau_{\gamma\gamma} \leq 1$, so that a reduction of $\tau_{\gamma\gamma}$ (Eq. 2.6) by a factor in the order of 10^{13} leads to a lower limit on the Lorentz factor of about 100. So, to overcome the compactness problem, highly relativistic motion towards the observer is required. Relativistic motion had indeed been inferred from radio afterglows of GRBs using VLBI (see Sec. 1.1; Frail et al. 1997).

2.3.2 The fireball model

The assumption of an ultra-relativistic motion towards us has led to the *relativistic fireball model* (Rees & Mészáros 1992). It has been shown that this model is equally valid for long and short bursts, even if the central engine (the progenitor) that powers the fireball might be different in the two classes (Sec. 2.4). As described in the previous section, because of

relativistic effects the real size of the source would then be $\Gamma^2 c \Delta t \gtrsim 10^{13}$ cm and the duration of the burst of the order of days or even years at the source.

According to the fireball model, decelerating relativistic ejecta produce the GRB and its afterglow (see Fig. 2.4). In this model an object of stellar mass undergoes a catastrophic event that leads to the formation of the GRB central engine. This source rapidly releases a large amount of energy in a compact region of $\sim 10^6 - 10^7$ cm. Since the initial opacity of the relativistic outflow is very high, the inner engine is hidden and cannot be observed directly. This makes it difficult to constrain GRB models and leaves only circumstantial evidence on the nature of the sources. First of all, the central source has to provide a large energy-to-rest mass ratio ($\Gamma = E/Mc^2 \gtrsim 100$) in order to make the fireball accelerate under its own pressure to ultra-relativistic velocities. During the expansion, the fireball transforms most of its thermal energy into kinetic energy of its baryons so that the outcome of this process is a “small” amount of ultra-relativistic particles. The baryonic mass M must to be smaller than

$$M = \frac{E}{\Gamma c^2} = 6 \cdot M_{\odot} \left(\frac{E}{10^{51} \text{erg}} \right) \left(\frac{100}{\Gamma} \right). \quad (2.7)$$

The initial energy does not produce the observed *prompt GRB emission*, but from the central source it is transported relativistically to distances larger than about 10^{13} cm, where the system becomes optically thin. Once the optical depth inside the fireball drops below unity, its photons escape. If the inner engine is active for some time, shells with different Lorentz factors may be produced. Collisions between these shells, the so-called *internal shocks*, are generally assumed to power the GRB itself. The shocked electrons produce gamma-rays via synchrotron and/or inverse Compton radiation.

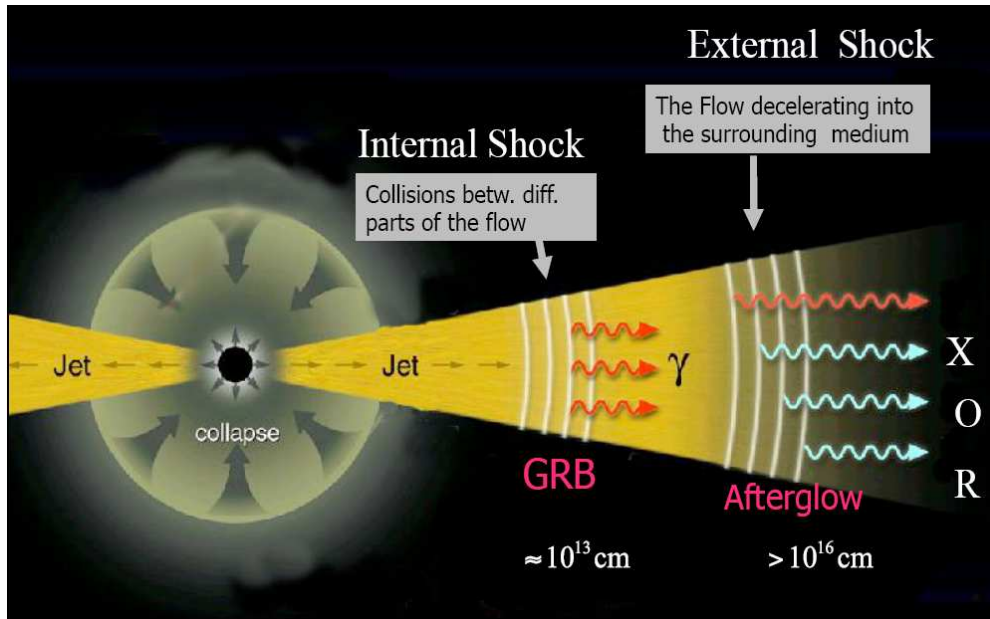


Figure 2.4: *Cartoon of the fireball model (Mészáros 2006). It is assumed here that the central engine is a massive star.*

Internal shocks dissipate only a fraction of the flow energy, the rest is transferred at larger radii ($\sim 10^{16} - 10^{18}$ cm) into the external medium via *external shocks*, where the

decelerating blast wave produces electromagnetic emission at lower frequencies, the so-called afterglow. The circumburst ambient can be either the interstellar medium, or in the case of long GRBs, the dense stellar wind produced by the progenitor. The blast waves are the relativistic analogues of supernova remnants. Magnetic fields cause the swept-up electrons to produce synchrotron radiation. When the external forward shock is formed, a *reverse shock* is also produced moving back into the ejecta. This reverse shock can produce a bright *optical flash* minutes after the burst (e.g., GRB 990123; Akerlof et al. 1999).

The brightness of the reverse shock emission decays very rapidly as t^{-2} (Sari et al. 1999), after which the forward shock dominates. Since the shock decelerates while it is sweeping-up mass, the blast wave will become sub-relativistic ($\Gamma \lesssim 2$) usually after days or weeks.

2.3.3 Afterglow spectral energy distribution and light curves

In the standard fireball model the afterglow is caused by external shocks. The fireball decelerates when the rest frame energy of the swept-up material is similar to the kinetic energy of the ejecta. Consequently, the evolution and the emission properties of the afterglow depend on the structure of the circumburst medium.

The temporal evolution and the spectral energy distribution (SED) of the afterglow is described by

$$F_\nu(t) \propto t^{-\alpha} \nu^{-\beta}, \quad (2.8)$$

where F_ν is the flux density, t is the time after the onset of the burst, ν is the frequency, α is the temporal decay slope and β is the spectral index (also designated as spectral slope; Mészáros 2006; Piran 2005).

The energy distribution of the shocked electrons is described by

$$N(E)dE \propto E^{-p}dE \quad (2.9)$$

where N is the number of electrons with the energy ($E, E + dE$) and p is the electron index. Numerical simulations predict $p > 2$ (e.g., Achterberg et al. 2001; Kirk et al. 2000) which is supported by most of the observational data (e.g., Kann et al. 2006). However, the electron distribution diverges at low energies. Consequently, there must be a low-energy cut-off, which is determined by the available energy density (see Sari et al. 1998; Piran 2000):

$$E_{\min} = \frac{(p+2)e_e}{(p+1)n_e}, \quad (2.10)$$

where n_e and e_e are the electron density and their energy density, respectively. The largest number of electrons is around E_{\min} which is the characteristic electron energy. We denote by ν_m the synchrotron frequency of an electron with this energy.

The electron energy density as well as the magnetic field energy density are characterised as a fraction ε_e and ε_B of the total internal energy. In other words, they represent the efficiency of the conversion of the fireball kinetic energy in electron energy and in energy of the magnetic field. Typical values, deduced from observational data, are $0.05 < \varepsilon_e < 0.5$ and $10^{-3} < \varepsilon_B < 0.1$ (Panaitescu et al. 2001; Yost et al. 2003).

Starting from these considerations, Sari et al. (1998) were able to estimate the instantaneous spectrum of the afterglow by means of three characteristic frequencies: the cooling

frequency ν_c , the synchrotron self-absorption frequency ν_a , and the already mentioned synchrotron frequency ν_m . The cooling frequency ν_c is the synchrotron frequency of an electron that cools during the local hydrodynamic time scale, while the self-absorption frequency ν_a is the frequency for which the optical depth $\tau(\nu_a) = 1$. The resulting spectrum is a combination of four power-laws, with three of the four slopes fixed and one depending on whether the electrons are fast cooling or not (Fig. 2.5).

In the fast cooling case ($\nu_m > \nu_c$), even the less energetic e^- of the electron ensemble have energies of $E_{\min} > h\nu_c$. In other words all e^- are cooling. This case might hold at early times up to a couple of hours after the burst in the observer frame. In this case the electrons lose their energy very fast due to radiation losses.

In the slow cooling case ($\nu_m < \nu_c$) the electrons loose their energy very slowly. This means to a good approximation the fireball evolution is adiabatic. Consequently, this case will dominate at late times.

The spectral slope and temporal evolution of each of the spectral segments in the interstellar medium (ISM) model (i.e., a circumburst medium with a constant density profile) are parametrised in Eqs. (2.11) and (2.13). The spectral breaks have a temporal evolution themselves, as shown in the equations 2.12 and 2.14 for the fast and slow cooling, respectively. The spectral behaviour is schematised in Fig. 2.5.

In detail, fast cooling:

$$F_\nu \propto \begin{cases} \nu^2 t^{1/2} & \text{for } \nu < \nu_a, \\ \nu^{1/3} t^{1/6} & \text{for } \nu_a < \nu < \nu_c, \\ \nu^{-1/2} t^{-1/4} & \text{for } \nu_c < \nu < \nu_m, \\ \nu^{-p/2} t^{-\frac{3p-2}{4}} & \text{for } \nu_m < \nu \end{cases} \quad (2.11)$$

$$\begin{aligned} \nu_a &\propto t^{-1/2} \\ \nu_c &\propto t^{-1/2} \\ \nu_m &\propto t^{-3/2}. \end{aligned} \quad (2.12)$$

Slow cooling:

$$F_\nu \propto \begin{cases} \nu^2 t^{1/2} & \text{for } \nu < \nu_a, \\ \nu^{1/3} t^{1/2} & \text{for } \nu_a < \nu < \nu_m \\ \nu^{-(p-1)/2} t^{-\frac{3}{4}(p-1)} & \text{for } \nu_m < \nu < \nu_c, \\ \nu^{-p/2} t^{-\frac{3p-2}{4}} & \text{for } \nu_c < \nu \end{cases} \quad (2.13)$$

$$\begin{aligned} \nu_a &\propto t^0 \\ \nu_c &\propto t^{-1/2} \\ \nu_m &\propto t^{-3/2}. \end{aligned} \quad (2.14)$$

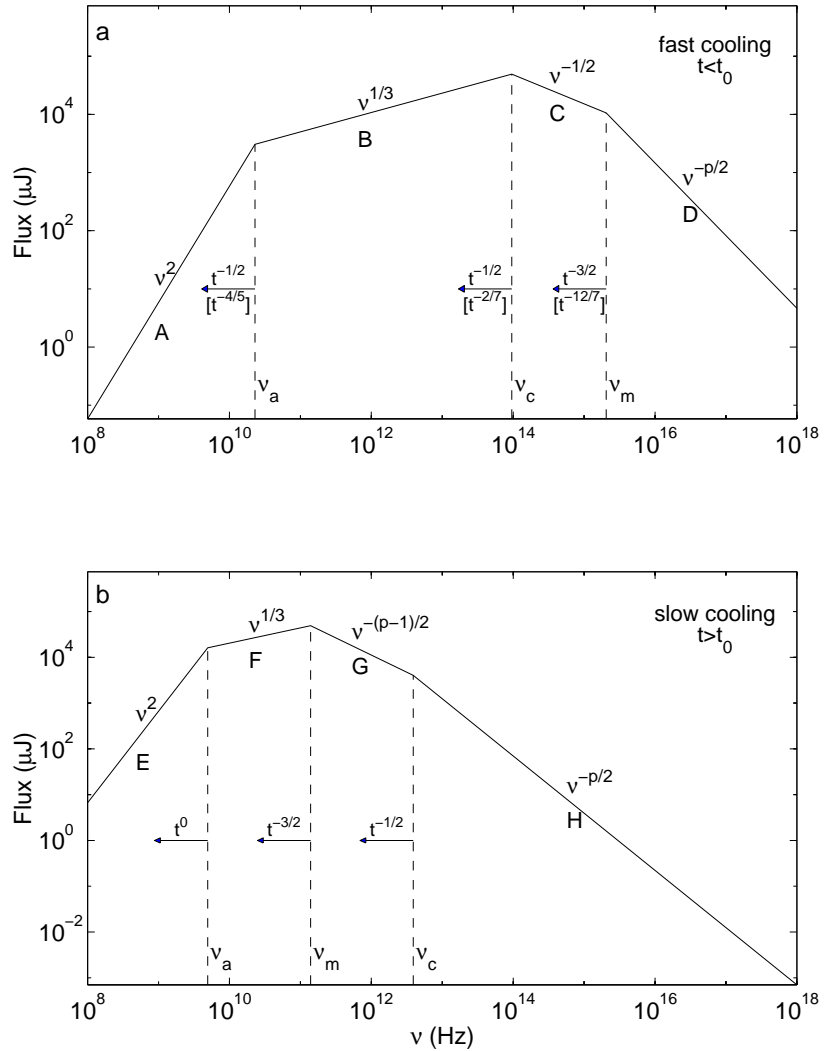
Similar formulae can be derived for the wind case, in which the density profile is $\propto r^{-2}$ and r is the distance from the source (Chevalier & Li 2000).

In both extreme cases, the fast and slow cooling case, the following inequality is valid:

$$|\dot{\nu}_c| < |\dot{\nu}_m|. \quad (2.15)$$

Consequently, there is always a transition phase when ν_m overtakes ν_c . In other words, even in the optical bands the spectrum evolves with time. From this a functional dependence

Figure 2.5: *Synchrotron spectrum of a relativistic shock with a power-law electron distribution (Sari et al. 1998). t_0 represents the time corresponding to the change from radiative expansion to fully adiabatic expansion of the fireball, when $\nu_c = \nu_m$. (a) Fast cooling, which is expected at early times ($t < t_0$). The spectrum consists of four segments, identified as A, B, C, and D. Self-absorption is important below ν_a . The frequencies, ν_m , ν_c and ν_a , decrease with time as indicated; the scalings above the arrows correspond to an adiabatic evolution, and the scalings below, in square brackets, correspond to a fully radiative evolution. (b) Slow cooling, which is expected at late times ($t > t_0$). The evolution is always adiabatic. The four segments are identified as E, F, G, and H.*



between the spectral slope β and the temporal slope α can be inferred. These dependencies are called “closure relations” since they can be written in the form $a \cdot \alpha + b \cdot \beta + c = 0$, where a, b, c are constants. In the following they are referred to by writing $\alpha = \alpha(\beta)$.

For the ISM and the wind models these relations can be explicitly given (Tab. 2.1).

Before the launch of *Swift* there was usually a gap of a few hours between the prompt emission and the first observations of the afterglow. Early-time observations with robotic optical telescopes in the pre-*Swift* era showed some spectacular optical flashes in the first minute after the burst (e.g., GRB 990123; Akerlof et al. 1999), sometimes also accompanied by a radio flare at ~ 1 day (e.g., GRB 990123; Kulkarni et al. 1999). *Swift* was expected to observe many of these optical flashes, but this turned out not to be the case.

Swift provided and provides a large number of GRBs with well sampled X-ray light curves, often overlapping the prompt emission. Soon after its launch, it was realized that X-ray light curves were much more complex than expected, specially during the early hours after the

	β	α	$\alpha(\beta)$
ISM, slow cooling			
$\nu < \nu_a$	-2	$-\frac{1}{2}$	
$\nu_a < \nu < \nu_m$	$-\frac{1}{3}$	$-\frac{1}{2}$	$\frac{3}{2}\beta$
$\nu_m < \nu < \nu_c$	$\frac{1-p}{2}$	$\frac{3(p-1)}{4} \sim 1.0$	$\frac{3}{2}\beta$
$\nu > \nu_c$	$\frac{p}{2}$	$\frac{3p-2}{4} \sim 1.2$	$\frac{3\beta-1}{2}$
ISM, fast cooling			
$\nu < \nu_a$	-2	-1	
$\nu_a < \nu < \nu_c$	$-\frac{1}{3}$	$-\frac{1}{6}$	$\frac{\beta}{2}$
$\nu_c < \nu < \nu_m$	$\frac{1}{2}$	$\frac{1}{4}$	$\frac{\beta}{2}$
$\nu > \nu_m$	$\frac{p}{2}$	$\frac{3p-2}{4} \sim 1.2$	$\frac{3\beta-1}{2}$
Wind, slow cooling			
$\nu < \nu_a$	-2	-1	
$\nu_a < \nu < \nu_m$	$-1/3$	0	$\frac{3\beta+1}{2}$
$\nu_m < \nu < \nu_c$	$\frac{p-1}{2}$	$\frac{3p-1}{4} \sim 1.5$	$\frac{3\beta+1}{2}$
$\nu > \nu_c$	$\frac{p}{2}$	$\frac{3p-2}{4} \sim 1.2$	$\frac{3\beta-1}{2}$
Wind, fast cooling			
$\nu < \nu_a$	-2	-2	
$\nu_a < \nu < \nu_c$	$-\frac{1}{3}$	$\frac{2}{3}$	$\frac{1-\beta}{2}$
$\nu_c < \nu < \nu_m$	$\frac{1}{2}$	$\frac{1}{4}$	$\frac{1-\beta}{2}$
$\nu > \nu_m$	$\frac{p}{2}$	$\frac{3p-2}{4} \sim 1.2$	$\frac{3\beta-1}{2}$
Jet, slow cooling			
$\nu < \nu_a$	-2	0	
$\nu_a < \nu < \nu_m$	$-\frac{1}{3}$	$\frac{1}{3}$	$2\beta - 1$
$\nu_m < \nu < \nu_c$	$\frac{1-p}{2}$	$p \sim 2.3$	$2\beta - 1$
$\nu > \nu_c$	$\frac{p}{2}$	$p \sim 2.3$	2β

Table 2.1: *Temporal index α and spectral index β in various afterglow models. The convention $F_\nu(t) \propto t^{-\alpha} \nu^{-\beta}$ is adopted. Closure relations $\alpha(\beta)$ are given for a spherically blast wave expanding in two different circumburst density profiles (ISM and wind) for early (fast cooling) and late times (slow cooling). The jet model applies for the sideways expanding phase (see Sec. 2.3.5), which is valid for both ISM and wind cases and is usually in the slow cooling regime. $p > 2$ and $p = 2.3$ are assumed (Zhang & Mészáros 2004).*

burst.

Figure 2.6 shows the canonical X-ray light curve (Nousek et al. 2006b; Zhang et al. 2006) observed by XRT. The light curve presents the following features: an initial very steep decay (A), followed by a flat phase (B), then a steeper decay (C) that was already observed in the pre-*Swift* era, and finally a steepening (D) like those explained as due to the jet geometry (see Sec. 2.3.5). The breaks that mark the transition between A and B and between B and are usually produced at ~ 500 s and between 10^3 and 10^4 s after the burst, respectively. Intense and long-lasting flaring activity (F) has been seen superposed to the X-ray light curve.

Based on what is explained above, the typically observed X-ray afterglow light curve (Fig. 2.6) can be described as follows. The initial steep decay (A) can be attributed to the tail of the prompt emission, from photons that are emitted at large angles relative to our line of sight, the so-called high-latitude emission (Nousek et al. 2006b; Zhang 2007). The

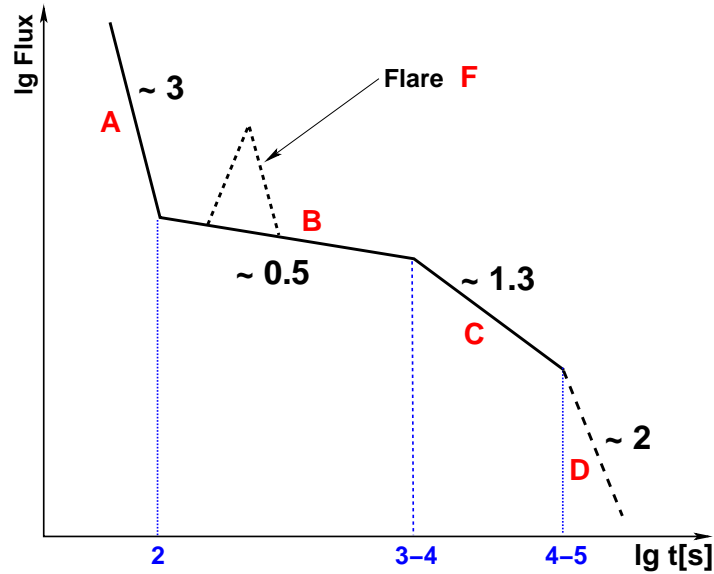


Figure 2.6: *Canonical X-ray light curve based on the observational data from Swift X-ray Telescope (Nousek et al. 2006b; Zhang et al. 2006). Four power-law light-curve segments together with a flaring component are identified in the afterglow phase. Typical temporal indices in the four segments and breaks times are indicated. Segments C (normal decay phase) and D (jet break phase) have been observed in the pre-Swift era, while the other segments have been discovered by Swift. Segments A (steep decay phase) and C are most common. The other three components are only observed in a fraction of bursts; segment B denotes the shallow decay phase and F the X-ray flares.*

transition from the steep to the shallow decay (B), at $10^2 - 10^3$ s, marks the time when the emission from the forward moving blast wave becomes dominant. The shallowness of the decay can find an explanation in a phase of “refreshment” of the relativistic flow. This might be caused by either energy injection of a long-lived central engine or slow shells in the relativistic outflow are catching-up with and refreshing the decelerating blast wave.

X-ray flares might be explained by the GRB central engine being still active after the prompt gamma-ray emission is over, releasing significant amounts of energy and material quite irregularly for a long period, sometimes up to days after the initial burst, but with reduced activity at later times. The decay of the flares is also very steep and might due to high-latitude emission too (Liang et al. 2006).

The decays C and D, already observed in the pre-*Swift*, are due to the external shocks, as predicted by the fireball model.

The behaviour of the X-ray afterglow has a correspondence in the optical/NIR bands, even if sometimes the breaks do not occur simultaneously in both regions of the electromagnetic spectrum, causing the optical/NIR and X-ray light curves depart. These deviations have not been yet satisfactorily explained.

2.3.4 Dark GRBs

During the first few years of GRB afterglow observations, X-ray afterglows were found for almost every burst, while optical/NIR emission could only be found for about 50% of the

bursts. This has led to the designation of “dark” GRBs for those which remained undetected in the optical/NIR bands. Empirically, Djorgovski et al. (2001) defined a dark GRB as a burst without an optical afterglow brighter than about $R \sim 23$ mag found within at most 2 days of the event. On the other hand, Jakobsson et al. (2004) and Rol et al. (2005) give a more quantitative definition of a dark burst, based on the relation between the X-ray flux and the optical flux. This means that a GRB is dark, when it turns out to be “darker” of what expected by extrapolating its optical brightness from the X-ray band. This is valid for late time observations, when optical and X-ray emission come from the same spectral component (afterglow). At early times this is incorrect, as other contributions such as reverse shocks (see for a definition of reverse shocks Sec. 2.3.2) can be present and emit more in the optical band than in the X-ray range.

However, several explanations have been brought forward to address the absence of detectable optical flux: 1) dark bursts could be intrinsically fainter at optical wavelengths (Jakobsson et al. 2004; Rol et al. 2005); 2) they could be at high redshift (e.g., Lamb & Reichart 2000), which would result in their optical/NIR light being suppressed because of hydrogen ($\text{Ly } \alpha$) absorption; 3) they could be heavily extinguished by gas and dust in the host galaxy. The latter solution seems unlikely, as observational evidence for substantial dust extinction in a large fraction of all GRB host galaxies is very small (Kann et al. 2006) and even the gas-to-dust ratio in GRB host galaxies deduced from the afterglow is very low (Stratta et al. 2004).

2.3.5 Jets and energetics

Assuming isotropic emission, the enormous amount of energy release, up to 10^{54} erg, implied by the cosmological distances of GRBs, posed severe problems for models of the engine powering the GRB. One of the brightest and intrinsically most energetic GRBs ever detected was GRB 990123, with an incredible amount of energy release of about 2×10^{54} erg at $z = 1.6$ (Kulkarni et al. 1999), if isotropic emission is assumed. However, it was already noted in the early 90’s that the outflow in a GRB might be collimated along the rotation axis of the progenitor (Woosley 1993), which would reduce the required energy. Rhoads (1997, 1999) showed that a collimated outflow, a *jet*, relaxes the energy output by a factor 10^{2-3} and would lead to an observed steepening of the afterglow light curve. This observed break in the light curve is the best evidence for such a collimated relativistic outflow.

The afterglow theory gets much more complicated if the relativistic ejecta are not spherical. The “jets” correspond to relativistic matter ejected into a cone of half opening angle θ_{jet} . Since the collimated outflow is feeded with matter only for a short period of time (seconds), a “flying pancake” is a better description for these jets (Piran 2000, 2005).

In the standard jet model (e.g., Frail et al. 2001; Panaitescu & Kumar 2002) it is assumed that the Lorentz factor Γ and energy per unit solid angle are uniform across the jet. When observing a jetted outflow roughly along the jet axis, the GRB will at first appear isotropic, due to the high Lorentz factor that causes the emission to be relativistically beamed in the forward direction, within an angle $1/\Gamma$ (Fig. 2.7). Typically after about a day in the host frame, this angle becomes larger than the physical jet opening angle (θ_{jet}) and the observer will start to see less flux compared to the isotropic case and becomes aware of the jet nature

of the outflow. At roughly the same time, the sideways expansion becomes significant due to the slowing down of the outflow, the jet widens and a break appears in the light curve. Such a break has been seen in several afterglows, for example in the optical light curve of GRB 030226 (Fig. 2.8). As this break is due to geometrical reason, it is *achromatic*, i.e. it should simultaneously occur in all photometric bands.

For a spherical adiabatic evolution we have (Sari et al. 1999)

$$\Gamma(t) = 6 \left(\frac{E_{iso,\gamma}}{n\eta_\gamma} \right)^{1/8} \left(\frac{1+z}{t_{day}} \right)^{3/8}, \quad (2.16)$$

where $E_{iso,\gamma}$ is the isotropic-equivalent energy of the explosion, n the mean surrounding interstellar medium particle density, t_{day} the observer's time in days, and η_γ is the efficiency of the fireball in converting the energy in the ejecta into γ -rays and we have inserted typical values.

From the time at which the jet break occurs (t_{jet})¹, the jet opening angle equals the relativistic opening angle, $\theta_{rel} = 1/\Gamma$. Hence, $\theta_{jet} = 1/\Gamma$, i.e.

$$\theta_{jet} = 0.057 \left(\frac{t_{jet}}{1day} \right)^{3/8} \left(\frac{1+z}{2} \right)^{-3/8} \left[\frac{E_{iso,\gamma}}{10^{53}erg} \right]^{-1/8} \left(\frac{\eta_\gamma}{0.2} \right)^{1/8} \left(\frac{n}{0.1cm^{-3}} \right)^{1/8}, \quad (2.17)$$

where we have inserted typical values.

Typical values for long bursts are spread around opening half-angles of 4 degrees (Zeh et al. 2006). As the observations give a GRB rate in the order of 1 events per day, the current estimates for the beaming angles suggest that there are at least 100-1000 GRBs per day in the Universe. This is easily shown if we consider that the outflow is collimated into two cones of opening half-angle θ_{jet} (a jet and a corresponding counter jet) and the solid angle Ω covered by an opening angle θ_{jet} is

$$\Omega = 2\pi(1 - \cos \theta_{jet}) = \pi\theta_{jet}^2 \quad \text{for } \theta_{jet} \ll 1, \quad (2.18)$$

we get for an opening half-angle of $\theta_{jet} \sim 4$ degrees

$$\frac{4\pi}{2\Omega} = \frac{2}{\theta_{jet}^2[\text{rad}]} \sim 1000. \quad (2.19)$$

After the jet break the light curve evolves as follows (from Nakar 2007):

$$F_\nu \propto \begin{cases} \nu^2 t^0 & \text{for } \nu < \nu_a, \\ \nu^{1/3} t^{-1/3} & \text{for } \nu_a < \nu < \nu_m, \\ \nu^{-(p-1)/2} t^{-p} & \text{for } \nu_m < \nu < \nu_c, \\ \nu^{-p/2} t^{-p} & \text{for } \nu_c < \nu. \end{cases} \quad (2.20)$$

Up to now we have assumed a uniform external medium, which has been found to reproduce most afterglows, however, in some cases, a wind-like external medium (with a density profile that follows $n = Ar^{-2}$) is preferred (Chevalier & Li 2000; Panaitescu & Kumar 2000; Li & Chevalier 2001; Zeh et al. 2006). This would be expected if the progenitor of the GRB

¹In the following, the break time might be also designated as t_b .

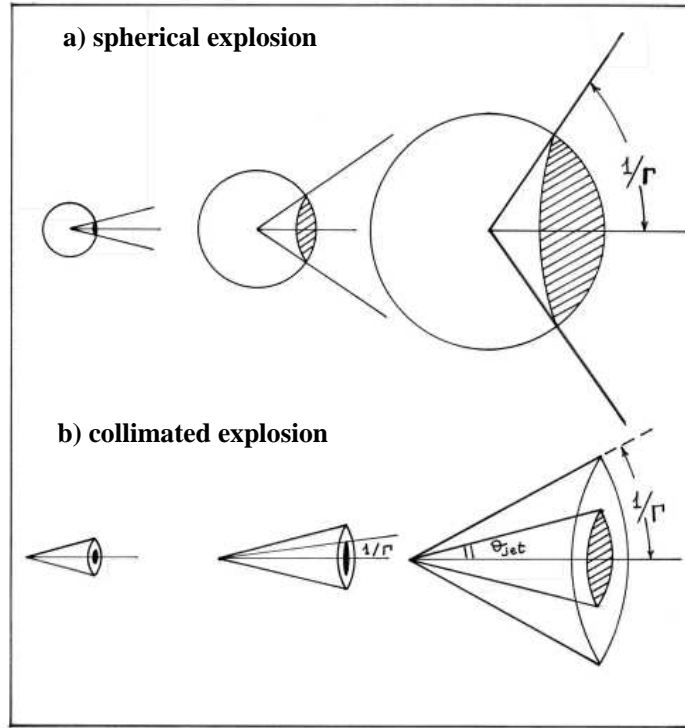


Figure 2.7: Illustration of the differences between an isotropic and a collimated explosion (Adapted from Ghisellini 2001). During the initial phase of the afterglow, the bulk Lorentz factor is large, and consequently the observer sees only a fraction of the emitting area inside a relativistically beamed cone with aperture angle $\theta_{rel} \sim 1/\Gamma$. There is no detectable difference between a sphere and a jet during this phase. In the spherical case the emitting area continues to increase both because the radius of the sphere increases and because Γ decreases, allowing more area to be within the $1/\Gamma$ cone. In the case of a collimation in a jet, once $1/\Gamma$ becomes comparable to the jet opening angle θ_{jet} , the observed area increases only because the distance to the jet apex increases. The light curve predicted in the two cases is therefore the same at early times, but in the jet case there will be a break at a particular time (when $1/\Gamma \sim \theta_{jet}$), after which the light curve decreases more rapidly than in the spherical case.

has been expelling a stellar wind during the last phase of its evolution. In this case inverting the equation (Chevalier & Li 2000)

$$\Gamma(t) = 5.9 \left(\frac{1+z}{2} \right)^{-1/4} E_{iso,\gamma}^{1/4} n A_*^{-1/4} t_{day}^{-1/4}, \quad (2.21)$$

(cf. Bloom et al. 2003) it follows

$$\theta_{jet}(wind) = 0.169 \left(\frac{1+z}{2} \right)^{+1/4} \left(\frac{E_{iso,\gamma}}{10^{52} erg} \right)^{-1/4} A_*^{1/4} \left(\frac{t_{jet}}{day} \right)^{1/4}, \quad (2.22)$$

where typical values has been inserted In the two equations A_* is related to the mass-loss rate \dot{M} of the massive star, that ejects the wind at constant velocity v_{wind} , in the following way:

$$A_* = \frac{\dot{M}/10^{-5} M_\odot \text{ yr}^{-1}}{v_{wind}/10^3 \text{ km s}^{-1}}. \quad (2.23)$$

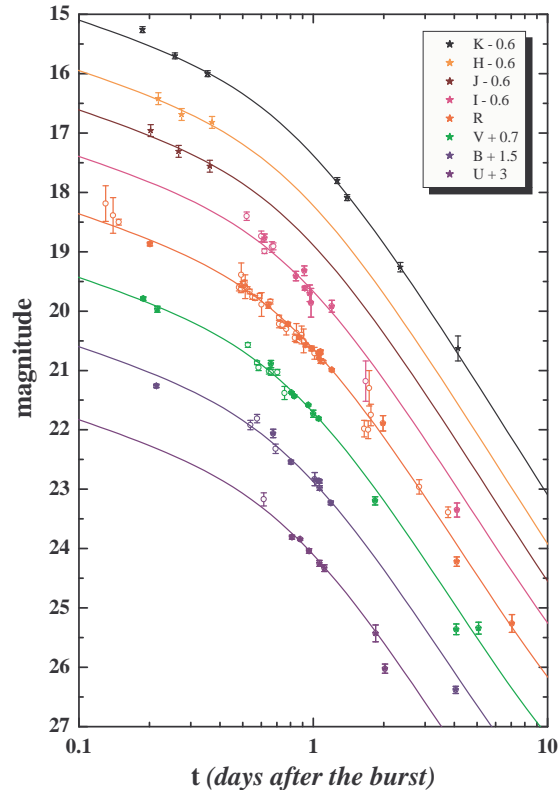


Figure 2.8: *Light curves in different optical bands of the afterglow of GRB 030226. The smooth break around $t = 1$ days appears to be achromatic pointing to a collimated explosion. From Klose et al. (2004).*

The last part of Tab. 2.1 describes the parameters α and β for a post-jet-break evolution. The jet break usually takes place, after the radiative transition, therefore in the slow cooling phase. The closure relations presented for the ISM and wind circumburst medium in the slow cooling model are equally valid to describe the pre-jet-break evolution (Zhang & Mészáros 2004).

Rossi et al. (2002) considered an alternative model in which the jet has a beam pattern where the luminosity per unit solid angle (and perhaps also the initial Lorentz factor) decreases smoothly with increasing angular distance from the axis, rather than having a well-defined cone angle within which the flow is uniform. They show that the break in the afterglow light curve then occurs at a time that depends on the viewing angle. Instead of implying a range of intrinsically different jets, the data on afterglow breaks could be consistent with a standardized jet, viewed from different angles.

Collimation is not the only suggested explanation for the observed breaks in the light curves. Alternative possibilities are: a sudden change in the circumburst density (Panaitescu & Kumar 2001), a fast transition from relativistic to non-relativistic bulk motion of the shock due to a dense circumburst medium (Wang et al. 2000), a break in the power-law distribution of electrons in the shock (Li & Chevalier 2001), usually assumed to be a single power-law.

However, in literature the jet model is still the most accepted model to explain breaks

in the afterglow light curves. Moreover the jet model can explain the XRFs as GRBs which occurs when the observer is “off-axis” with respect the opening angle of the emission. This indicate that XRFs and GRBs are either closely related phenomena or that they are the same events seen from different angles (Heise et al. 2001).

2.4 The progenitors

2.4.1 Long bursts, collapsars, and supernova bumps

In the early 1990s a detailed model of the death of a rapidly rotating, massive star had been constructed by Woosley (1993). In the collapsar model, as it is called, a GRB accompanied by a supernova is produced in the collapse of a massive stellar core into a central compact object. This compact object is generally considered to be a black hole, although it has been suggested that at first a super-massive rapidly rotating neutron star is formed, which collapses to a black hole after it has lost the angular momentum it needs to support the mass against gravity. In both cases the end-product of the collapse is a black hole and a torus of stellar material surrounding it, which produces a collimated outflow, a jet, which is the source of the GRB. The fact that the jet has to escape the stellar envelope puts constraints on the massive star: the star must have undergone a severe mass-loss by means of a stellar wind, e.g. a Wolf-Rayet star.

However, it was with the GRB occurred on April 25, 1998 that the first observational evidence of the connection between supernovae (SNe) and GRBs came out. Galama et al. (1998) reported the discovery of an optical transient, in the *BeppoSAX* WFC error box of GRB 980425, within about a day of the γ -ray burst. Its optical light curve, spectrum and location in a spiral arm of the galaxy ESO184-G82, at a redshift $z = 0.00856$ (to date still the nearest known)², showed that the transient was a very luminous type Ic supernova, now named SN 1998bw.

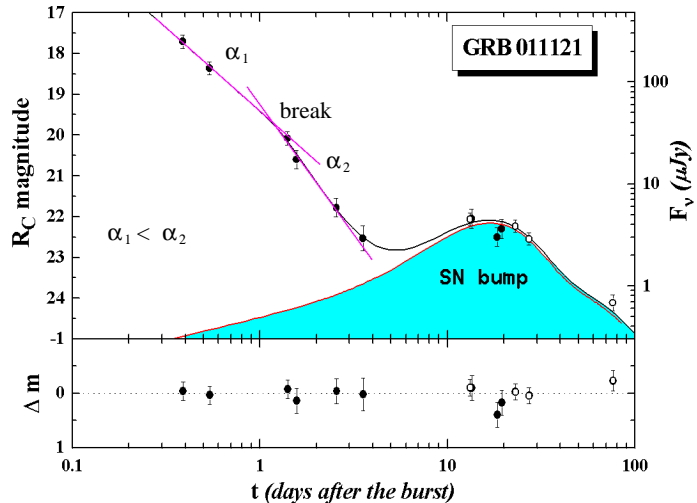
The presumed association of the GRB with a supernova brought much support to the collapsar model, although the hypothesis that SNe and GRBs are physically related was at first highly debated.

Another non-definitive evidence for the GRB-SN connection came with the fact that several bursts showed a small bump in their late-time optical afterglow light curves (e.g., Bloom et al. 1999; Zeh et al. 2004), the so-called supernova bump.

In Figure 2.9 a typical optical afterglow light curve is shown. In general the afterglow light curve decays, initially, as a power law with $\alpha_1 \approx 1.2$ (large variations around this value are however possible), then in many cases an achromatic break to a steeper decline with $\alpha_2 \approx 2$ is found. This break is usually interpreted, like in the X-ray band, as a jet break. In most of the cases the afterglow fades rapidly and becomes significantly dimmer than its host galaxy and the light curve reaches a plateau corresponding to the brightness of the host. For several GRBs red bumps are seen at late times (several weeks to a month) and they are interpreted as evidence for an underlying SN. The physics behind the afterglow light curve is discussed at the end of Sec. 2.3.3.

²The X-ray flash 080109 associated with a bright supernova in NGC 2770 (Soderberg et al. 2008) had a shorter redshift ($z=0.0065$), but no GRB was detected for that event.

Figure 2.9: An example of optical afterglow light curve: R_C -band light curve of GRB 011121 based on observational data with the addition of an underlying SN component (Greiner et al. 2003) to explain, at late times, the magnitude values of the afterglow brighter than predicted by the power law decay. All the data are corrected for Galactic extinction and the contribution of the underlying host galaxy has been removed. Δm stands for observed minus fitted magnitude.



It was the GRB 030329 that provided the first spectroscopic evidence that a very energetic supernova (“hypernova”) was temporally and spatially coincident with a GRB (Fig. 2.10, left panel). The monitoring of the supernova indicated that it exploded within a few days of the GRB (Hjorth et al. 2003). Stanek et al. (2003) and Hjorth et al. (2003) reported on the early observations of the afterglow of GRB 030329 and the spectroscopic discovery of its associated supernova SN 2003dh. They obtained spectra (wavelength range of 350–850 nm) of the afterglow each night from March 30.12 (0.6 days after the burst) to April 8.13 (UT) (9.6 days after the burst). The early spectra consist of a power-law continuum ($F_\nu \propto \nu^{-0.9}$) with narrow emission lines originating from HII regions in the host galaxy, indicating a low redshift of $z = 0.1687$. However, their spectra taken after 2003 April 5 show broad peaks in flux characteristic of a supernova. Correcting for the afterglow emission, they found that the spectrum of the supernova was remarkably similar to the type Ic “hypernova” SN 1998bw. This further on strongly suggested that core collapse events can give rise to GRBs, thereby favoring the “collapsar” model.

After GRB 980425 and 030329, other two GRBs with a spectroscopically identified supernova associated with them were discovered: GRB 031203 (Malesani et al. 2004) and GRB 060218 (Masetti et al. 2006).

At $z = 0.1055$ the GRB 031203 is the third nearest GRB known. The optical and infrared monitoring of the afterglow carried out by Malesani et al. (2004) revealed a brightening source embedded in the host galaxy, which they attributed to the presence of a supernova (SN 2003lw) related to the GRB. A rebrightening in the optical light curve was detected in all bands, peaking in the R -band about 18 rest-frame days after the burst. This rebrightening closely resembled the light curve of a supernova like SN 1998bw and also spectra taken close to the maximum of the rebrightening showed extremely broad features as in SN 1998bw (Malesani et al. 2004). Since it was an intrinsically faint GRB, the optical light curve was dominated by the SN after the first few days.

Finally, GRB 060218 was associated to SN 2006aj. This is the second closest GRB (redshift $z = 0.033$). Modeling of the spectra and light curve of the associated SN 2006aj (Cobb et al. 2006; Mirabal & Halpern 2006; Pian et al. 2006; Sollerman et al. 2006) suggested

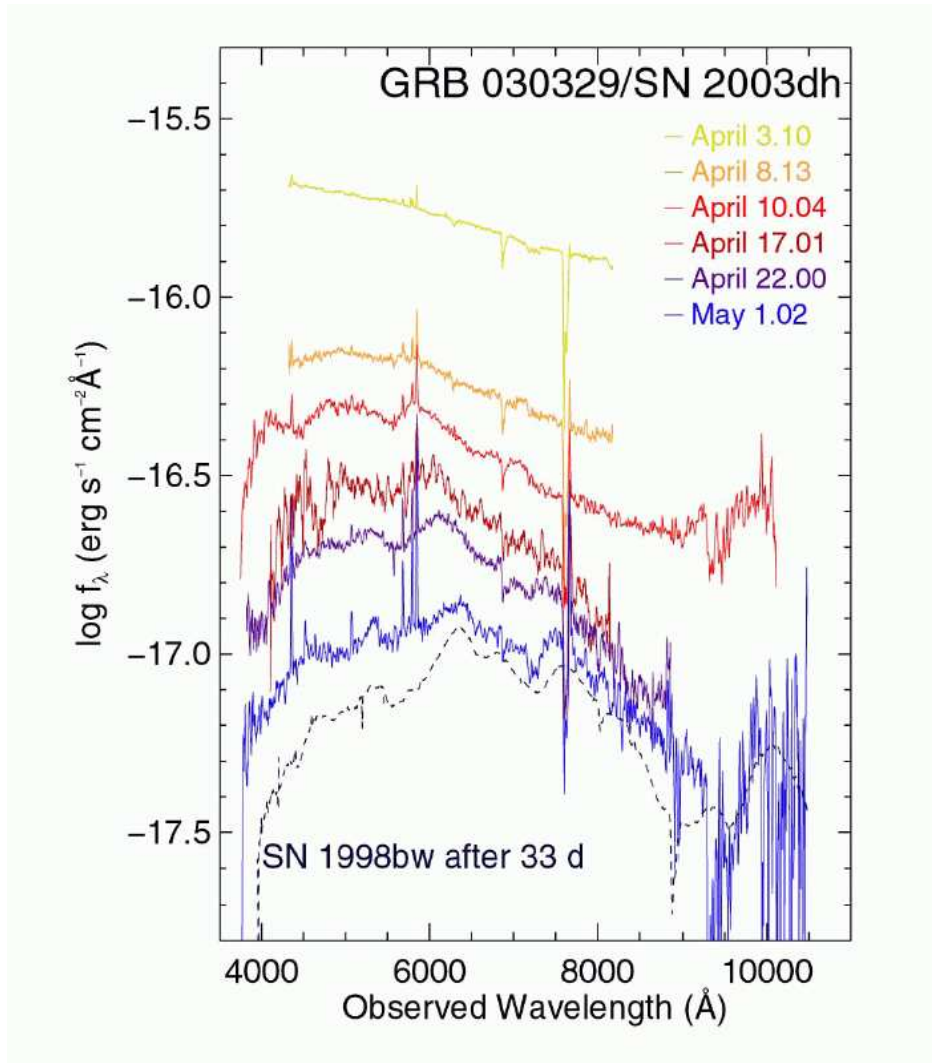


Figure 2.10: *The optical spectra of GRB 030329/SN 2003dh at various epochs (Hjorth et al. 2003).*

a progenitor star whose initial mass was $20 \pm 1 M_{\odot}$ (Mazzali et al. 2006b). For an extended study of this object see Sects. 3.2 and 4.1 in this Thesis.

However, just after the connection GRB-SN was confirmed by several cases, two nearby long GRBs were discovered which both showed no evidence of an associated supernova: GRB 060505 and GRB 060614 (Fynbo et al. 2006), with a redshift of 0.089 and 0.125, respectively. The lack of detected supernova emission in these bursts indicated that the peak luminosity had to be at least 10^2 times smaller than the one of GRB 980425. This shed a new light upon the GRB-SN connection, in particular it has risen the question whether all long GRBs are really coming from the collapse of a massive star. Host galaxy studies for these two GRBs have shown that their environments are similar to typical long GRB host galaxies (Thöne et al. 2008), hinting at a massive stellar progenitor.

2.4.2 Short bursts and neutron star mergers

Much less is known about the progenitors of short GRBs. As there is a clear distinction in their temporal and spectral characteristics (see Sec. 2.2.1), it has been widely adopted that they have different origins. The discovery of the first X-ray afterglow with the *Swift* satellite of a short burst, GRB 050509B, showed that this event is most likely associated with a giant elliptical galaxy, in which hardly any star formation is still present (Gehrels et al. 2005). After this one, more short GRBs afterglows have been found, also at optical and radio wavelengths (e.g., Fox et al. 2005; Hjorth et al. 2005b; Berger et al. 2005). Optical observations of their environments show that there is a wide variety of host galaxies for short GRBs (see Sec. 2.5.2).

For short GRBs a model with a binary merger of two compact objects, neutron star-neutron star or neutron star-black hole, has been suggested (e.g., Blinnikov et al. 1984; Goodman 1986; Paczyński 1986). In this binary merger model, the GRB is expected to occur far away from the place of birth of the binary. The supernova explosions that made the compact objects, will give the binary kick velocities that move it away from its place of birth, maybe even outside of its host galaxy given the timescale for the merger process, $10^5 - 10^{10}$ years.

The fact that a significant fraction of short GRBs is found in the outskirts of their host galaxies, or even entirely outside them, means that the immediate environment of short GRBs on average has a lower density than that of long GRBs (Nakar 2007).

The ambient medium density has a significant influence on the brightness of the afterglow: a lower ambient density causes a fainter afterglow. This makes the afterglows of short GRBs in comparison to those of long GRBs harder detectable. For a comprehensive study on the differences between short and long GRB afterglows see Kann et al. (2008).

2.5 Host galaxies

Host galaxies give important clues about the environment in which GRBs progenitors are formed, which indirectly points to the nature of progenitors of the explosions. Different host galaxies have been found for short and long gamma-ray bursts, indicating that we are looking at different progenitor populations.

2.5.1 Host galaxies of long GRBs

Long gamma-ray bursts are generally found in extremely blue, sub-luminous host galaxies of magnitude M_B from about -15.9 to -21.9 mag (Christensen et al. 2004; Fruchter et al. 2006; Bloom & Prochaska 2006; Savaglio et al. 2006), usually not located in dense clusters. They present strong emission lines and a very high specific star formation rate ($SSFR_{\text{long}}$) with a median value of $10 M_{\odot}\text{yr}^{-1}(L/L_*)^{-1}$ (Christensen et al. 2004), where L_* is the luminosity of a galaxy at the break of the Schechter luminosity function (Schechter 1976), suggesting a significant abundance of young massive stars. This supports the generally accepted idea that long GRBs arise from the death of young massive stars, similarly to core-collapse supernovae.

However, significant differences have been found in the environments of long GRBs and core-collapse supernovae. In a sample of 42 host galaxies observed by the *Hubble Space*

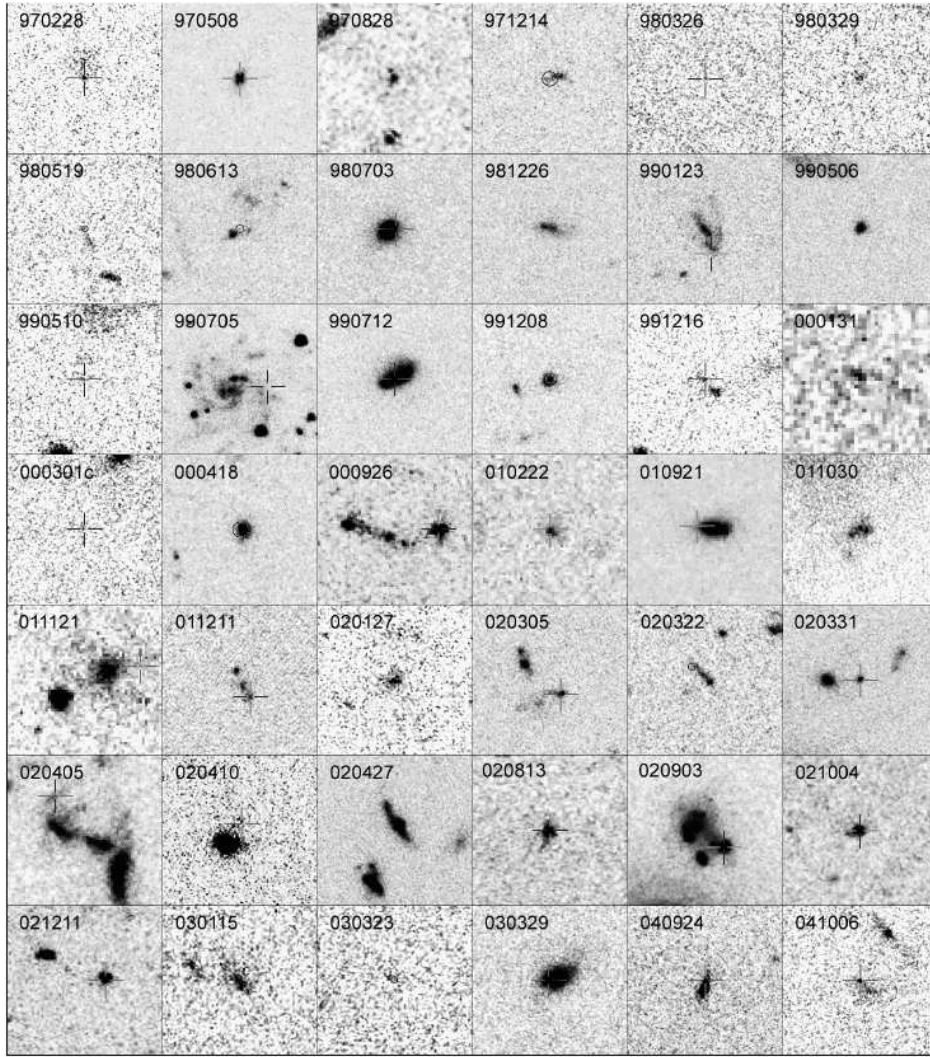


Figure 2.11: *Sample of 42 GRB host galaxies observed by the Hubble Space Telescope (Fruchter et al. 2006). The boxes have a size of $3.75'' \times 3.75''$.*

Telescope, Fruchter et al. (2006) found that only one host was a grand-design spiral, and the rest irregular galaxies (see Fig. 2.11), while supernovae not associated with GRBs are equally distributed in irregulars and spirals. In addition, gamma-ray bursts are concentrated in the brightest regions of their hosts, in the most active star-forming regions, while SNe are more uniformly distributed across their host galaxies. This is best understood if GRBs are formed from the core-collapse of extremely massive ($25 - 30 M_{\odot}$, Woosley & Bloom 2006), low metallicity (around one-third of the solar one; Fruchter et al. 2006), very short-living stars ($\lesssim 0.1$ Gyr; Christensen et al. 2004).

2.5.2 Host galaxies of short GRBs

Host galaxies of short bursts include both early and late-type galaxies, as well as field and cluster galaxies (see Fig. 2.12), in contrast to the very uniform sample of long burst hosts. Berger (2008) shows that despite the fact that most short GRBs occur in star-forming galax-

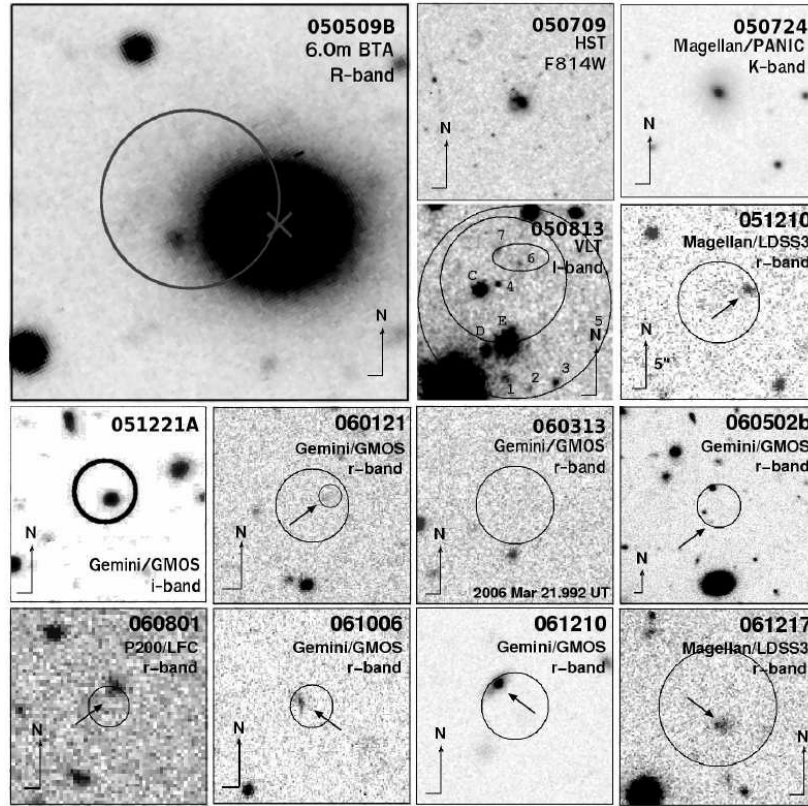


Figure 2.12: *Short GRB host galaxies.* Adapted from Castro-Tirado et al. (2005), Fox et al. (2005), Berger et al. (2005), Soderberg et al. (2006a), Ferrero et al. (2007b), Berger et al. (2007). The boxes have a size of $20'' \times 20''$, except for GRB 050509B, where it is $40'' \times 40''$. Figure from de Ugarte Postigo (2007).

ies, their properties are strongly distinct from those of long GRB hosts. First of all, the rest-frame B -band luminosity distribution of the short GRB hosts is systematically brighter than for long GRB hosts in the same redshift range. Additionally, the specific star formation rates of the short GRB hosts is lower by about an order of magnitude ($\sim 1 M_{\odot} \text{yr}^{-1} (L/L_*)^{-1}$), and the metallicities are higher by a factor of about 0.6 dex.

Fruchter et al. (2006) and Gorosabel et al. (2006) argue that a statistical test rejects the hypothesis that the two populations come from the same parent distribution with a significance greater than 99%.

According to Berger (2008), the progenitor ages span a wide range, of about 0.1 – 10 Gyr and the overall dissimilarity to the hosts of long GRBs, which appear dominated by young stellar populations, indicates that only a small fraction of short GRBs ($\lesssim 1/3$) are likely to arise from a young population of progenitors. This provides additional support to the binary coalescence model for short GRBs.

2.6 Redshift distribution

There is currently a great interest to push the redshift record beyond $z=7$, not only in order to get an answer about the re-ionization history of the universe but also about its chemical evolution. Due to their extraordinary luminosity GRBs might be the very best tool we have in the near future to obtain an answer to several questions related to the evolution of the universe after the Dark Ages.

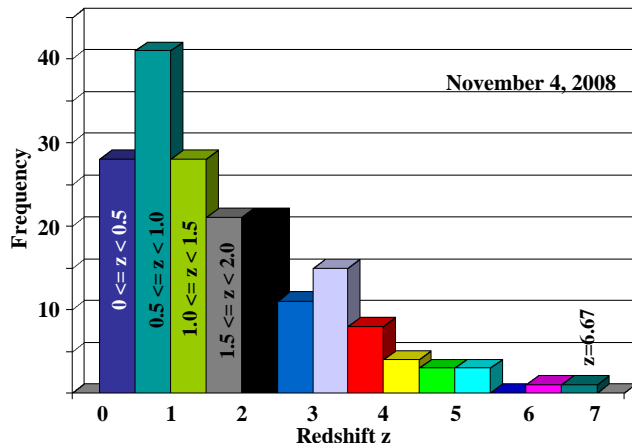


Figure 2.13: *The redshift distribution of altogether 185 afterglows with secure redshift by November 4, 2008. Based on Jochen Greiner's webpage: <http://www.mpe.mpg.de/~jcg/grbgen.html>.*

By November 4, 2008, the currently leading GRB satellite (*Swift*), launched in November 2004, has detected about 370 GRBs. In about 125 cases a redshift could be measured, i.e. for 1/3 of the entire sample. The current (spectroscopically confirmed) redshift record for galaxies is 6.96 (Iye et al. 2006) and for quasars 6.56 (Hu et al. 2002). Until Summer 2008, for GRBs the redshift record was 6.29 (Kawai et al. 2006), while for the nearest GRB the record was $z=0.00856$ (GRB 980425; Galama et al. 1998). Meanwhile, using GROND mounted on the 2.2m telescope on La Silla, Chile, observations of our group have pushed the GRB redshift record to 6.7 (Greiner et al. 2008).

The median of the redshift distribution is currently $z \sim 2$ (see Fig. 2.13). It is not clear which could be the maximum of the redshift distribution. It has been suggested that GRBs may occur at redshifts around up to z about 15 – 20, and that their afterglows should also be detectable (Lamb & Reichart 2000). Bursts at this redshift will not be detectable in the optical bands due to absorption by the Ly- α forest, but in the X-ray, IR and radio bands. At further redshift probably GRBs do not occur, as their progenitors might have not formed yet.

Chapter 3

The bursts: observational data

In this Chapter the data samples for the three *Swift* gamma-ray bursts, and information about the data reduction process are presented.

3.1 The short burst GRB 050813

3.1.1 The event

GRB 050813 was detected by the *Swift* satellite on 2005 August 13, 6:45:09.76 UT (Retter et al. 2005). Its duration in the 15-350 keV band was $T_{90} = 0.6 \pm 0.1$ seconds (Sato et al. 2005), making it after GRB 050509B and 050724 the third short burst that *Swift* localized quickly and precisely. According to its observed duration (T_{90}), GRB 050813 can be associated with the class of short bursts with very high (99.9%) probability (Donaghy et al. 2006). In addition, its measured spectral lag is consistent with zero, another important property of short bursts (Donaghy et al. 2006; Norris & Bonnell 2006). Furthermore, the small original *Swift* XRT error circle encompasses parts of an anonymous cluster of galaxies with ellipticals inside and close to the error circle (Gladders et al. 2005; Gorosabel et al. 2005; Prochaska et al. 2006). Taken together, these observations suggest that GRB 050813 should be considered as a typical short burst.

It is reminiscent of GRB 050509B, which had a very faint X-ray afterglow (Gehrels et al. 2005). Ground analysis of the X-ray data revealed a faint, uncatalogued source at coordinates R.A., Decl. (J2000) = $16^{\text{h}} 07^{\text{m}} 57^{\text{s}}.0$, $+11^{\circ} 14' 52''$ with an uncertainty of 10 arcsec radius (Morris et al. 2005). This position was later refined by Moretti et al. (2006) to R.A., Decl. (J2000) = $16^{\text{h}} 07^{\text{m}} 57^{\text{s}}.07$, $+11^{\circ} 14' 54''.2$ with an uncertainty of 6.5 arcsec radius; an even smaller error region was reported by Prochaska et al. (2006). No optical or near-infrared afterglow candidate was found. Li (2005) reported an unfiltered upper limit of magnitude 18.6 at 49.2 seconds after the burst. UVOT observations started 102 seconds after the trigger and a 3-sigma upper limit of $V = 19.1$ was derived from a 188 seconds exposure (Blustin et al. 2005). Sharapov et al. (2005) found a limiting *I*-band magnitude of ~ 21 at 10.52 hours after the burst, while Bikmaev et al. (2005) reported an *R*-band upper limit of ~ 23 at 12.75 hours after the event.

Spectroscopy of galaxies close to and inside the XRT error circle revealed a mean redshift of $z = 0.72$ (Berger 2005; Foley et al. 2005; Prochaska et al. 2006), indicating the possibility

that this may also be the redshift of the GRB. This was later refuted by Berger (2006), who argued that the host is a background galaxy at a (photometric) redshift of about 1.8, possibly related to a background cluster of galaxies. This would make GRB 050813 the second most distant (after GRB 060121, de Ugarte Postigo et al. 2006; Levan et al. 2006) short burst for which a redshift could be estimated.

However, besides the efforts, the short burst GRB 050813 belongs to the small set of short bursts for which up to date it has not been possible to define precisely the host galaxy.

3.1.2 OSN, CAHA and VLT data

A first imaging of the GRB error box was performed with the 1.5-m OSN telescope at Observatorio Sierra Nevada and the Calar Alto (CAHA) 2.2-m telescope equipped with CAFOS starting already 0.5 days after the burst (Gorosabel et al. 2005). Unfortunately, these observations resulted only in upper limits for the magnitude of any optical transient (Table 3.1). In order to set constraints on a rising SN component, we have then carried out deep follow-up observations using VLT/FORS2 in standard resolution (SR) imaging mode with a scale of 0.25 arcsec per pixel (field of view $6'8 \times 6'8$). Observations were performed in the Bessel *I* band in order to minimize the potential influence of host extinction on the discovery of a fading (afterglow) or a rising (supernova) source. A first run was performed on August 19.061 to 19.088 UT, 5.8 days after the burst. Ten frames were obtained, 200 seconds exposure time each. Seeing conditions were very good, ~ 0.5 arcsec. A second run using the same instrumental setup was performed on August 24.990 to 25.017 UT, 11.7 days after the burst. Atmospheric seeing conditions were even better than during the first observing run, approaching 0.35 arcsec. Both nights were photometric.

Date (days)	$t - t_0$ (days)	Mag	Exposure (s)	Filter	Telescope
13.8333	0.5519	22.8	10×600	I	1.5m OSN
13.8708	0.5894	23.3	23×180	R	2.2m, CAFOS
14.8475	1.5661	23.1	24×300	R	2.2m, CAFOS
19.0606	5.7792	25.1	10×200	I	8.2m, FORS2
24.9901	11.7087	25.5	10×200	I	8.2m, FORS2

Table 3.1: *Observing log of the GRB 050813 field. t_0 , the time of the burst, is August 13.2814, 2005. All dates refer to August 2005 and give the time of the start of the first exposure. Mag is the limiting magnitude of the combined image.*

The FORS2 images were bias-subtracted and flat-fielded with standard reduction procedures provided within IRAF¹. Frames obtained on the same night and in the same band were summed together in order to increase the signal-to-noise ratio. Photometry was performed with standard Point Spread Function (PSF) fitting using the DAOPHOT II image data analysis package “PSF-fitting algorithm²” (Stetson 1987) within the MIDAS³ platform. In addition, we performed aperture photometry using the IRAF Aperture Photometry Package Apphot.

¹<http://iraf.noao.edu>

²The PSF-fitting photometry is accomplished by modeling a two-dimensional Gaussian profile with two free parameters (the half width at half maxima along *x* and *y* coordinates of each frame) on at least five unsaturated bright stars in each image.

³<http://www.eso.org/projects/esomidas>

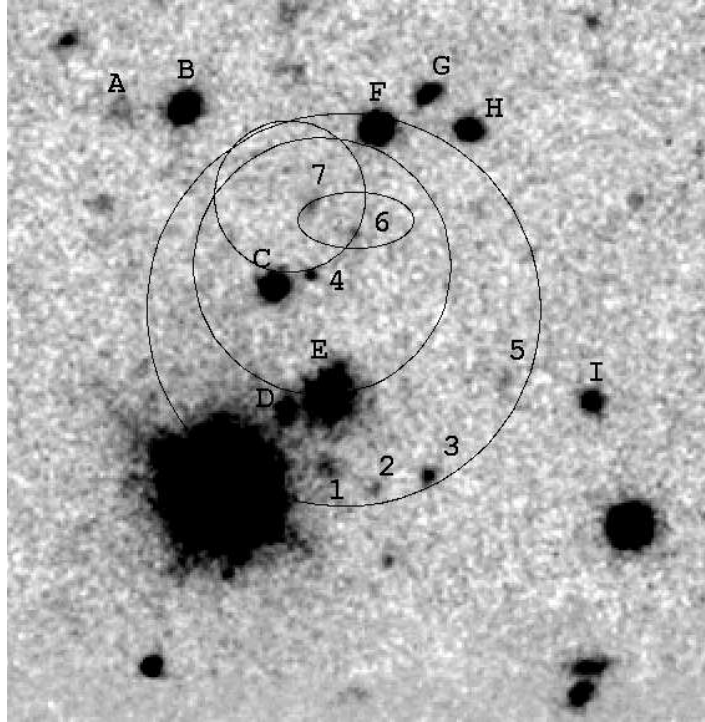


Figure 3.1: VLT I-band image of the GRB field obtained 11 days after the burst, showing the original 10 arcsec (radius) XRT error circle of GRB 050813 (large circle, Morris et al. 2005), the refined error circle by Moretti et al. (2006) (small circle, center around source #4), the revised error ellipse (Prochaska et al. 2006), the refined error circle by Butler (2007) (small circle, centered around source #7) and the objects listed in Tables 3.2 and 3.3.

Table 3.2: List of objects used for the calibration of the photometry (A,B,F,G,H,I) and the brightest galaxies in the XRT error circle (C,D,E). The numbering follows Fig. 3.1.

Object	R.A. (J2000) d m s	Decl. (J2000) ° ' "	I mag
A	16:07:57.72	+11:15:02.24	24.68 ± 0.35
B	16:07:57.50	+11:15:02.13	21.83 ± 0.09
C	16:07:57.19	+11:14:53.15	22.43 ± 0.12
D	16:07:57.16	+11:14:46.86	23.38 ± 0.22
E	16:07:57.01	+11:14:47.61	22.74 ± 0.28
F	16:07:56.85	+11:15:01.80	20.88 ± 0.03
G	16:07:56.66	+11:15:02.87	23.61 ± 0.19
H	16:07:56.53	+11:15:01.11	22.85 ± 0.14
I	16:07:56.10	+11:14:47.34	23.50 ± 0.17

Table 3.3: Photometry of the fainter sources in the XRT error circle. As in Tab. 3.2, the numbering follows Fig. 3.1. Run 1 and run 2 refer to the first and second VLT/FORS observations, respectively.

Object	R.A. (J2000) d m s	Decl. (J2000) ° ' "	I run 1 mag	I run 2 mag
1	16:07:57.00	+11:14:43.83	$24.7 < I < 24.9$	$24.4 < I < 25.4$
2	16:07:56.85	+11:14:42.91	> 25.1	$24.4 < I < 25.5$
3	16:07:56.66	+11:14:43.58	24.69 ± 0.24	24.44 ± 0.10
4	16:07:57.07	+11:14:53.65	24.63 ± 0.30	24.67 ± 0.13
5	16:07:56.40	+11:14:48.35	> 25.1	25.47 ± 0.25
6	16:07:56.91	+11:14:55.91	> 25.1	25.64 ± 0.28
7	16:07:57.07	+11:14:57.43	$24.7 < I < 25.1$	25.41 ± 0.25

Additional spectroscopic observations covering the entire original $r=10$ arcsec XRT error circle (Morris et al. 2005) were performed with the Integral Field Unit VIMOS/IFU at the

ESO-VLT starting 20 hours after the burst. Unfortunately, these observations could not be implemented into this study due to technical problems with the data.

Figure 3.1 shows the *Swift* XRT 90% containment radius reported by Morris et al. (2005) (large circle), the refined error circle by Moretti et al. (2006) (small circle) and, as a small ellipse, the re-analyzed X-ray error box (68% containment radius) given by Prochaska et al. (2006). In the original $r=10$ arcsec XRT error circle there are 11 sources, designated by the letters C, D, E, F and the numbers from 1 to 7. Note that $B = X$, $C = B$, $4 = B^*$ and $E = C$ in the nomenclature of Prochaska et al. (2006). The X-ray error box published by Prochaska et al. (2006) contains only two sources, of which #6 is the one identified by Berger (2006) as the possible host galaxy possibly related to a cluster of galaxies⁴ at $z=1.8$. Nothing can be said at this stage about the redshift of source #7, however. Here, we assume that it is a member of the cluster of galaxies at $z=0.72$ (Berger 2005; Foley et al. 2005; Prochaska et al. 2006).

3.2 The GRB-SN event GRB 060218

3.2.1 The burst

On 2006 February 18, at 03:34:30 UT, the Burst Alert Telescope (BAT) on board the *Swift* satellite detected the bright GRB 060218 (Cusumano et al. 2006). The *Swift* X-ray Telescope (XRT) and the UV/Optical Telescope (UVOT) also detected its afterglow in the X-ray and optical bands (Cusumano et al. 2006; Kennea et al. 2006), respectively, leading to a precise localization of the optical counterpart at coordinates R.A., Decl. (J2000) = $03^{\text{h}} 21^{\text{m}} 39^{\text{s}}.71$, $+16^{\circ} 52' 02''.6$ with an estimated 1-sigma error of about $1''.0$ (Marshall et al. 2006). Due to its unusual properties in the gamma-ray band (Campana et al. 2006) and its odd behavior (Gehrels 2006), its nature was not clear till the determination of its redshift ($z= 0.033$, Mirabal & Halpern 2006) and the discovery of an association with a supernova (Masetti et al. 2006). GRB 060218 is classified as an X-ray Flash (Campana et al. 2006), with E_{iso} comparable with other GRB-SNe and consistent with the Amati relation (Amati et al. 2006). It is probably not an off-axis (see page 22) event (Nousek et al. 2006a).

The low redshift and the brightness of the object allowed extensive follow-up observations with ground-based facilities (Ferrero et al. 2006; Mirabal et al. 2006; Modjaz et al. 2006; Pian et al. 2006; Soderberg et al. 2006b; Sollerman et al. 2006).

3.2.2 VLT data

We observed SN 2006aj (see Fig. 3.2) both spectroscopically and photometrically with the ESO Very Large Telescope FORS1 and FORS2 instruments. Results from the spectroscopic VLT campaign are presented in our paper Pian et al. (2006) and modeled in Mazzali et al. (2006a).

The photometric observations presented in this Thesis were performed until 26 days after the burst (Table 3.4). After this point in time, the SN location was no longer observable due to

⁴E. Berger, talk given at “Swift and GRBs: Unveiling the Relativistic Universe”, San Servolo, Venice (Italy), 2006 June 5-9.

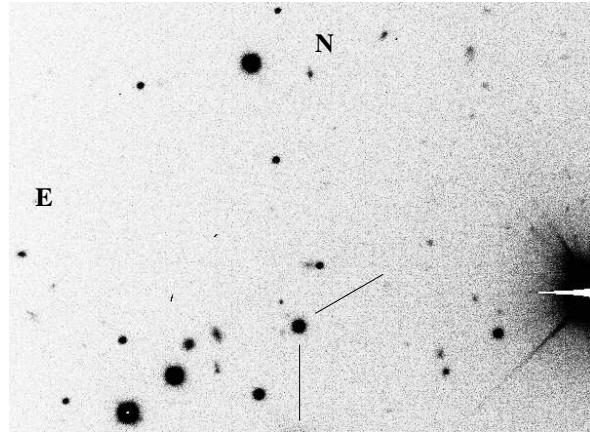


Figure 3.2: The location of SN 2006aj is shown here in a VLT/FORS2 R-band image taken on 2006 March 1, at 00:52 UT (30 sec exposure time). The field of view is approximately 2×3 arcmin.

high airmass. The exposure time was between 30 and 60 seconds. The images, in the Bessell B , V , R , and I filters, were bias-subtracted and flat-fielded with standard reduction procedures using IRAF and final photometry was performed with standard Point Spread Function (PSF) fitting using the DAOPHOT II image data analysis package (Stetson 1987) within MIDAS. Photometric calibration of the images was performed using the standard star 685 of the field SA98 (Landolt 1992), imaged during the same night of our first observational run, which was used to create 16 secondary standards in the field around the SN that were subsequently used for all individual images to draw a linear regression among instrumental and reference magnitudes and calculate the value of the optical transient. The accuracy of the photometry was confirmed by considering the zero point values of several stars in the calibration field in all bands for different nights. In addition, we investigated a possible influence of color terms. We found that they could affect the photometry with an additional error of up to 0.02 magnitudes, which was then added in quadrature to the individual photometric measurement errors.

3.2.3 Liverpool Telescope data and KAIT data

Further photometric data were obtained with the 2 m robotic Liverpool Telescope on La Palma on several occasions over a period of about 2.5 weeks post-burst. Observations were made in Bessell B , V and SDSS r' filters and zero-point deduced by comparison to two field stars (star S1 and star 4 of Modjaz et al. 2006). The magnitudes were transformed into Johnson B , V and Cousins R -band via equations previously derived for the camera (Steele et al. 2004). The quoted errors reflect the scatter in individual measurements for subexposures at each epoch, and include an estimate of the calibration uncertainty.

Additional data were also obtained with the 0.8 m robotic KAIT at Lick Observatory on four consecutive nights between 3 to 6 days post-burst. Unfiltered observations were obtained in all four nights, and Bessell B , V , R , and I filtered observations were made in the last three nights. The images were bias-subtracted and flat-fielded with standard reduction procedures using IRAF, and the final photometry was performed with PSF-fitting technique in IRAF/DAOPHOT.

The secondary standards calibrated with VLT data were used for the final photometric calibration. The unfiltered magnitudes were converted to the R band following the method

described in Li et al. (2003).

Table 3.4: *The photometry of SN 2006aj from the Very Large Telescope (VLT), the Liverpool Telescope (LT) and the Katzman Automatic Imaging Telescope (KAIT), including the acquisition images for the VLT spectroscopy (Pian et al. 2006). The date is the UT exposure mid-time. Column $t - t_0$ refers to the time in days after the burst trigger at $t_0 = 3:34:30$ UT of Feb. 18, 2006 (Cusumano et al. 2006). The third column gives measured magnitudes which are corrected neither for extinction nor flux from the host galaxy. The fourth column gives the pure supernova magnitudes after correcting for Galactic extinction, host-galaxy flux and host-galaxy extinction.*

	Date	$t - t_0$	Mag. (measured)	Mag. (corrected)	Exposure s	Filter	Telescope
Feb.	20.8924	2.7434	18.63 ± 0.06	18.14 ± 0.06	8×150	B	LT
Feb.	21.0307	2.8817	18.57 ± 0.03	18.07 ± 0.03	2×30	B	VLT
Feb.	22.1219	3.9729	18.41 ± 0.08	17.87 ± 0.08	450	B	KAIT
Feb.	23.0550	4.9060	18.24 ± 0.04	17.68 ± 0.04	2×30	B	VLT
Feb.	23.1209	4.9719	18.29 ± 0.08	17.74 ± 0.08	450	B	KAIT
Feb.	24.1218	5.9728	18.13 ± 0.08	17.56 ± 0.08	450	B	KAIT
Feb.	25.0467	6.8977	18.11 ± 0.04	17.54 ± 0.04	2×30	B	VLT
Feb.	26.0398	7.8908	18.05 ± 0.03	17.47 ± 0.03	2×30	B	VLT
Feb.	27.0483	8.8993	18.01 ± 0.03	17.43 ± 0.03	60	B	VLT
Feb.	28.0037	9.8547	18.07 ± 0.04	17.49 ± 0.04	2×30	B	VLT
Mar.	1.0337	10.8847	18.14 ± 0.03	17.57 ± 0.03	2×30	B	VLT
Mar.	2.0297	11.8807	18.22 ± 0.03	17.66 ± 0.03	2×30	B	VLT
Mar.	3.0330	12.8840	18.35 ± 0.03	17.81 ± 0.03	2×30	B	VLT
Mar.	4.0303	13.8813	18.47 ± 0.03	17.95 ± 0.03	2×30	B	VLT
Mar.	5.0119	14.8629	18.61 ± 0.03	18.11 ± 0.03	2×30	B	VLT
Mar.	6.0364	15.8874	18.66 ± 0.03	18.17 ± 0.03	2×30	B	VLT
Mar.	7.8899	17.7409	18.97 ± 0.07	18.56 ± 0.07	5×100	B	LT
Mar.	8.0332	17.8842	19.03 ± 0.03	18.64 ± 0.04	60	B	VLT
Mar.	8.9983	18.8493	19.10 ± 0.03	18.73 ± 0.04	60	B	VLT
Mar.	10.0009	19.8519	19.26 ± 0.04	18.95 ± 0.05	60	B	VLT
Mar.	11.9977	21.8487	19.40 ± 0.04	19.16 ± 0.05	$60+30$	B	VLT
Mar.	13.0145	22.8655	19.57 ± 0.05	19.43 ± 0.07	60	B	VLT
Mar.	13.9976	23.8486	19.57 ± 0.05	19.43 ± 0.07	60	B	VLT
Feb.	20.8787	2.7279	18.19 ± 0.06	17.86 ± 0.06	5×150	V	LT
Feb.	21.0323	2.8833	18.17 ± 0.03	17.83 ± 0.03	2×30	V	VLT
Feb.	22.1277	3.9787	17.92 ± 0.08	17.54 ± 0.08	300	V	KAIT
Feb.	23.0573	4.9083	17.80 ± 0.03	17.41 ± 0.03	2×30	V	VLT
Feb.	23.1266	4.9776	17.77 ± 0.08	17.37 ± 0.08	300	V	KAIT
Feb.	24.1275	5.9785	17.69 ± 0.08	17.28 ± 0.08	300	V	KAIT
Feb.	24.8713	6.7223	17.61 ± 0.06	17.19 ± 0.06	5×100	V	LT
Feb.	25.0483	6.8993	17.58 ± 0.03	17.16 ± 0.03	2×30	V	VLT
Feb.	26.0413	7.8923	17.51 ± 0.03	17.08 ± 0.03	2×30	V	VLT
Feb.	26.8720	8.7230	17.48 ± 0.06	17.05 ± 0.06	5×100	V	LT

Table 3.4: continued

	Date	$t - t_0$	Mag. (measured)	Mag. (corrected)	Exposure s	Filter	Telescope
Feb.	27.0156	8.8666	17.45 ± 0.03	17.02 ± 0.03	60	V	VLT
Feb.	27.0497	8.9007	17.46 ± 0.03	17.03 ± 0.03	60	V	VLT
Feb.	28.0053	9.8563	17.45 ± 0.03	17.02 ± 0.03	2×30	V	VLT
Mar.	1.0353	10.8863	17.45 ± 0.03	17.02 ± 0.03	2×30	V	VLT
Mar.	2.0313	11.8823	17.47 ± 0.03	17.04 ± 0.03	2×30	V	VLT
Mar.	2.8673	12.7183	17.50 ± 0.06	17.07 ± 0.06	3×100	V	LT
Mar.	3.0345	12.8855	17.51 ± 0.03	17.08 ± 0.03	2×30	V	VLT
Mar.	4.0331	13.8841	17.56 ± 0.03	17.14 ± 0.03	2×30	V	VLT
Mar.	5.0134	14.8644	17.60 ± 0.03	17.18 ± 0.03	2×30	V	VLT
Mar.	6.0379	15.8889	17.68 ± 0.03	17.27 ± 0.03	2×30	V	VLT
Mar.	6.8912	16.7422	17.67 ± 0.08	17.26 ± 0.08	2×100	V	LT
Mar.	8.0018	17.8528	17.85 ± 0.03	17.46 ± 0.03	60	V	VLT
Mar.	8.0347	17.8857	17.86 ± 0.03	17.47 ± 0.03	60	V	VLT
Mar.	8.9998	18.8508	17.92 ± 0.03	17.54 ± 0.03	60	V	VLT
Mar.	9.0067	18.8577	17.92 ± 0.03	17.54 ± 0.03	60	V	VLT
Mar.	10.0024	19.8534	18.01 ± 0.03	17.65 ± 0.03	60	V	VLT
Mar.	10.0080	19.8590	17.98 ± 0.03	17.61 ± 0.03	60	V	VLT
Mar.	11.9987	21.8497	18.14 ± 0.03	17.80 ± 0.03	60+30	V	VLT
Mar.	13.0157	22.8667	18.22 ± 0.04	17.89 ± 0.04	60	V	VLT
Mar.	13.9991	23.8501	18.30 ± 0.03	17.99 ± 0.03	60	V	VLT
Mar.	14.9992	24.8502	18.41 ± 0.03	18.12 ± 0.03	2×30	V	VLT
Mar.	16.0023	25.8533	18.42 ± 0.05	18.14 ± 0.05	2×30	V	VLT
Feb.	20.8578	2.7088	18.10 ± 0.06	17.88 ± 0.06	6×150	R	LT
Feb.	20.9362	2.7872	18.10 ± 0.06	17.88 ± 0.06	6×150	R	LT
Feb.	21.0339	2.8849	18.02 ± 0.03	17.78 ± 0.03	2×30	R	VLT
Feb.	21.0374	2.8884	18.02 ± 0.03	17.78 ± 0.03	30	R	VLT
Feb.	21.1294	2.9804	17.98 ± 0.08	17.73 ± 0.08	120	R	KAIT
Feb.	21.1312	2.9822	17.96 ± 0.08	17.71 ± 0.08	120	R	KAIT
Feb.	21.1330	2.9840	17.97 ± 0.08	17.73 ± 0.08	120	R	KAIT
Feb.	21.1349	2.9859	17.98 ± 0.08	17.73 ± 0.08	120	R	KAIT
Feb.	21.1367	2.9877	17.96 ± 0.09	17.71 ± 0.09	120	R	KAIT
Feb.	22.1317	3.9827	17.76 ± 0.08	17.48 ± 0.08	300	R	KAIT
Feb.	22.1398	3.9908	17.79 ± 0.09	17.51 ± 0.09	120	R	KAIT
Feb.	23.0224	4.8734	17.66 ± 0.03	17.37 ± 0.03	60	R	VLT
Feb.	23.0590	4.9100	17.66 ± 0.03	17.37 ± 0.03	2×30	R	VLT
Feb.	23.1306	4.9816	17.60 ± 0.08	17.30 ± 0.08	300	R	KAIT
Feb.	23.1387	4.9897	17.60 ± 0.10	17.29 ± 0.10	120	R	KAIT
Feb.	24.1315	5.9825	17.50 ± 0.09	17.19 ± 0.09	300	R	KAIT
Feb.	24.1395	5.9905	17.50 ± 0.10	17.19 ± 0.10	120	R	KAIT
Feb.	24.8645	6.7155	17.44 ± 0.07	17.12 ± 0.07	5×100	R	LT
Feb.	25.0499	6.9009	17.40 ± 0.04	17.08 ± 0.04	2×30	R	VLT

Table 3.4: continued

	Date	$t - t_0$	Mag. (measured)	Mag. (corrected)	Exposure s	Filter	Telescope
Feb.	26.0429	7.8939	17.31 ± 0.04	16.98 ± 0.04	2×30	R	VLT
Feb.	26.8677	8.7187	17.29 ± 0.06	16.96 ± 0.06	3×100	R	LT
Feb.	27.0512	8.9022	17.28 ± 0.03	16.95 ± 0.03	60	R	VLT
Feb.	28.0068	9.8578	17.25 ± 0.03	16.91 ± 0.03	2×30	R	VLT
Mar.	1.0370	10.8880	17.23 ± 0.03	16.89 ± 0.03	2×30	R	VLT
Mar.	2.0328	11.8838	17.23 ± 0.03	16.89 ± 0.03	2×30	R	VLT
Mar.	2.8604	12.7114	17.26 ± 0.06	16.93 ± 0.06	5×100	R	LT
Mar.	3.0360	12.8870	17.24 ± 0.03	16.90 ± 0.03	2×30	R	VLT
Mar.	3.8601	13.7111	17.25 ± 0.07	16.91 ± 0.07	2×100	R	LT
Mar.	4.0346	13.8856	17.26 ± 0.03	16.93 ± 0.03	2×30	R	VLT
Mar.	5.0148	14.8658	17.24 ± 0.04	16.90 ± 0.04	2×30	R	VLT
Mar.	6.0082	15.8592	17.33 ± 0.03	17.00 ± 0.03	60	R	VLT
Mar.	6.0394	15.8904	17.33 ± 0.03	17.00 ± 0.03	2×30	R	VLT
Mar.	6.8834	16.7344	17.36 ± 0.07	17.03 ± 0.07	4×100	R	LT
Mar.	7.8841	17.7341	17.41 ± 0.06	17.09 ± 0.06	5×100	R	LT
Mar.	8.0361	17.8871	17.46 ± 0.03	17.14 ± 0.03	60	R	VLT
Mar.	9.0012	18.8522	17.56 ± 0.03	17.26 ± 0.03	60	R	VLT
Mar.	10.0038	19.8548	17.60 ± 0.03	17.30 ± 0.03	60	R	VLT
Mar.	11.9997	21.8507	17.62 ± 0.04	17.32 ± 0.04	60+30	R	VLT
Mar.	13.0169	22.8679	17.68 ± 0.03	17.39 ± 0.03	60	R	VLT
Mar.	14.0013	23.8523	17.89 ± 0.03	17.63 ± 0.03	60	R	VLT
Feb.	21.0358	2.8868	17.86 ± 0.03	17.80 ± 0.03	2×30	I	VLT
Feb.	22.1357	3.9867	17.69 ± 0.08	17.60 ± 0.08	300	I	KAIT
Feb.	23.0604	4.9114	17.54 ± 0.03	17.41 ± 0.03	2×30	I	VLT
Feb.	23.1346	4.9856	17.49 ± 0.09	17.36 ± 0.09	300	I	KAIT
Feb.	24.1356	5.9866	17.31 ± 0.09	17.15 ± 0.09	300	I	KAIT
Feb.	25.0514	6.9024	17.25 ± 0.03	17.08 ± 0.03	2×30	I	VLT
Feb.	26.0444	7.8954	17.16 ± 0.03	16.98 ± 0.03	2×30	I	VLT
Feb.	27.0526	8.9036	17.10 ± 0.03	16.91 ± 0.03	60	I	VLT
Feb.	28.0083	9.8593	17.05 ± 0.04	16.85 ± 0.04	2×30	I	VLT
Mar.	1.0386	10.8896	17.04 ± 0.03	16.84 ± 0.03	2×30	I	VLT
Mar.	2.0328	11.8854	17.03 ± 0.03	16.83 ± 0.03	2×30	I	VLT
Mar.	3.0376	12.8886	17.03 ± 0.03	16.83 ± 0.03	2×30	I	VLT
Mar.	4.0362	13.8872	17.07 ± 0.04	16.87 ± 0.04	2×30	I	VLT
Mar.	5.0165	14.8675	17.01 ± 0.06	16.81 ± 0.06	2×30	I	VLT
Mar.	6.0410	15.8920	17.08 ± 0.03	16.89 ± 0.03	2×30	I	VLT
Mar.	9.0026	18.8536	17.21 ± 0.03	17.03 ± 0.03	60	I	VLT
Mar.	10.0052	19.8562	17.26 ± 0.03	17.09 ± 0.03	60	I	VLT
Mar.	11.9993	21.8503	17.35 ± 0.05	17.19 ± 0.05	60+30	I	VLT
Mar.	13.0181	22.8691	17.37 ± 0.05	17.21 ± 0.05	60	I	VLT
Mar.	14.0027	23.8537	17.48 ± 0.03	17.34 ± 0.03	60	I	VLT

3.2.4 The magnitudes of the host galaxy

The host galaxy of GRB 060218/SN 2006aj was imaged pre-burst by the Sloan Digital Sky Survey (Adelman-McCarthy et al. 2006; Cool et al. 2006). It was pointed out (Modjaz et al. 2006; Hicken et al. 2006) that there are offsets between the SDSS calibration and later efforts, rendering the transformed host-galaxy magnitudes of Cool et al. (2006) too bright. The values used for the host galaxy in this work are $B = 20.57 \pm 0.07$, $V = 20.18 \pm 0.04$, $R = 20.03 \pm 0.03$ and $I = 19.58 \pm 0.06$, not corrected for Galactic extinction. These magnitudes have been evaluated from those reported by Cool et al. (2006), by applying the corrections recommended by Modjaz et al. (2006) and Hicken et al. (2006). Our $BVRI$ magnitudes have been obtained from Cool et al.'s $u^*b^*v^*r^*i^*$ magnitudes by adopting the conversion of Lupton (2005)⁵ and taking into account that the offsets determined by Modjaz et al. (2006) in the BVR bands are 0.40, 0.27, 0.20 mag, respectively⁶. In order to determine the offset in the I band, we have considered that the offset determined by Hicken et al. (2006) and Modjaz et al. (2006) in the i^* -filter is 0.15 mag, and we have used the SDSS transformations⁷ to derive from this the offset in the i -band. Our host-galaxy magnitudes are consistent to those of Sollerman et al. (2006) within the errors.

3.2.5 The extinction correction

As the host galaxy and SN 2006aj were not separated at the resolution of the images, the host magnitudes have to be subtracted. For the extinction correction, we used the values derived by Guenther et al. (2006) from an analysis of the Na I D2 absorption lines in our Galaxy ($A_V = 0.39$ mag) and the host galaxy ($A_V = 0.13$ mag) in a VLT/UVES spectrum, obtained during this campaign close to SN maximum. This host-galaxy extinction is typical of the lines of sight toward GRBs (Kann et al. 2006). Using these extinction and host magnitude values, we derived the magnitudes of the pure SN light component.

3.3 The long burst GRB 060605

The detailed study of this burst was triggered by our goal to use integral field spectroscopy (IFS) to perform rapid follow-up observations of arcsec-sized *Swift* X-ray error circles. While in this particular case our observations were performed only some hours after the event, we could obtain useful spectra. One can imagine that a much faster response with an integral field unit (IFU), immediately after the announcement of an arcsec-sized *Swift* X-ray error circle, can provide early spectral information on bursts. A brief overview of this technique is provided in Appendix A.

3.3.1 Swift BAT data: the burst

GRB 060605 was detected by the BAT instrument on-board *Swift* on June 5, at $T_0 = 18:15:44.61$ UT (trigger 213630; Page et al. 2006) with an accuracy of 3 arcmin radius (90% containment,

⁵see also <http://www.sdss.org/dr4/algorithms/sdssUBVRITransform.html#Rodgers2005>

⁶see http://www.cfa.harvard.edu/supernova/sn2006aj_compstars.html

⁷see http://www.sdss.org/dr4/algorithms/jeg_photometric_eq_dr1.html#usno2SDSS

including systematic uncertainty). The BAT on-board calculated location of the burst was R.A., Decl. (J2000) = $21^h 28^m 35^s$, $-06^\circ 3' 36''$ (Page et al. 2006), while ground analysis resulted in coordinates R.A., Decl. (J2000) = $21^h 28^m 37.6^s$, $-06^\circ 2' 44''.7$ with an accuracy of 1.5 arcmin radius.

The time-averaged spectrum of the burst (from $T_0 - 2.580$ s to $T_0 + 20.450$ s) can be described by a cutoff power law with $\alpha = 0.3_{-0.9}^{+0.7}$, and the peak energy at 90_{-20}^{+150} keV (Butler et al. 2007). According to Sato et al. (2006), in the 15-350 keV band the burst had a duration of $T_{90} = 15 \pm 2$ s, while according to Butler et al. (2007) $T_{90} = 19 \pm 1$ s.

3.3.2 Swift XRT data

X-ray data of the afterglow of GRB 060605 were collected on 5 and 6 June 2006 with XRT. Pointed observations on target started 93 s after the BAT trigger and the monitoring was organized in two sequences, with a total net exposure time of ~ 37.4 ks in photon counting (PC) mode and ~ 13 s in windowed timing (WT) mode. In order to obtain a better S/N ratio in the spectral analysis, only the data of the first ~ 30.5 ks of the PC mode observation were used.

The data reduction was performed using the XRTDAS v2.0.1 standard data pipeline package (`xrtpipeline` v0.10.3), in order to produce the final cleaned event files.

During sequence 000 the count rate of the burst was high enough to cause pile-up in the PC mode data, which covered the entire first three orbits of XRT observation from $T_0 + 126$ s to about $T_0 + 1.8 \times 10^4$ s. Therefore, to account for this effect, the PC data were extracted in a circle of 25 pixels radius, with a circular region of 4 pixels radius excluded from its centre. The size of the inner region was determined following the procedure described in Vaughan et al. (2006).

The X-ray background was measured within a circle with 40 pixels radius located far from any source. The ancillary response file was generated with the task `xrtmkarf` (v0.5.2) within FTOOLS⁸ (Blackburn 1995), and accounts for the size of the extraction region. We used the latest spectral redistribution matrices (`swxpc0to12_20010101v008.rmf`) in the Calibration Database⁹ (CALDB 2.3) maintained by HEASARC.

3.3.3 Swift UVOT data

Swift started settled observations of GRB 060605 with its UV/Optical Telescope (Romig et al. 2005) 78 s after the trigger. The very first image was in the *v*-band, while the satellite was slewing. *Swift* found an afterglow at coordinates R.A., Decl. (J2000) = $21^h 28^m 37.32^s$, $-06^\circ 3' 31''.3$ (Page et al. 2006), confirming the optical transient already identified at that time by the robotic ROTSE IIIa telescope (Rykoff & Schaefer 2006).

The afterglow was only detected in the *white*, *v* (see Fig. 3.3), and *b* filters. The lack of detection in the UV filters (Blustin & Page 2006) is consistent with the redshift of $z = 3.7 - 3.8$ based on observations with the Australian National University ANU 2.3-m (Peterson & Schmidt 2006) and the 10-m Southern African Large Telescope (SALT; Still et al. 2006).

⁸<http://heasarc.gsfc.nasa.gov/ftools/>

⁹http://heasarc.gsfc.nasa.gov/docs/heasarc/caldb/caldb_intro.html

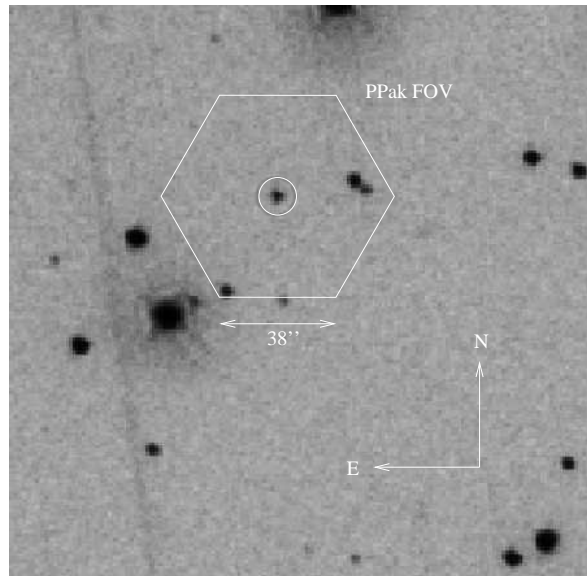


Figure 3.3: *Swift* UVOT *v*-band image of the field of GRB 060605. The optical afterglow is indicated by a circle. The overplotted hexagon shows the sky coverage of PMAS/PPak during our observing campaign (see also Fig. 3.4).

The initial observations, namely the *white* and *v* finding charts, were performed in event mode (photon counting), while the rest of the exposures were taken predominately in image mode.

The source counts were extracted using a region of $5''$ radius. As the source fades it is more accurate to use smaller source apertures (Poole et al. 2008). Therefore, when the count rate fell below $0.5 \text{ counts s}^{-1}$, the source counts were extracted using a region with $3''$ radius. These counts were corrected to $5''$ using the curve of growth contained in the calibration files. Background counts were extracted using a circular region of radius $15''$ from a blank area of sky situated near to the source position. The count rates were obtained from the event lists using `uvotevtlc` and from the images using `uvotsource`. The used software can be found in the software release, Headas 6.3.2 and version 20071106 (UVOT) of the calibration files.

For each filter, the count rates were binned by taking the weighted average in time bins of $\Delta t/t = 0.2$. They were then converted to magnitudes using the UVOT photometric zero points (Poole et al. 2008). The log of the observations is presented in Tab. 3.5.

3.3.4 Spectroscopic data

Low-resolution integral field spectroscopy of the field was acquired starting about 7.5 hours after the burst. Even if at that time the afterglow position was already precisely known, we decided to perform the IFS observing run, in order to learn the handling of the data.

The observations were carried out starting at UT 01:43:41 (June 6), at the 3.5-m telescope equipped with the Potsdam Multi-Aperture Spectrograph (PMAS; Roth et al. 2005) in the PPak (PMAS fiber Package) mode (Verheijen et al. 2004; Kelz et al. 2006), using 2×2 pixel binning. We used the V300 grating, which covers a wavelength range between 3698 and 7010 Å, resulting in a reciprocal dispersion of 3.4 Å per pixel . The PPak fiber bundle consists of 382 fibers of $2.7''$ diameter each (see fig. 5 in Kelz et al. 2006). Of them, 331 fibers (the science fibers) are concentrated in a single hexagonal bundle covering a field-of-view of $74'' \times 64''$ with a filling factor of $\sim 65\%$.

Table 3.5: *Log of the Swift UVOT observations. The first column gives the logarithmic mid-time in seconds after the onset of the GRB. The second and the third columns give the start/end of the observations. The data are not corrected for Galactic extinction.*

t	$\Delta t-$	$\Delta t+$	Magnitude	Filter	t	$\Delta t-$	$\Delta t+$	Magnitude	Filter
106.6	4.9	5.1	$18.23^{+0.18}_{-0.16}$	<i>white</i>	4281	49	49	> 20.39	<i>u</i>
126.6	4.9	5.1	$17.97^{+0.15}_{-0.13}$	<i>white</i>	5713	49	49	> 20.22	<i>u</i>
151.6	7.3	7.7	$18.06^{+0.13}_{-0.12}$	<i>white</i>	15799	224	227	> 21.89	<i>u</i>
181.5	7.3	7.6	$17.83^{+0.11}_{-0.10}$	<i>white</i>	22560	224	227	> 21.57	<i>u</i>
4690	49	49	$19.81^{+0.16}_{-0.14}$	<i>white</i>	29221	148	149	> 20.19	<i>u</i>
6122	49	49	$20.14^{+0.31}_{-0.24}$	<i>white</i>	43093	1831	1913	> 22.68	<i>u</i>
17560	193	195	$20.90^{+0.30}_{-0.23}$	<i>white</i>	60462	1843	1901	> 21.79	<i>u</i>
85.7	7.6	8.4	17.72 ± 0.66	<i>v</i>	4077	49	49	> 19.87	<i>uvw1</i>
220	9	9	$16.66^{+0.16}_{-0.14}$	<i>v</i>	5509	49	49	> 19.27	<i>uvw1</i>
263	12	13	$16.69^{+0.14}_{-0.12}$	<i>v</i>	11768	191	194	> 19.92	<i>uvw1</i>
318	15	15	$16.37^{+0.10}_{-0.09}$	<i>v</i>	21645	220	222	> 21.54	<i>uvw1</i>
383	17	18	$16.67^{+0.12}_{-0.11}$	<i>v</i>	28460	220	222	> 20.90	<i>uvw1</i>
463	22	23	$16.45^{+0.10}_{-0.09}$	<i>v</i>	42229	1852	1937	> 21.28	<i>uvw1</i>
551	21	22	$16.60^{+0.12}_{-0.10}$	<i>v</i>	59599	1864	1925	> 22.37	<i>uvw1</i>
5100	49	49	$18.45^{+0.22}_{-0.18}$	<i>v</i>	73712	221	221	> 21.22	<i>uvw1</i>
10013	223	228	$19.33^{+0.14}_{-0.13}$	<i>v</i>	3872	49	49	> 21.95	<i>uvm2</i>
34052	225	226	> 20.57	<i>v</i>	5304	49	49	> 21.85	<i>uvm2</i>
51412	225	226	> 20.58	<i>v</i>	10916	219	223	> 21.58	<i>uvm2</i>
68768	225	226	> 20.53	<i>v</i>	27553	220	222	> 20.93	<i>uvm2</i>
116954	8680	8845	> 21.40	<i>v</i>	34905	195	196	> 21.36	<i>uvm2</i>
184147	3318	3379	> 21.32	<i>v</i>	48416	2051	2142	> 22.44	<i>uvm2</i>
4486	49	49	$20.10^{+0.27}_{-0.22}$	<i>b</i>	65785	2063	2130	> 21.52	<i>uvm2</i>
5918	49	49	$20.20^{+0.41}_{-0.30}$	<i>b</i>	4895	48	49	> 20.19	<i>uvw2</i>
16711	224	227	$21.06^{+0.30}_{-0.24}$	<i>b</i>	6304	37	37	> 20.18	<i>uvw2</i>
23377	177	179	$21.27^{+0.65}_{-0.40}$	<i>b</i>	33138	221	222	> 21.59	<i>uvw2</i>
40696	197	198	> 21.02	<i>b</i>	50495	220	221	> 21.24	<i>uvw2</i>
58053	395	396	> 20.98	<i>b</i>	67853	221	222	> 22.16	<i>uvw2</i>

The sky is sampled by 36 additional fibers, distributed in 6 bundles of 6 fibers each, located following a circular distribution at $\sim 90''$ from the center and at the edges of the central hexagon. The sky-fibers are distributed among the science ones in the pseudo-slit, in order to have a good sampling of the sky. The remaining 15 fibers are used for calibration purposes.

Given that PMAS/PPak has a filling factor less than 1, during the observations a dithering scheme was applied. The observations consisted of 9 single exposures of 15 min each, i.e. 3 images for every dither pointing. As 3 of the 9 exposures had a low S/N due to the presence of clouds, only six of them were considered. Figure 3.4 shows the average of the second dither pointing images, when the magnitude of the afterglow was about $R_C=19.5$. The field of view is sampled into discrete spatial elements named SPAXELs.

The data reduction was performed twice using two different softwares: PPAK_online,

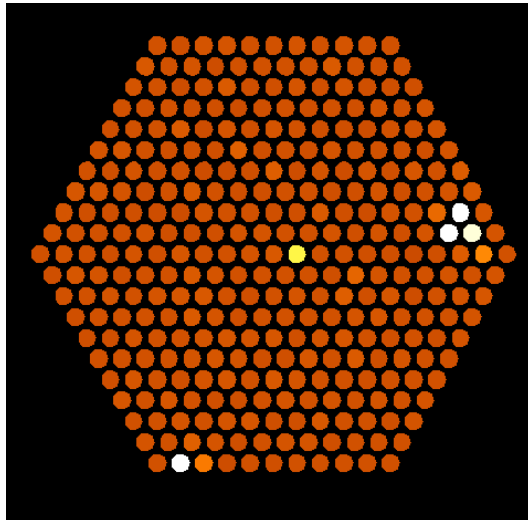


Figure 3.4: *The field of GRB 060605 seen by the PPAk spaxels. The image is the average of three exposures when the afterglow (the yellow spot in the middle) had a magnitude of about $R_C=19.5$. The other bright spaxels are stars (see Fig. 3.3).*

which is part of P3D¹⁰ (Becker 2002), and R3D¹¹ (Sánchez & Cardiel 2005; Sánchez 2006). In combination with the previous ones, IRAF, MIDAS and the E3D¹² visualization tool (Sánchez 2004) were used. The results obtained using the two packages were consistent.

The reduction of spectroscopic data obtained with fiber-based integral-field units consists of the following standard steps: bias subtraction, flat field correction, location of the spectra on the CCD (the so-called tracing), spectra extraction, wavelength calibration, fiber flat correction, sky subtraction, cosmic ray rejection and flux calibration.

The bias frame, obtained immediately after the target frame, was cleaned and smoothed using boxsizes of 5 pixels in x and y to create the final bias frame. Domeflat exposures of 5 s were taken before and after the object observations to produce a trace mask, i.e. to locate the spectra along the cross-dispersion direction on the CCD (for a detailed description of tracing, see Becker 2002). Once this mask is defined one can easily extract the spectra from the CCD, producing a so-called row-stacked-spectra image, where one row represents one spectrum.

For wavelength calibration a combined He/Rb-emission lamp exposure of 15 s was obtained at the beginning of the night with the additional illumination of 15 separate calibration fibers with ThAr. Simultaneous ThAr-exposures of these calibration fibers during lamp flat and object observations as well were used to correct for flexure effects of the instrument (Kelz et al. 2006). We defined some (at least two) of the ThAr spots in the lamp flat image as reference and calculated their shifts in x and y versus the same ThAr spots in the object images. These shift values were taken into account during tracing, spectra extraction, and wavelength calibration as well.

For the sky subtraction the spaxels not contaminated by sources were selected and the average extracted spectrum was then subtracted from the science spectrum. For this purpose we used the E3D package (Sánchez 2004).

After cosmic ray rejection, the final spectrum was flux calibrated using the spectrophoto-

¹⁰A package of IDL routines developed for the reduction of PMAS data.

¹¹<http://www.caha.es/sanchez/r3d/index.html>

¹²<http://www.aip.de/Euro3D/E3D/#Docu>

metric standard star Hz 44 (Oke 1990). As the spectra of the optical afterglow were extracted on one spaxel, the spectra of the standard star were extracted in the same way. A cross check on the flux calibration was performed using the observed R_C -band photometric magnitude.

Chapter 4

Identifying the GRB progenitors

As I have already outlined in Chapter 1, among the three bursts studied, GRB 060218 developed a bright GRB-SN. On the other hand, GRB 050813 was a short burst where we could only set an upper limit on any rising SN component and GRB 060605 was at too high redshift in order to detect any SN bump in the afterglow light.

4.1 GRB 060218 – a collapsar

The burst 060218 turned out to develop the second brightest GRB-SN ever seen since 1998, the year of the discovery of the first GRB-SN (SN 1998bw; Galama et al. 1998). It was in detail studied by several groups, and our group contributed a substantial work to understand this event. In particular, it was in our work where this GRB-SN was in detail compared to all GRB-SNe known at that time (Ferrero et al. 2006) and where the spectral evolution of the SN was in detail investigated (Pian et al. 2006). The first paper is still an up-to-date reference for an observational summary of GRB-SNe.

4.1.1 The supernova light curve

We followed previous works (Zeh et al. 2004, 2005) and modeled the light curve of SN2006aj using SN 1998bw as a template (Galama et al. 1998) that was shifted to the corresponding redshift¹ and scaled in luminosity (in the SN rest frame) by a stretch factor k and in time evolution by a factor s , while zero host extinction was assumed for SN 1998bw (Patat et al. 2001). In doing so, we found an additional component visible in the early data that makes the light curve systematically brighter than that of SN 1998bw. This component has also been noted by Mirabal et al. (2006). Furthermore, strong spectral evolution is noticeable, with the flux excess being stronger toward shorter wavelengths. The most reasonable explanation for this additional blue component is the light due to shock break-out through a dense progenitor wind (Campana et al. 2006). However, we note that at least part of this additional component may be the result of an intrinsically different (as compared to SN 1998bw) early SN light

¹Here and in the following, the adopted world model is always a closed universe with a Hubble constant $H_0 = 71 \text{ km s}^{-1} \text{ Mpc}^{-1}$, a matter density $\Omega_M = 0.27$, and a cosmological constant $\Omega_\Lambda = 0.73$. For $z=0.033$ this yields a distance modulus of 35.78 mag. For the flux density of the afterglow the usual convention $F_\nu(t) \propto t^{-\alpha} \nu^{-\beta}$ is used (see also Sec. 2.3.3).

curve. SN 2002ap was also overluminous at early times in comparison to SN 1998bw, and has been compared, both photometrically and spectroscopically, with SN 2006aj (e.g., Pian et al. 2006). But the early multi-color evolution of SN 2002ap was achromatic, showing no evidence for strong spectral evolution as seen in SN 2006aj.

We thus used two different methods to fit the SN light curve. In the first fit, we excluded all data earlier than 8.8 days, but fitted only the SN 1998bw model light curve to the data, without any additional contributions. The result is shown in Fig. 4.1. The early excess blue flux is clearly visible in the residuals. The data after 8.8 days are matched very well by the SN 1998bw model. Note that for typical GRB-SNe we also fit only the peak and decaying part of the SN, as the early flux is typically dominated by the GRB afterglow.

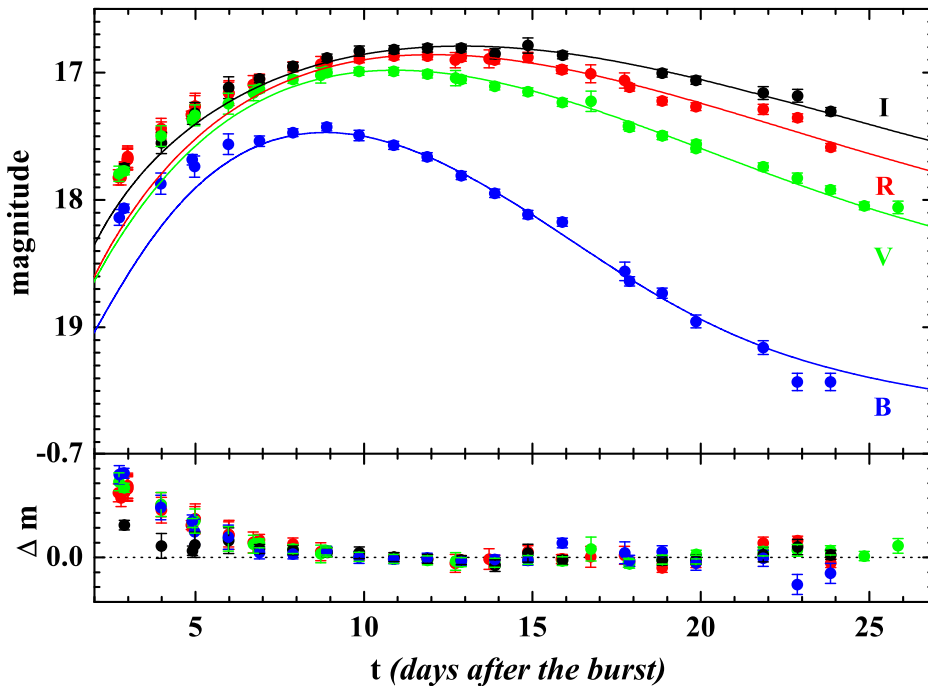


Figure 4.1: The light curves of SN 2006aj based on our *BVRI* data after correcting for extinction and host flux contribution. The data were fitted using the light curves of SN 1998bw as a template, not considering data from SN 2006aj that was taken before 8.8 days post burst. The residuals Δm represent observed values minus the fit.

In the second fit, we assumed that an additional component the afterglow decays according to a power-law, with the decay index α ($F_\nu \propto t^{-\alpha}$) being a free parameter of the fit, and independent for each band (Fig. 4.2). The derived values of the luminosity ratio k and the stretch factor s as well as the decay index α are given in Table 4.1. It is apparent that while the results derived from the two methods are similar, they do in fact differ by as much as 10% (in k). The additional component improves the quality of the fit in all bands. The steeper decay at shorter wavelengths is also in agreement with the *Swift* UVOT photometry of the blue shock break-out (Campana et al. 2006). The strong wavelength dependence of the decay (Table 4.1) argues against this component being the optical afterglow of the GRB. On the other hand, the very shallow decay in *VRI* indicates that the time evolution of the SED of this additional component is probably more complex than a simple decay according to a pure

power-law, as assumed in our analysis.

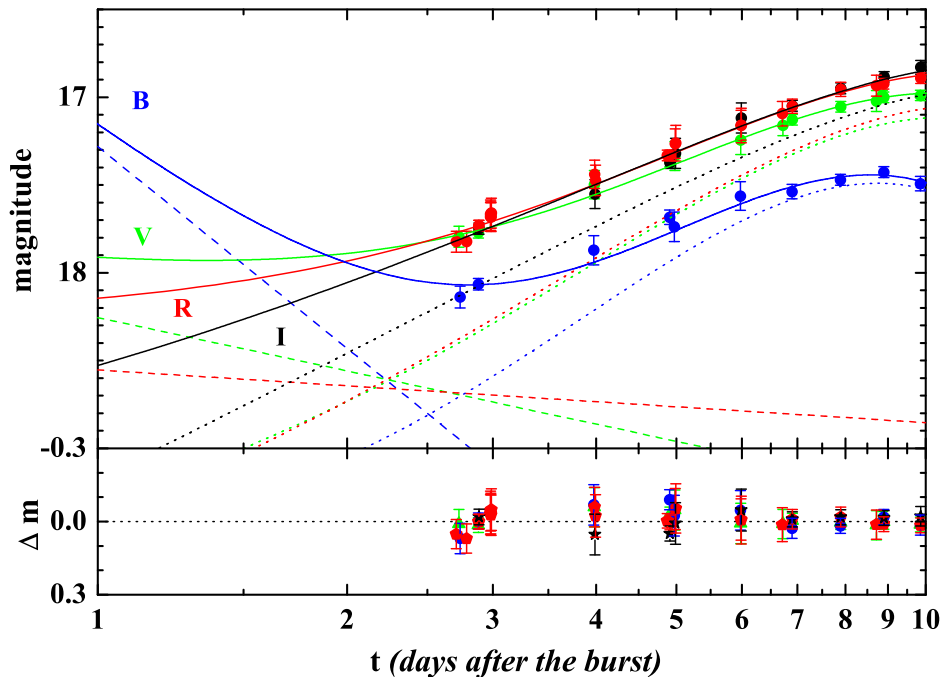


Figure 4.2: The light curves of SN 2006aj fitted by including an additional early component which decays according to a power-law. Solid lines mark the fit, the dashed lines are the power-law component and the dotted lines are the SN component. The time scale is logarithmic to show in detail the earlier data.

Table 4.1: Fitting results for the light curves of SN 2006aj attained by either excluding early data (top) or including an additional power-law component decaying with index α (see text for details).

	$\chi^2/\text{d.o.f}$	k	s	α
<i>B</i>	1.83	0.734 ± 0.014	0.620 ± 0.006	...
<i>V</i>	1.02	0.724 ± 0.007	0.682 ± 0.005	...
<i>R</i>	1.93	0.735 ± 0.007	0.689 ± 0.006	...
<i>I</i>	0.71	0.761 ± 0.008	0.686 ± 0.008	...
<i>B</i>	1.79	0.721 ± 0.022	0.613 ± 0.005	1.53 ± 0.43
<i>V</i>	0.35	0.640 ± 0.014	0.659 ± 0.008	0.40 ± 0.09
<i>R</i>	0.94	0.621 ± 0.022	0.656 ± 0.012	0.12 ± 0.10
<i>I</i>	0.48	0.667 ± 0.039	0.663 ± 0.022	-0.10 ± 0.34

The small value of the stretch factor s means that SN 2006aj evolved much faster than SN 1998bw (see also Cobb et al. 2006; Mirabal et al. 2006; Modjaz et al. 2006; Pian et al. 2006; Soderberg et al. 2006b; Sollerman et al. 2006). Furthermore, SN 2006aj had a slightly different color than SN 1998bw, being brighter in the *B* and *I* band than in the *V* and *R* band. The k values we obtained are also in accordance with the values found by the authors cited above. In all bands, SN 2006aj was about 30% less luminous than SN 1998bw. From the light curve data, independent of any fit, we found the following peak absolute magnitudes of the SN: $M_B = -18.29 \pm 0.05$, $M_V = -18.76 \pm 0.05$, $M_R = -18.89 \pm 0.05$, $M_I = -18.95 \pm 0.10$.

Table 4.2: *Luminosity ratio k and stretch factor s for GRB-SNe with known redshift normalized to SN 1998bw before and after correcting for host extinction. In cases where no extinction could be derived, only the non-corrected values are given. In all cases the SN fits were derived in the observer R -band frame. This list is complete up to the end of 2005, with the exception of GRB 040924 (Soderberg et al. 2006c). These results supersede those presented in Zeh et al. (2005). Differences compared to Zeh et al. (2005) are basically due to the inclusion of new observational data or a revision of the used value for the Galactic extinction along the line of sight. Furthermore, note that we use different cosmological parameters than those in Zeh et al. (2004, 2005).*

GRB/XRF/SN	k	s	k (corrected)
970228	0.40 ± 0.29	1.45 ± 0.95	...
990712	0.35 ± 0.09	0.83 ± 0.13	...
991208	0.93 ± 0.25	1.12 ± 0.20	$2.62^{+1.10}_{-0.65}$
000911	0.63 ± 0.29	1.40 ± 0.32	$0.85^{+0.44}_{-0.26}$
010921	0.68 ± 0.43	0.69 ± 0.25	$1.85^{+2.82}_{-0.79}$
011121/2001ke	0.59 ± 0.02	0.80 ± 0.02	$0.88^{+0.08}_{-0.07}$
020405	0.74 ± 0.05	0.97 ± 0.07	$0.90^{+0.15}_{-0.11}$
020903	0.62 ± 0.09	0.92 ± 0.08	...
021211/2002lt	0.40 ± 0.19	0.98 ± 0.26	...
030329/2003dh	1.06 ± 0.11	0.85 ± 0.10	$1.50^{+0.19}_{-0.16}$
031203/2003lw	0.67 ± 0.05	1.09 ± 0.07	$1.28^{+0.18}_{-0.16}$
041006	0.90 ± 0.05	1.38 ± 0.06	$1.03^{+0.22}_{-0.09}$
050525A/2005nc	0.49 ± 0.04	0.77 ± 0.04	$0.66^{+0.10}_{-0.08}$

4.1.2 Comparison to other GRB-supernovae

In order to place SN 2006aj in the context of the presently known GRB-SNe, we started with the results presented in Zeh et al. (2004, 2005), updated them in cases where new data were available, and corrected the k value using host-galaxy extinctions derived in Kann et al. (2006), including uncertainties. We added two further GRB-SNe to the sample. The result for XRF 020903 is based on data from Bersier et al. (2006). We found that the SN of this event was also superimposed on an underlying power-law afterglow component. Unfortunately, the afterglow data are too sparse to derive any conclusions on the extinction in the host galaxy. For GRB 031203, we used the extinction derived by Mazzali et al. (2006b). In the case of GRB 050525A, we employed the data presented by Della Valle et al. (2006b) and applied the extinction found by Blustin et al. (2006). In those cases where no extinction could be found in Kann et al. (2006), we only present the observed values and note that these are lower limits on the luminosity of the SNe (Table 4.2). On the other hand, the line of sight extinction is often low and the true values are thus not expected to be much higher.

SN 2006aj was a rare nearby GRB-SN, with a distance of only about 140 Mpc. Its luminosity was about 70% of that of SN 1998bw, confirming that GRB-selected supernovae may not qualify for the label “standard candle”. Given the UVES data of SN 2006aj, taken close to SN maximum light (Guenther et al. 2006; Wiersema et al. 2007), it is unlikely that the deficiency in luminosity is the result of dust extinction in the host galaxy of SN 2006aj.

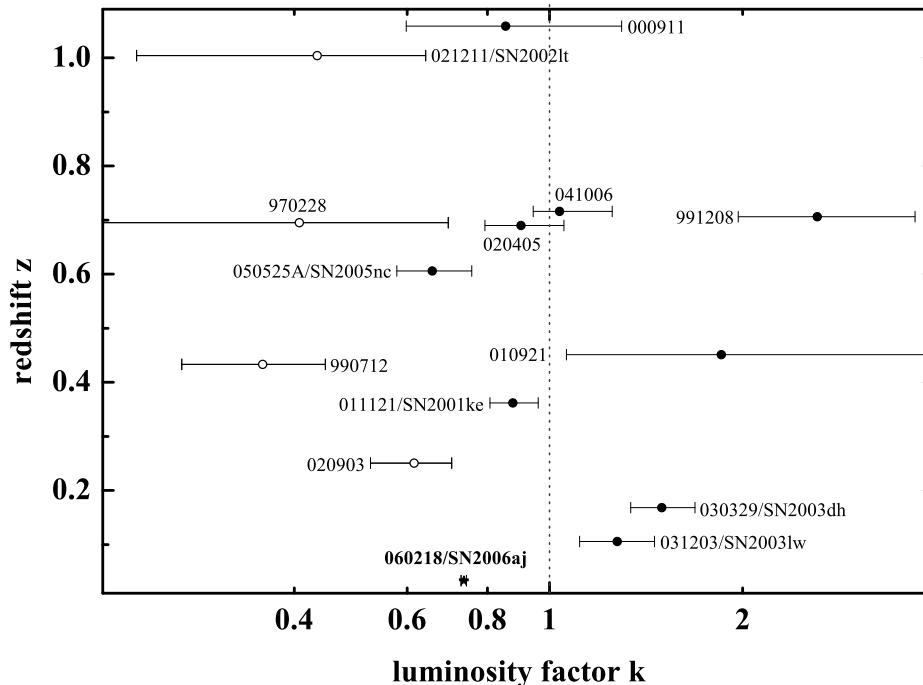


Figure 4.3: *The distribution of the luminosity factor k in the R band with redshift z . There is no apparent correlation with redshift, even though we caution that all the k values refer to the R band in the observer frame, corresponding to different wavelengths in the host frame. Filled symbols mark the k values that have been corrected for host extinction, open symbols represent supernovae for which this correction could not be applied. A star marks the value derived from the R -band light curve of SN 2006aj by removing data before 8.8 days from the fit. SN 1998bw is at $k = 1$, by definition.*

By the end of 2005, there were 14 optical afterglows²³ with known redshifts that showed evidence for extra light in the R band at late times (GRBs 970228, 990712, 991208, 000911, 010921, 011121, 020405, 021211, 030329, 031203, 040924⁴, 041006, 050525A, XRF 020903). For eight afterglows with a known SN bump (GRBs 991208, 000911, 010921, 011121, 020405, 021211, 030329, 041006) Kann et al. (2006) were able to derive a host extinction value. We used these to determine the extinction-corrected luminosities of these SNe in the observer frame (Fig. 4.3). It turned out that only two (030329, 031203) or perhaps three (including 991208) of the 14 SNe were actually more luminous than SN 1998bw with high significance (but see, e.g., Deng et al. 2005, for a spectroscopic modeling of SN 2003dh that results in $k < 1$). Remarkably, most extinction corrected SNe cluster around $0.6 < k < 1.5$. We found that the four SNe not corrected for extinction (GRBs 970228, 990712, 020903, 021211) are typically fainter, implying that a correction for host galaxy extinction will probably also shift them into this range. While one might worry about the fact that for each individual GRB-SN, due to the different redshifts, the k factor refers to a different wavelength region, SN 2006aj does not contradict our assumption that k is not strongly dependent on wavelength (Fig. 4.4).

²Compared to Zeh et al. (2004, 2005), GRB 980703 has been removed as we now have reason to doubt the identification of a SN bump.

³This number has not substantially changed by the end of 2008.

⁴This event is not included in our study as sufficient photometry has not been published yet.

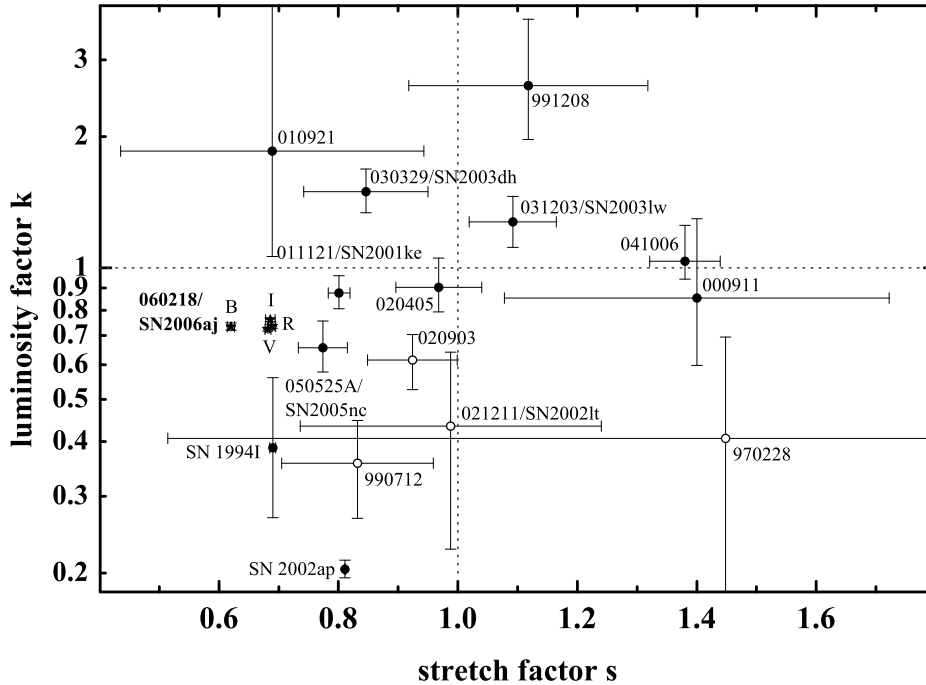


Figure 4.4: Luminosity factor k versus stretch factor s in the R band for all GRB-SNe in our sample (Table 4.2). The symbols are identical to those used in Fig. 4.3. SN 1998bw defines $k = 1$, $s = 1$. Note that in the case of SN 2006aj the values for $BVRI$ are plotted. Furthermore, we plot the Type Ic supernova SN 1994I and the Type Ic broad-lined SN Ic SN 2002ap, neither of which are associated with GRBs. Both are fainter than any GRB-SN in our sample for which the host extinction has been corrected.

Obviously, the present data, even though some have large uncertainties, indicate that the width of the GRB-SN luminosity function is at least 2 mag, comparable to what is known for the other types of SNe (cf. Richardson et al. 2002, 2006). In particular, there is no evidence that the luminosity function evolves with redshift: the width of the luminosity function for $z < 0.2$ is comparable to the width at $z \approx 0.7$. It is also much narrower than the distribution of intrinsic afterglow luminosities (Kann et al. 2006).

4.1.3 Comparison to other local stripped-envelope supernovae

It is also interesting to compare the light curve properties of SN 2006aj and other GRB-SNe with well-studied local stripped-envelope (i.e. types Ib, Ic, IIb) supernovae, as is shown in Fig. 4.5. Distance moduli and absolute magnitudes for these SNe were taken from Richardson et al. (2006) (who use $H_0 = 60 \text{ km s}^{-1} \text{ Mpc}^{-1}$) and have been transformed to the world model used here ($H_0 = 71 \text{ km s}^{-1} \text{ Mpc}^{-1}$) by adding $-5 \log 71/60 = -0.365$ mag to the former and $+0.365$ mag to the latter values. Similarly, for the world model used here SN 1998bw is 0.19 mag less luminous than given in Galama et al. (1998), who use $H_0 = 65 \text{ km s}^{-1} \text{ Mpc}^{-1}$, i.e. $k=1$ corresponds to $M_V = -19.16$. The absolute visual magnitudes of the GRB-SNe in our sample were then calculated according to $M_V^{GRB-SN} - M_V^{98bw} = -2.5 \log k$, assuming that k is independent of wavelength. Figure 4.5 shows the result obtained in this way. Most notable is that the ensemble of GRB-SNe is at the bright end of the luminosities of local stripped-

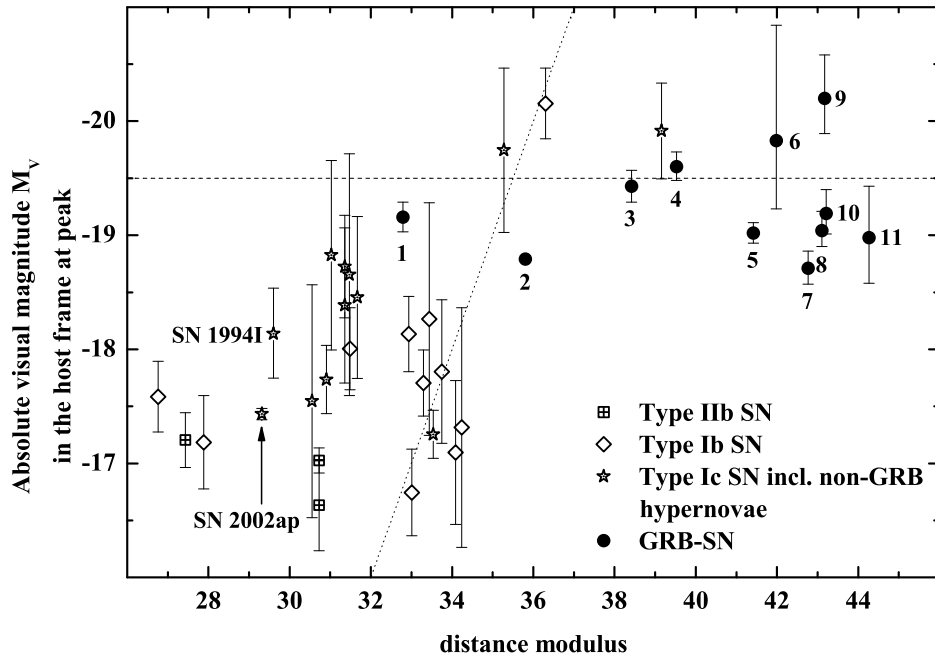


Figure 4.5: The absolute V -band magnitude M_V of stripped-envelope supernovae versus their distance modulus. This is an expanded version of Figure 1 in Richardson et al. (2006), and the values for SN of Type IIb, Ib and Ic have been taken from that work but transformed according to the world model used here. The individual GRB-SNe have the same numbers as in Fig. 4.6. We have also labeled two local Type Ic SNe we have included in our study (Fig. 4.4). GRB-SNe without known host extinction are not included. The dashed line at $M_V = -19.5$ denotes the typical absolute magnitude of Type Ia SNe (the “ridgeline”). The slanted dotted line denotes a constant visual magnitude $m_V = 16$ in the case of no extinction.

envelope supernovae. In other words, the present data indicate that Type Ic supernovae with associated (detected) GRBs are on average more luminous in the optical bands than those without detected GRBs. In particular, SN 2006aj is no exception from this rule. Note, however, that our assumption of wavelength-independence of k could be an oversimplification. The larger the redshift, the more uncertain is the absolute V -band magnitude of a GRB-SN derived in this way. This uncertainty is not included in the error bars plotted in Fig. 4.5.

Finally, note that an observational bias might affect the interpretation of Fig. 4.5: the larger the redshift, the more difficult it is to observe less luminous stripped-envelope supernovae.

Richardson et al. (2006) give host extinction values for all 27 events in their sample. Therefore, we investigated whether host extinction of GRB-SNe is different from those of local stripped-envelope supernovae. No substantial differences are apparent (Fig. 4.6). While it is interesting that SN 2006aj is less affected by host extinction compared to the local sample of Type Ic SNe, the current sample is too small to draw reliable conclusions from this finding.

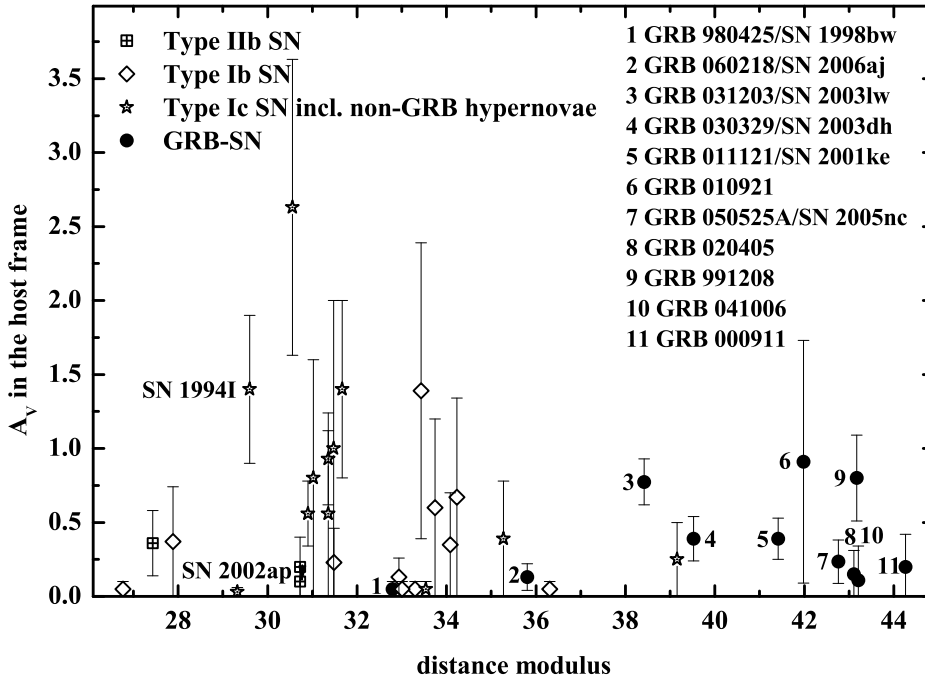


Figure 4.6: The visual host-galaxy extinction A_V (in the host frame) of stripped-envelope supernovae versus their distance modulus. The values for SNe of Type IIb, Ib and Ic have been taken from Richardson et al. (2006), while the data for the GRB-SNe are from Kann et al. (2006). We labeled individual GRB-SNe and the two Type Ic SNe we have also studied. GRB-SNe without known host extinction were not included.

4.1.4 The stretch factor

A statistics of the stretch factor s is in some sense more reliable since it is not affected by the extinction issue. First of all, among all known GRB-SNe, SN 2006aj has the smallest s value, i.e. it was the fastest GRB-SN ever seen (Mazzali et al. 2006a; Modjaz et al. 2006; Pian et al. 2006). Interestingly, about half of the GRB-SNe have $s < 1$, i.e., they were evolving faster than SN 1998bw. In contrast, the evolution of the SN associated with GRB 041006 was very slow (Fig. 4.4) with high significance (Stanek et al. 2005). Basically only two SNe (000911, 970228) occupy the ($k < 1$, $s > 1$) region, i.e., they were slow and subluminous, contrary to the general trend, but both have large error bars. Stanek et al. (2005) noted that for GRB-SNe a relation may exist between light curve shape and luminosity, similar to the one established for Type Ia SNe (see Figure 3 in Stanek et al. 2005). Fig. 4.4 neither supports nor contradicts the existence of such a potential relation. While a trend of rising k with rising s seems to be visible, a fit to the data does not support this trend with reasonable statistical significance.

It should be stressed, however, that the procedure applied here has shortcomings that are basically related to cosmological effects on one hand and to data quality on the other.

As long as one is only concerned with broad-band photometry, which is the case in this study, the observed light curves of GRB-SNe usually refer to different wavelength bands in their host frames. However, for SN 1998bw it has been shown that the light curve shape, the time of the peak flux, and the peak flux itself were a function of wavelength (as is the case

for other SN types, too). Unfortunately, the available photometric data base is in most cases restricted to R -band observations (in the observer frame). In order to be able to compare light curves of GRB-SNe that occurred at various redshifts with light curves of SN 1998bw, the simplest and in some sense only useful approach is then to assume that the luminosity ratio k and the stretch factor s , which are both normalized to SN 1998bw, are independent of wavelength. In other words, we assume that the SED of all GRB-SNe (in their host frame) is the same at all times.

In addition, the data base used for our light curve fits is usually weighted to data obtained past the peak time of a GRB-SN under consideration. The reason is that before the peak time usually the afterglow dominates the light of the optical transient, while after the peak time usually the SN light dominates. This problem is difficult to overcome. Therefore, for basically all cosmologically remote SNe we have no information about the details of the SN light curves at early times up to several days after the corresponding burst. In particular the stretch factor s is then mainly affected by the late-time behaviour of the SN light curves.

It is therefore by no means clear if a relation between s and k indeed exists. It is possible that such a relation is hidden by the relatively large error bars for individual (k, s) values of the GRB-SNe on the one hand (Fig. 4.4) and by the basic assumptions that went into the procedure we applied here on the other hand. More spectral data from GRB-SNe might finally solve this issue. However, progress made in this regard during the last years was only modest, at best. Most *Swift* detected GRBs are at such a high redshift that no SN spectroscopy can be performed with current telescopes within a reasonable amount of observing time. Therefore, the photometric approach utilized here derives some of its justification from these spectroscopic limitations.

Independent of these considerations, our photometric (Ferrero et al. 2006) and spectroscopic (Pian et al. 2006) data leave no doubt on the fact that the progenitor of GRB 060218 was a collapsing massive star (see also Mazzali et al. 2006a).

4.2 GRB 050813 – favouring a NS-NS merger

While GRB 050813 was a short burst, and no classical SN component was expected to be seen, the non-existence of such a component is still one of the strongest criteria to identify the nature of the progenitor. In the present case, based on theoretical grounds (see Nakar 2007), we expected that the GRB was most likely not due to a collapsar but due to a compact stellar merger. Therefore, it is of utmost importance to set constraints on any SN light following a short burst. In Kann et al. (2008) we discuss in detail the search for a mini-SN following a short burst, while here, given the available data set, we constrain the appearance of (classical) SN light peaking usually $(1+z)15..20$ days after the burst.

In the following, let us first start with the question: was GRB 050813 a short burst at all?

4.2.1 What is a short burst?

Short bursts, according to phenomenological classification introduced by Kouveliotou et al. (1993), are bursts whose T_{90} duration measured with BATSE was less than 2 sec. Even

though it has already been known in the 1990s that T_{90} is a function of energy (and of detector properties), this definition, because of its simplicity, has been widely used even in the *HETE-2* and in the *Swift* era. In principle, having now much more observational data at hand for individual bursts than in the BATSE era, this phenomenological definition/classification scheme calls for a more accurate, namely a physical classification scheme. This, however, is a difficult task that is not yet solved in a satisfactory manner.

The observed bimodality in the T_{90} distribution of all BATSE bursts clearly showed that there are two kinds of bursters. It can be fitted very well by two overlapping Gaussian functions, suggesting that there are two different populations of progenitors responsible for the emission of GRBs (for the potential existence of a third group see, e.g., Horváth et al. 2006). This statement however refers to the GRB ensemble as a whole. Difficulties arise if one wants to classify an individual burst, because both Gaussian functions overlap.

In the *Swift* era, the observational situation has improved a lot. First at all, given that this is a different satellite/detector, any statistics of the GRB duration distribution has to be established again based on *Swift* bursts alone and it has to be checked at which duration T_{90} the two fitted Gaussians overlap.

However, *Swift* has shown that the observational situation is much more complex, too. For example, some bursts have long soft tails extending over several hundred seconds after the trigger while starting with a short spike (e.g., GRB 061006; Krimm et al. 2006). The question is, can we find any observational parameters that tell us exactly for any individual burst whether it was a member of the long or of the short burst class? In a more accurate and much more physical way, the question is (see also Zhang 2006): Which criteria apply for the GRBs and their follow-up phenomena if the burster was a collapsing single star or a compact merger event? Fortunately, the former does indeed provide us with a clear signal, namely the appearance of a SN 1998bw-like component in the GRB afterglow. Any such bright component rules out a merger event according to our present understanding of mergers of compact stars. Similarly, any GRB originating in an early-type galaxy cannot, according to our present understanding of ellipticals, be related to the collapse of a single massive star because there is no ongoing star-formation in elliptical galaxies anymore (at least at low redshifts). Unfortunately, these two are the only clearly observationally founded criteria so far that can help to classify an individual burst unambiguously with respect to the nature of its progenitor. If no SN is seen following a GRB then the burst can still be due to the collapse of a single star, but then for sure something was very different in the collapse compared to the progenitors of the other GRB-SNe known so far (e.g., GRB 060614: Della Valle et al. 2006a; Fynbo et al. 2006; Gal-Yam et al. 2006; Gehrels et al. 2006). On the other hand, the non-detectability of a SN component does not automatically imply that the burst was due to a merger event. In a same way, merger events can also occur in late-type spirals. So, if any GRB originates in a late-type spiral it cannot be classified based on the nature of the underlying host galaxy alone.

It is clear that the classification of individual bursts with respect to the nature of their progenitor is difficult. Recent investigations tackle this problem and have led to the suggestion of much more than just one criterium in order to classify a GRB (Donaghy et al. 2006; Norris & Bonnell 2006). As long as no consensus has been reached in the literature what the ultimate criteria are for a burst to be classified as being due to a merger event, in several cases only

arguments can be provided that favor one scenario for the other (merger vs. collapse). The detection or non-detection of a SN signal plays a key role in this approach but has come into question recently (see Della Valle et al. 2006a; Fynbo et al. 2006; Gal-Yam et al. 2006; Gehrels et al. 2006; Zhang 2006). This leaves the nature of the host galaxy as the strongest argument to detect a GRB due to a merger event, namely if the host is an elliptical galaxy. But the potentially broad range in merger times and hence distances of the merger events from their host galaxies (cf. Belczynski et al. 2006) might also call into question the application of this criterium. GRB 050813 belongs to those bursts that demonstrate all these problems in detail.

4.2.2 Upper limits on a rising supernova component

Our two FORS2 observing runs were arranged such that they would allow us to search for a fading (afterglow) as well as for a rising (supernova) component following GRB 050813, supposing $z=0.72$ ⁵. Initially we searched for a transient isolated point source in the original 10 arcsec XRT error circle, but we did not find one. The fact that the sources #2, #5 and #6 (Fig. 3.1; Table 3.3) are not detected in the combined image of the first VLT/FORS2 observing run might be due to the presence of the Moon, causing an enhanced sky background level. During the second FORS2 run the sky background was much lower and the seeing even better than during the first observing run. We conclude that any well-isolated afterglow or supernova in this field was fainter than the magnitude limits at the time of the two FORS2 observing runs, $I=25.1$ and 25.5 , respectively.

One of the main observational characteristics of a short burst should be the absence of a SN component in the late-time afterglow, as the merger is not expected to result in the kind of radioactivity-powered optical display typical for thermonuclear (Type Ia) and core-collapse (Types II and Ib/c) supernovae. However, mergers may have sub-relativistic explosions with low amount of ejected mass (Li & Paczyński 1998; Kulkarni 2005), but they should have a small luminosity. In agreement with these expectations, strong upper limits could be set so far on any potential SN component accompanying short bursts (cf. Hjorth et al. 2005a; Fox et al. 2005).

The constraints we can place on a rising SN component for GRB 050813 are less severe, given the potentially relatively high redshift of this burst. For the cosmological parameters employed here, SN 1998bw (Galama et al. 1998) redshifted to $z=0.72$ would have magnitudes of $I=24.7$ and $I=23.9$ during our first and second VLT/FORS observing run, respectively, after taking into account a Galactic reddening of $E(B - V)=0.056$ mag (Schlegel et al. 1998) in the direction of GRB 050813. At that brightness level we would have detected the SN if not superimposed on a much brighter host or strongly extinguished by dust. More precisely, we conclude that at the time of our second FORS2 observation any supernova following GRB 050813 was at least about 1.5 mag less luminous than SN 1998bw. While constraints placed on any SN component underlying the afterglow of e.g. GRB 050509B (Hjorth et al. 2005a) and GRB 050709 (Fox et al. 2005; Covino et al. 2006) are much stronger, this makes a potential SN component following GRB 050813 already fainter than any of the 11 GRB-SNe

⁵The adopted world model for this redshift gives a distance modulus of 43.22 mag. The luminosity distance is 1.36×10^{28} cm and 1 arcsec corresponds to 7.23 kpc. If $z=1.8$, the corresponding numbers are 45.7 mag, 4.26×10^{28} cm, and 8.55 kpc.

of long bursts known to date (Ferrero et al. 2006, their Figure 6).

On the other hand, we would have been able to detect (at 3σ) a rising SN component superimposed on the bright galaxy E (Fig. 3.1) only if its I -band magnitude had been 23.5 at the time of the second FORS2 observation. In other words, a SN 1998bw-like component would be missed in this case. The same holds for a typical type Ia supernova (Krisciunas et al. 2003), which would have had $I=26.9$ and $I=25.4$ at the time of our first and second FORS2 observing run, respectively.

Based on these data we conclude: the lack of detection of a SN component following GRB 050813 strongly support the view that the progenitor of this event was not a collapsar.

4.3 The high- z GRB 060605

Due to its high redshift no SN bump was expected to be seen in the afterglow light curve of GRB 060605 and, even less likely was the possible spectroscopic verification of SN light. However, we still might get indirect evidence on the nature of the GRB progenitor via two observational signatures: (a) evidence for a wind profile as deduced from the $\alpha - \beta$ relations (see Sect. 2.3.3), and (b) the occurrence of multiple absorption line systems in the afterglow spectrum, which might be due to the (not fastly moving) interstellar medium (ISM) in the GRB host galaxy (at $z=3.78$) and the (rapidly expanding) stellar wind from the luminous GRB progenitor, the wind into which the GRB fireball expands.

Unfortunately, for this burst the $\alpha - \beta$ relations do not favour a wind profile but do instead point to an ISM profile (see Sect. 5.1.4). This is not unusual since indeed found in several cases (cf. Zeh et al. 2006). It might just indicate that, when the bright afterglow developed, the fireball shock front was already at a such large distance from the GRB progenitor that the surrounding medium was not shaped by the stellar wind anymore.

The second indicator on the nature of the GRB progenitor is at a first view more promising since evidence for two absorption line systems was indeed found by us for this burst in our PMAS/PPak data (see Sect. 6.3.1). Similar to the arguments presented in Klose et al. (2004), we might interpret this as evidence for a complex stellar wind from the GRB progenitor. However, it should be stressed that there is no general consensus in the literature about the nature of such absorption line systems found in GRB afterglows (see Sect. 6.3.1). So, we are left with the conclusion that in the case of GRB 060605 we cannot claim with certainty to have found strong observational signs on the nature of the GRB progenitor, even though according to our present understanding there might be no doubt that the progenitor of this long burst must have been a collapsar as well.

Chapter 5

Analysis of the afterglows

In this Chapter I present the analysis of the GRB afterglow data. While in the case of GRB 060605 the detection of the afterglow in all the bands has allowed us a deep study of the event, and given hints on the circumburst medium, for the other two burst a minor number of information has been derived. For GRB 050813 an upper limit on the magnitude of a possible optical afterglow component has been obtained. Finally, the brightness of SN 2006aj was higher than the afterglow one, has prevented us to see clearly the afterglow component and only an excess of blue light has been found in the early data (see Sect. 4.1.1).

5.1 GRB 060605: a detailed afterglow analysis

5.1.1 The X-ray afterglow

The X-ray afterglow of GRB 060605 was detected by *Swift* for more than 1 day after the trigger. When analyzing the data we rebinned them by taking 30 counts/bin in order to obtain a good S/N ratio. As already noted by Godet et al. (2006), the X-ray light curve (Fig. 5.1) consists of three segments which can be fitted with a smoothly double broken power-law. In doing so, we fixed the break smoothness parameter of the fitting equation (see Liang et al. 2008)¹ to -10 , 10 and 10 (for the method see Zeh et al. 2006) in the case of transition I to II and transition II to III, respectively. For the steep-to-shallow transition (I to II), we find a break time of 210 ± 30 s (0.0024 ± 0.0003 days), while the shallow-to-steep transition (II to III) took place at 7510 ± 410 s (0.0869 ± 0.0047 days) after the trigger. At the beginning, the afterglow decays with a slope of $\alpha_{\text{I}} = 2.19 \pm 0.42$, followed by $\alpha_{\text{II}} = 0.34 \pm 0.03$ during the shallow decay phase, and it continues to decay with $\alpha_{\text{III}} = 1.89 \pm 0.07$ ($\chi^2/\text{d.o.f.} = 55.5/42 = 1.32$). Within errors, these values are in agreement with the results reported by Godet et al. (2006).

After dividing the 0.3-6 keV² XRT spectrum, derived from PC data, in several spectra over small time intervals, as no spectral evolution was found, we took the overall spectrum between $t = 126$ s (0.0015 days) and $t = 7.4 \times 10^4$ s (0.8565 days) (Fig. 5.2). It is well fitted by an absorbed power-law with a spectral index $\beta_{\text{X}} = 1.06 \pm 0.16$ ($\chi^2/\text{d.o.f.} = 39.6/44 = 0.93$)

¹We realized that in their (Eq. 3) the $t_{b,2}$ has to be t_{jet} .

²The 0.3-10 keV XRT spectrum had no signal in the range 6-10 keV and for this reason only the first part was considered.

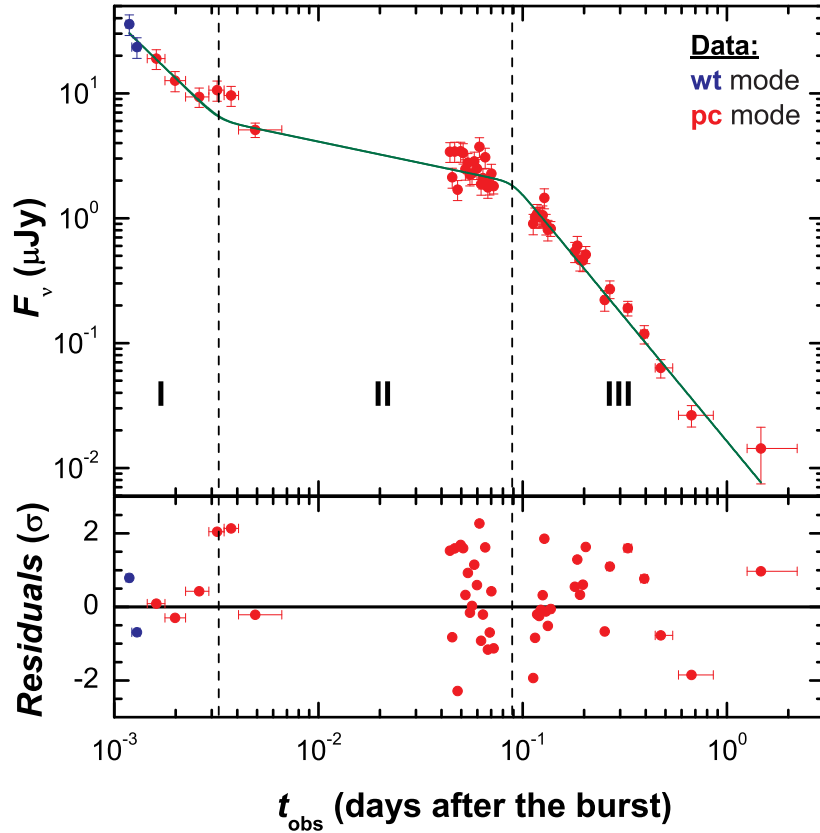


Figure 5.1: The X-ray light curve of the afterglow of GRB 060605 observed with Swift XRT (Evans et al. 2007). Formally, three power-law segments can be distinguished (Godet et al. 2006). A small flare is seen at the beginning of the second decay phase (II). The lower panel shows the residuals of the best fit. Fluctuations in the light curve ($> 2\sigma$) are mainly seen during the flare. The energy conversion factor is $4.6 \times 10^{-11} \text{ erg cm}^{-2} \text{ counts}^{-1}$.

and $N_{\text{H}} = 5.5_{-2.9}^{+3.3} \times 10^{20} \text{ cm}^{-2}$. Due to the big uncertainty this last value is consistent with both the Galactic hydrogen column density of $N_{\text{H}}^{\text{Gal}} = 5.1 \times 10^{20} \text{ cm}^{-2}$ by Dickey & Lockman (1990) and the lower value of $N_{\text{H}}^{\text{Gal}} = 4.1 \times 10^{20} \text{ cm}^{-2}$ given by the recent release of the Leiden/Argentine/Bonn Survey of Galactic HI (Kalberla et al. 2005). No additional rest frame hydrogen column density can be found in the X-ray spectrum. Adding such a component did not improve the fit. The lack of evidence for additional hydrogen in the host galaxy is in agreement with the finding of Grupe et al. (2007b) that high-redshift events usually do not show such a feature.

However, due to the large uncertainty on N_{H} (Ly α) and no strong constraints on N_{H} (X-ray), we cannot exclude that for GRB 060605 the optical and the X-ray data trace a different population of hydrogen at the redshift of the burst, as it has been found in many other cases (Watson et al. 2007).

5.1.2 The UV/optical light curve and its SED

We combined our UVOT data (Table 3.5) with further data reported in the GRB Coordinates Network Circulars (Rykoff & Schaefer 2006; Schaefer et al. 2006; Khamitov et al. 2006a,b;

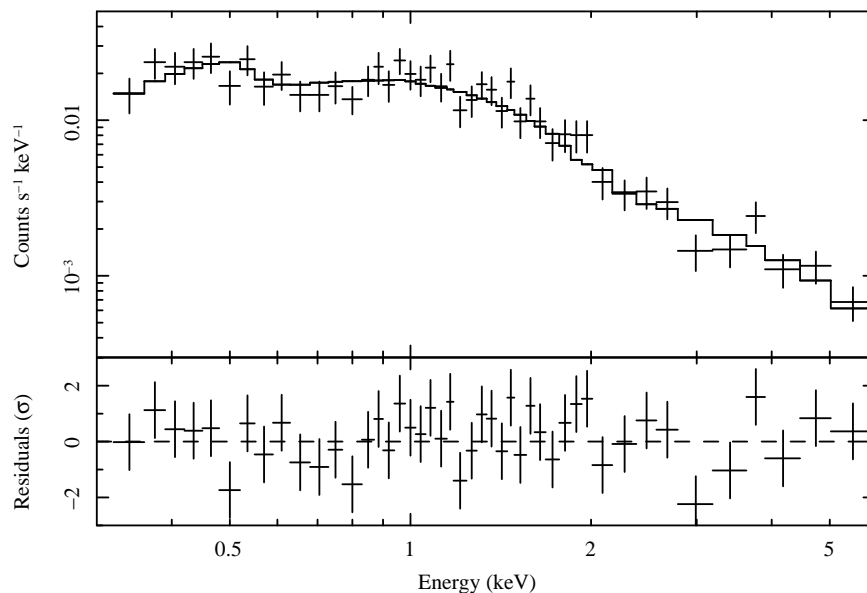


Figure 5.2: *X-ray spectrum of the afterglow of GRB 060605 obtained in photon counting mode between 0.0015 and 0.8565 days after the trigger. The lower panel shows the residuals of the best fit (for more details see Sect. 5.1.1).*

Malesani et al. 2006; Zhai et al. 2006; Karska & Garnavich 2006; Sharapov et al. 2006), all taken in the R_C filter, or unfiltered calibrated to the R_C band. Karska & Garnavich (2006) pointed out zero-point discrepancies between different USNO R_C magnitudes, and we can confirm that the magnitudes reported by Khamitov et al. (2006a) are about one magnitude fainter than what would be expected from the joint light curve (see below), whereas the late detection by Khamitov et al. (2006b) agrees well with the steep decay slope found by Karska & Garnavich (2006) and one additional point from Pozanenko et al. 2008, in preparation. We added an error of 0.1 magnitudes in quadrature to all GCN data points to account for the different filters and reference stars.

Using the R_C -band light curve as the most reliable template, and correcting all data for the foreground extinction of $E_{B-V} = 0.049$ (Schlegel et al. 1998), we derived colors for the UVOT detections. We found $v - R_C = 1.2 \pm 0.2$, $white - R_C = 2.3 \pm 0.2$, $b - R_C = 2.45 \pm 0.3$, $u - R_C > 3.3$, $uvw1 - R_C > 2.5$, $uvm2 - R_C > 4.5$, and $uvw2 - R_C > 2.5$. We note that, usually, *white* magnitudes are close in value to UVOT v -band values. Given the high redshift of the source, however, the large *white* – v color is due to the unfiltered UVOT bandpass being strongly affected by Lyman damping, making the afterglow much redder than usual (see below). We used the derived color indices to shift the UVOT detections (v , *white* and b) to the R_C -band and to construct a composite light curve (Fig. 5.3).

In the UV/optical bands the data are broadly consistent with an achromatic evolution, but we note that the data are sparse. We find an early rise, as reported by others (Schaefer et al. 2006; Zhai et al. 2006), which is followed by a “classical” broken power-law decay. Denoting the three slopes α_R (rise), α_1 and α_2 , we find $\alpha_R = -0.70 \pm 0.15$, $\alpha_1 = 0.89 \pm 0.04$ and $\alpha_2 = 2.58 \pm 0.15$. The break times are 0.0044 ± 0.0007 days for the break from rise to decay, and 0.27 ± 0.02 days for the second break. In both cases, we assumed that the host

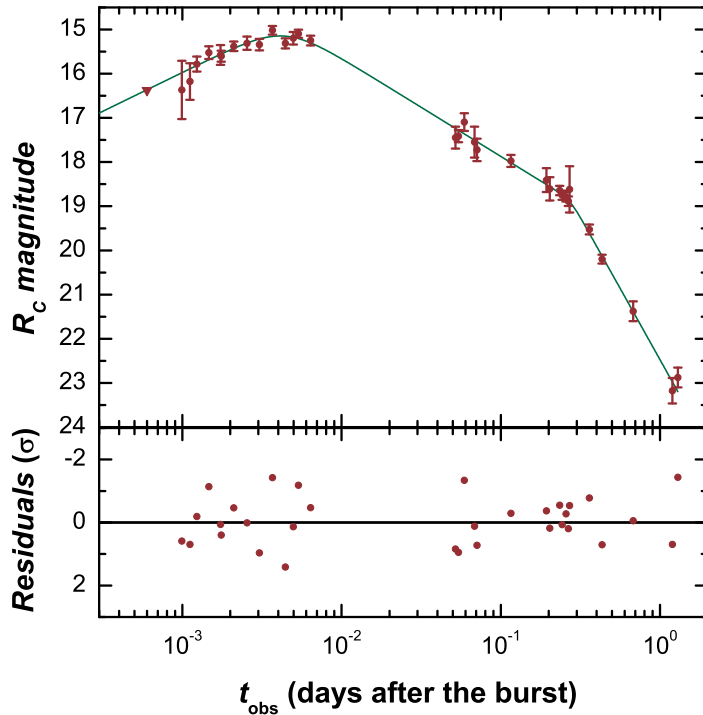


Figure 5.3: *The composite R_C -band light curve of the afterglow of GRB 060605, fitted with a double broken power-law. The lower panel gives the residuals of the fit. These data are corrected for Galactic extinction. See the text and Tab. 5.1 for the results of the fit.*

galaxy underlying the afterglow has an extinction-corrected magnitude of $R_C = 26.3$ (see Sect. 6.3.2). We fixed the break smoothness parameter n_2 according to Liang et al. (2008) to 10 for the second break. For the first break, while we were not able to leave n_1 as a free parameter of the fit, we find a minimum χ^2 and a good fit ($\chi^2/\text{d.o.f.} = 21.00/32 = 0.66$) for a rather smooth break $n_1 = 2.5$. A summary of the fit parameters is given in Tab. 5.1

Table 5.1: *Parameters of the fit of the optical afterglow light curve of GRB 060605.*

Parameter	Value
α_R	-0.70 ± 0.15
α_1	0.89 ± 0.04
α_2	2.58 ± 0.15
t_R (days)	0.0044 ± 0.0007
t_1 (days)	0.27 ± 0.02
n_1	2.5
n_2	10
$\chi^2/\text{d.o.f.}$	$21.00/32 = 0.66$

The peak time of 358 ± 61 s (0.0041 ± 0.0007 days) can be found from the light curve fit by setting $dF_\nu(t)/dt = 0$ and has a value that is comparable to what has been found for, e.g., the early phase of the optical afterglow of GRB 060418 and 060607A (Molinari et al. 2007). Our result for α_1 is in agreement with the value reported by (Schaefer et al. 2006) and the peak time we derive is in agreement with Zhai et al. (2006).

The afterglow of GRB 060605 belongs to the growing ensemble of optical afterglows for

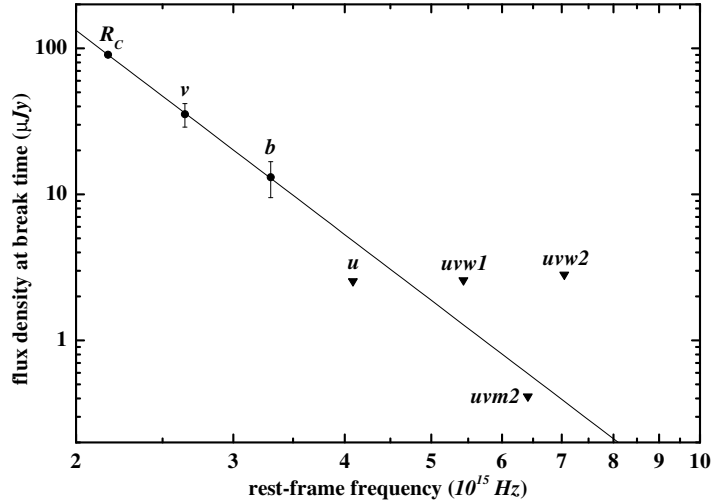


Figure 5.4: Spectral energy distribution (SED) of the afterglow of GRB 060605 in the optical bands at $t=0.27$ days. The line is the best-fit power law. Detections in three filters (bvR_C) and deep upper limits in u and in $uvw2$ show a very steep SED ($\beta_{\text{opt}} = 4.64 \pm 0.58$), a result of Lyman blanketing in the optical/UV due to the high redshift.

Table 5.2: The values plotted in Fig. 5.4. The u , $uvw1$, $uvm2$ and $uvw2$ data are upper limits. For all filters except R_C , λ is from Poole et al. (2008). Data refer to $t=0.27$ days. A redshift of $z=3.773$ was assumed. The values have been corrected for Galactic extinction. The fluxes have been calculated assuming the conversion factors from Bessell (1979) and Poole et al. (2008).

Filter	λ (Å)	$\nu(1+z)$ (10^{15} Hz)	mag	F_ν (μ Jy)
R_C	6588	2.17	18.83 ± 0.04	90.40 ± 3.33
v	5402	2.65	20.03 ± 0.2	35.38 ± 6.52
b	4329	3.31	21.28 ± 0.3	13.09 ± 3.62
u	3501	4.09	> 22.13	< 2.54
$uvw1$	2634	5.43	> 21.33	< 2.56
$uvm2$	2231	6.41	> 23.33	< 0.41
$uvw2$	2030	7.05	> 21.33	< 2.82

which thanks to a rapid response in the follow-up observations the data show the early rise of the afterglow, as predicted by theoretical models (Panaitescu & Kumar 2000; Sari 1997). With a peak magnitude of $R_C = 15.2$ at $t \approx 360$ s (0.0042 days) (Fig. 5.3) it is among the brightest optical afterglows ever detected (Nardini et al. 2008; Kann et al. 2007).

Using the colors derived above, we can construct the spectral energy distribution (SED; Fig. 5.4 and Table 5.2) at $t=0.27$ days. We have detections in only three filters (BVR_C). These three data points can be fit with a very steep SED: we find $\beta_{\text{opt}} = 4.64 \pm 0.58$. The steep slope is further confirmed by the u -band and $uvw2$ -band upper limits, the other two filters are less constraining. This is much steeper than typical afterglow slopes, which lie in the range from 0.5 to 1.1 (e.g., Kann et al. 2006, 2007). This is mostly due to the Lyman blanketing blueward of the rest-frame Ly α line, which at $z = 3.773$ falls between the observed v and R_C bands.

5.1.3 The issue of the jet break

According to Nousek et al. (2006b) and Zhang et al. (2006), a canonical X-ray light curve shows four well defined evolutionary phases (see Sec. 2.3.3 and Fig. 2.6): a steep initial decay followed by a flat (plateau) phase, then a steeper decay (a pre-jet break phase) and finally a post-jet break phase (e.g., GRB 050315; Vaughan et al. 2006; Panaitescu 2007; Liang et al. 2008). However, Fig. 5.1 shows only three segments. The question we are interested in here is if the break seen in the fitted X-ray light curve at around 0.0869 days (see Fig. 5.1) could

be a jet break. We consider two cases.

Case A: If we assume that this is a jet break, segment II of our Fig. 5.1 is the pre-break segment, while segment III is the post-break phase. Consequently the slopes of segment II (α_{II}) and of segment III (α_{III}) are the pre-jet break decay and the post-break decay slopes, usually designated as α_1 and α_2 , respectively.

Case B : The second possibility is that the jet break was in fact at much later times, i.e. $t_b \gtrsim 1.2$ days and $\alpha_1 = \alpha_{\text{III}}$. Indeed, most X-ray afterglows do not show jet breaks (Liang et al. 2007), with the most extreme example being GRB 060729 (Grupe et al. 2007a).

Which between these two possibilities is the preferred one will be provided by the $\alpha - \beta$ relations. For this reason, we considered the standard wind and ISM models for the isotropic case as well as for a jet with the cooling frequency ν_c below and above the observers window. In addition, we also considered models with a power-law index of the electron distribution function of less than 2, as they are listed in table 1 of Zhang & Mészáros (2004). Based on our data the latter models turned out to be excluded with high significance, however. So, we followed Greiner et al. (2003, their table 6), and present here the results for the eight standard cases.

Table 5.3: *Upper pannel: The parameters α_1 and α_2 found for the X-ray light curve in the cases A and B discussed in Sect. 5.1.3. Lower pannel: Predicted spectral slope β in the X-ray band, considering the parameters listed above, for different applied models. The spectral slopes have to be compared with the observed $\beta_X = 1.06 \pm 0.16$ (Sect. 5.1.1). The subscript on β compares the two different cases A and B, while in the models, the subscript f refers to $\nu_c < \nu_X$ (fast cooling), and the subscript s to $\nu_c > \nu_X$ (slow cooling). The values for t_b are just given for completeness and rounded to two digits after the comma.*

Parameter	Case A	Case B		
α_1	0.34 ± 0.03	1.89 ± 0.07		
α_2	1.89 ± 0.07	3.03 ± 0.30		
t_b (days)	0.09 ± 0.01	$\gtrsim 1.2$		
Model	$\beta(\alpha)$	β_A	β_B	
Fast cooling ($\nu_c < \nu_X$)				
ISM _{iso,f}	$(2\alpha_1 + 1)/3$	0.56 ± 0.02	1.59 ± 0.05	
ISM _{jet,f}	$\alpha_2/2$	0.94 ± 0.04	1.52 ± 0.15	
wind _{iso,f}	$(2\alpha_1 + 1)/3$	0.56 ± 0.02	1.59 ± 0.05	
wind _{jet,f}	$\alpha_2/2$	0.94 ± 0.04	1.52 ± 0.15	
Slow cooling ($\nu_c > \nu_X$)				
ISM _{iso,s}	$2\alpha_1/3$	0.23 ± 0.02	1.26 ± 0.05	
ISM _{jet,s}	$(\alpha_2 - 1)/2$	0.44 ± 0.04	1.02 ± 0.15	
wind _{iso,s}	$(2\alpha_1 - 1)/3$	-0.11 ± 0.02	0.93 ± 0.05	
wind _{jet,s}	$(\alpha_2 - 1)/2$	0.44 ± 0.04	1.02 ± 0.15	

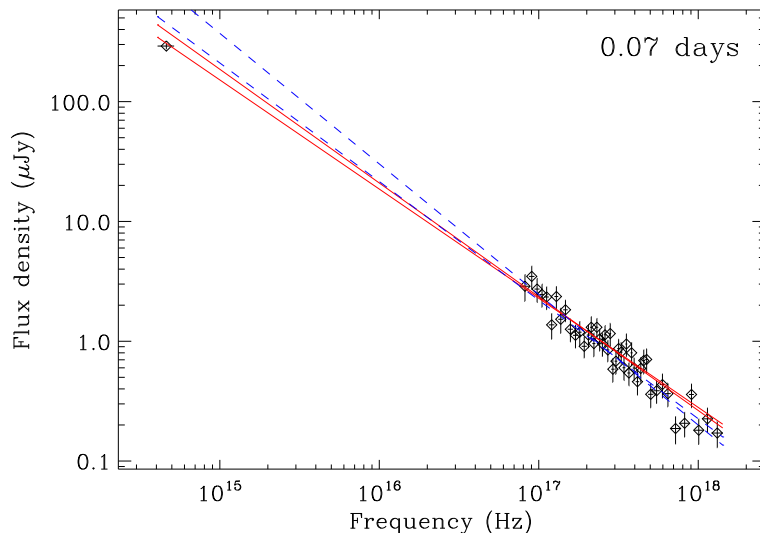
Table 5.3 shows the predicted values for the spectral slope β for the considered scenarios as a function of the observed light curve decay slope in the X-ray band. These results have

to be compared with the observed β in the X-ray band, $\beta_X = 1.06 \pm 0.16$ (Sect. 5.1.1). The subscript on β compares the two cases discussed before. For Case B we calculated α_2 via $\alpha_2 = \alpha_1 + 1.14$, with the latter being the mean value for $\Delta\alpha$ in our data base of GRB afterglows (S. Schulze et al. 2008, in preparation) with an error of 0.3 to be very conservative. We find that Case A is ruled out with high significance. The expected spectral slope before the break is inconsistent with the observed one after the flat decay phase and, thus, with the assumption of no break in the X-ray light curve. Case B suggests a wind model with $\nu_c > \nu_X$. The question, if a wind model is required can be answered by the observed temporal evolution of the SED of the afterglow.

5.1.4 The broad-band spectrum

In order to better discriminate among possible scenarios for the afterglow emission of GRB 060605 in the context of the standard fireball model, we studied the broad-band spectrum from the X-rays (0.3–6 keV) to the optical (R_C band) at two epochs. The first epoch, at 0.07 days (Fig. 5.5), was chosen because it is before any suspected X-ray jet break time, while the second epoch, at 0.43 days (Fig. 5.6), corresponds to the time of the R_C -band measurement by the Nordic Optical Telescope (NOT; Sharapov et al. 2006).

Figure 5.5: *Broad-band spectrum of the afterglow of GRB 060605 at 0.07 days. The lines show the 1- σ confidence regions of power-law fits. Solid lines: simultaneous fit of the X-ray and the R_C -band data; dashed lines: fit of the X-ray data only. The R_C -band data point was calculated from the UVOT data (Sect. 5.1.2). It lies beneath the spectral slope extrapolated from the X-ray band, indicating that the cooling frequency is in between the optical and the X-ray band.*



The R_C -band magnitude at 0.07 days was derived from UVOT data with the procedure described in Sect. 5.1.2. In order to check the reliability of this method, we computed in the same way the R_C magnitude at 0.43 days, finding a value fully consistent with the NOT measurement. The R_C -band fluxes were corrected for extinction in our Galaxy. The 0.3 to 6 keV spectra were derived in the following way: we deconvolved the average XRT count spectrum by assuming the best-fit power-law model, corrected it for the measured column density (Sect. 5.1.1), and rescaled it to the two epochs by using the multi-broken power-law model that fitted the XRT light curve best. The fit of the X-ray spectrum alone, with N_H

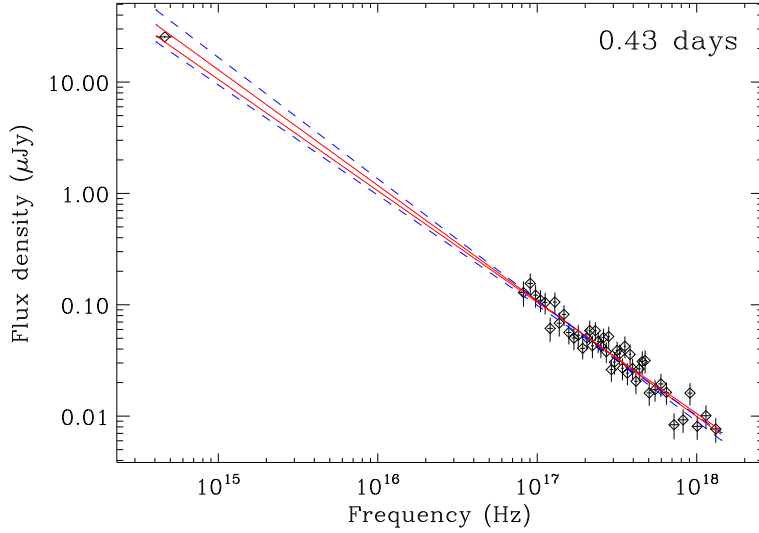


Figure 5.6: *The same as Fig. 5.5 but at 0.43 days. Here, the R_C -band data point is from Sharapov et al. (2006). A simultaneous fit of the X-ray and the R_C -band data gives the same result as a fit of the X-ray data only, suggesting a change of the SED compared to 0.07 days (Fig. 5.5).*

fixed at the Galactic value of $5.1 \times 10^{20} \text{ cm}^{-2}$, gives a spectral index of 1.04 ± 0.05 . Both, X-ray and R_C -band fluxes, were converted into flux densities (μJy), in order to build-up the SED and to allow for broad-band spectral fitting.

As it can be seen in Figs. 5.5 and 5.6, there is a hint of a spectral evolution between the two epochs. At 0.43 days the R_C -band flux density is fully consistent with the extrapolation of the power-law fit of the X-ray spectrum. This is confirmed by the joint fit with a simple power-law of the two data sets, which provides an acceptable chi-square value ($39.5/44=0.90$) and a spectral index of $\beta_{\text{OX}} = 1.02 \pm 0.02$. This is evidence that at this epoch the cooling frequency, ν_c , was already lower than the R_C band one. On the other hand, in the spectrum at 0.07 days the R_C -band data point is below the extrapolation of the power-law fit of the X-ray spectrum. Thus, at 0.07 days the cooling frequency was still at slightly higher frequencies than the R_C band, suggesting that in both spectra ν_c is below the X-ray band and decreasing with time. This points to an ISM model (Sari et al. 1998), since for a wind model ν_c is increasing with time (Chevalier & Li 2000). Based on these findings we conclude that even Case B (Sect. 5.1.3) is ruled out. Moreover, given that at $t=0.43$ days the R_C -band data point of the afterglow light curve lies exactly on the SED derived in the X-ray band (with a slope of $\beta_X = 1.02 \pm 0.02$; see Fig. 5.6), the power-law index p of the electron distribution function is $p = 2\beta = 2.04 \pm 0.04$, a value close to the observed mean (cf. Kann et al. 2006; see also Starling et al. 2008). If the cooling frequency were at higher values than the X-ray band ones, then $p = 2\beta + 1 = 3.04 \pm 0.04$, an unusually large number. Consequently, the data disfavour the hypothesis of a jet break occurring after about 1.2 days.

Since neither Case A or Case B lead to a reasonable agreement with the $\alpha-\beta$ relations, we conclude that a three segment X-ray light curve is ruled out, and a fourth segment is needed. In fact, this conclusion is supported by the joint fit of the optical and the X-ray light curve.

5.1.5 The X-ray vs. the optical light curve: a joint fit

Figure 5.7 shows the combined optical/X-ray light curve of the afterglow of GRB 060605. At early times, from about 0.0012 to 0.0046 days, the X-ray and the optical light curves show a completely different behaviour. The X-ray light curve is falling while the optical light curve is rising, similar to what was observed for e.g. GRB 060418 (Jin & Fan 2007). This rising optical component ends approximately at the same time as the plateau phase commences in X-ray band. The optical light curve might also include a plateau phase lasting for at least 100 s (0.0012 days) around the peak time.

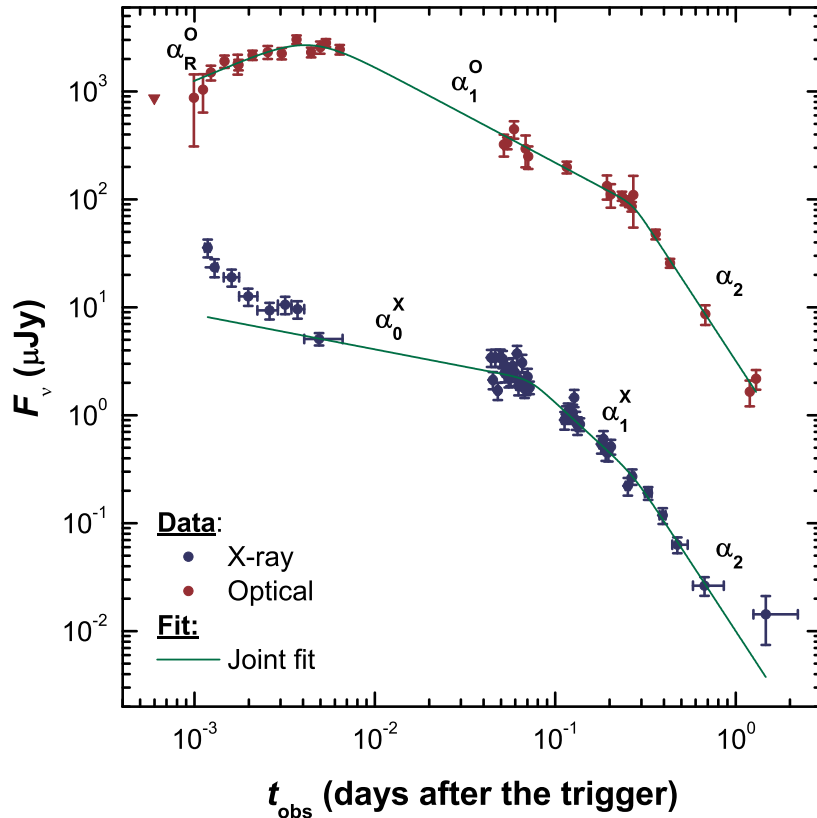


Figure 5.7: *The composite optical and X-ray light curve of the afterglow of GRB 060605. The first optical point is an upper limit (triangle). The green line shows the results of the joint fit of the optical and the X-ray light curve (see Sect. 5.1.5).*

The later behaviour of the light curve is difficult to interpret with certainty due to the lack of X-ray as well as optical data between about 0.006 and 0.041 days. Potentially, also the optical light curves could show a long-lasting plateau phase in this period if its peak was followed by a faster decay. But in this case there are no data published to check this hypothesis. Following the previous discussion, an additional power-law segment in the X-ray light curve must exist between about 0.04 and 0.2 days. While the most striking feature in the combined light curve is the obvious difference in the supposed jet break time, i.e. a chromatic evolution. On the other hand, as we had already emphasized, also the optical data are sparse in this evolutionary phase of the afterglow. For this reason, we have also performed a joint fit of the optical and X-ray light curves.

In doing the joint fit, the data of Khamitov et al. (2006a) have been excluded since they are roughly one magnitude too faint (Karska & Garnavich 2006). The data from 0.05 to 0.1 days are the UVOT *white*, *b* and *v* measures shifted to the R_C -band zero point using

Table 5.4: *Upper pannel: Fit parameters of the joint optical and X-ray fit ($\chi^2/\text{d.o.f.} = 62.11/65 = 0.96$). Lower pannel: Predicted spectral slope β considering the parameters listed above, for different applied models. The spectral slopes have to be compared with the observed $\beta_X = 1.06 \pm 0.16$ (Sect. 5.1.1). the subscript *f* refers to fast cooling, and the subscript *s* to slow cooling.*

Before the jet break	
Parameter	Value
α_R^O	-0.70 ± 0.15
α_1^O	0.89 ± 0.04
$t_{b,1}^O$ (days)	0.004 ± 0.0007
n_1^O	2.5
α_0^X	0.32 ± 0.06
α_1^X	1.54 ± 0.11
$t_{b,1}^X$ (days)	0.072 ± 0.008
n_1^X	10
After the jet break	
Parameter	Value
α_2	2.56 ± 0.13
$t_{b,2}$ (days)	0.27 ± 0.02
n_2	10

Model	$\beta(\alpha)$	β
Fast cooling		
ISM _{iso,f}	$(2\alpha_1^O + 1)/3$	0.93 ± 0.02
ISM _{iso,f}	$(2\alpha_1^X + 1)/3$	1.36 ± 0.07
ISM _{jet,f}	$\alpha_2/2$	1.28 ± 0.07
wind _{iso,f}	$(2\alpha_1^O + 1)/3$	0.93 ± 0.02
wind _{iso,f}	$(2\alpha_1^X + 1)/3$	1.36 ± 0.07
wind _{jet,f}	$\alpha_2/2$	1.28 ± 0.07
Slow cooling		
ISM _{iso,s}	$2\alpha_1^O/3$	0.59 ± 0.02
ISM _{iso,s}	$2\alpha_1^X/3$	1.03 ± 0.07
ISM _{jet,s}	$(\alpha_2 - 1)/2$	0.78 ± 0.07
wind _{iso,s}	$(2\alpha_1^O - 1)/3$	0.26 ± 0.02
wind _{iso,s}	$(2\alpha_1^X - 1)/3$	0.69 ± 0.07
wind _{jet,s}	$(\alpha_2 - 1)/3$	0.78 ± 0.07

the early R_C and UVOT observations, and thus may be incorrect if a strong color change occurred in between. However, no sign of a strong chromatic evolution is detected. Allowing for a different pre-break decay slope in the optical and in the X-ray band, but requiring an identical post-break decay slope, such a joint fit finds a break time of $t_b = 0.27 \pm 0.02$ days, a pre-break decay slope in the optical of 0.89 ± 0.04 , a pre-break decay slope in the X-ray band

of 1.54 ± 0.11 , and a post-break decay slope of 2.56 ± 0.13 (Fig. 5.7 and Tab. 5.4). Thereby, the smoothness parameter of the break was fixed to 10.

Including the suggested additional segment and hence a further break at 0.27 ± 0.02 days we fitted the X-ray light curve after 0.04 days with a double smoothly broken power law ($\chi^2/d.o.f. = 50.74/37 = 1.18$). To compute the improvement given by the previous fit, we also fitted the same time interval with a double smoothly broken power law ($\chi^2/d.o.f. = 54.21/39 = 1.39$).

Based on the joint fit and the results of the $\alpha - \beta$ relations (see Tab. 5.4), we conclude that an additional, 4th power-law segment between about 0.04 and 0.2 days delivers a unique solution with the cooling frequency at values lower than the R -band in the ISM model.

We can now use the observational data to constrain the density n in the circumburst medium and the parameter ε_B that measures the fraction of energy carried by the magnetic field. For an ISM medium the cooling frequency is given by (cf. Granot et al. 2000)

$$\nu_c = 2.9 \times 10^{15} \varepsilon_{B,-1}^{-3/2} E_{52}^{-1/2} n_0^{-1} t_2^{-1/2} (1+z)^{-1/2} \text{ Hz}, \quad (5.1)$$

where $n_0 = n/1 \text{ cm}^{-3}$, $\varepsilon_{B,-1} = \varepsilon_B/0.1$, and $t_2 = t/100 \text{ s}$. Using $\nu_c < 4.5 \times 10^{14} \text{ Hz}$ at $t=0.43$ days with $E_{52} = 2.5$ (Butler et al. 2007) and $z=3.773$ we can constrain the product $\varepsilon_{B,-1}^{-3/2} n_0^{-1}$ (Fig. 5.8). Since $\varepsilon_B < 1$, it must be $n \gtrsim 0.005 \text{ cm}^{-3}$, a reasonable result. On the other hand, the low deduced hydrogen column density along the line of sight in the GRB host (Sects. 5.1.1 and 6.3.1) might indicate a relatively low circumburst gas density. If we require $n < 100 \text{ cm}^{-3}$ then $\varepsilon_B > 0.001$, which is also a reasonable constraint.

In the following we consider the break at 0.27 days as a classical jet break and we use the results of the joint fit to discuss the energetics of the afterglow.

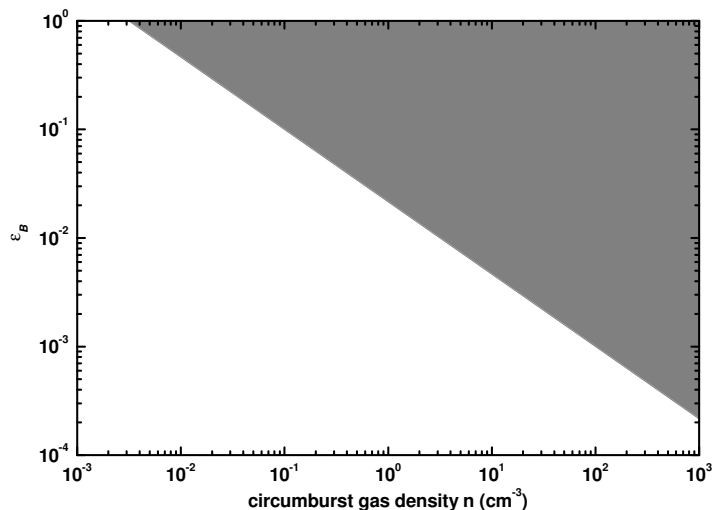


Figure 5.8: Constraints on the parameter space of the fractional energy carried by the magnetic field, ε_B , and the gas density (in units of cm^{-3}) in the circumburst medium into which the fireball was expanding. It was assumed here that at 0.43 days the cooling frequency was at frequencies less than $4.5 \times 10^{14} \text{ Hz}$ (R_C band). The allowed region is represented by the gray area.

5.1.6 Energetics of the burst and of the afterglow

5.1.6.1 The burst

We follow the standard approach to calculate the jet half-opening angle for an ISM environment (cf. Sari et al. 1999),

$$\theta_{\text{jet}}^{\text{ISM}} = \frac{1}{6} \left(\frac{t_b}{1+z} \right)^{3/8} \left(\frac{n_0 \eta_\gamma}{E_{52}} \right)^{1/8} \text{ rad.} \quad (5.2)$$

Here, E_{52} is the isotropic equivalent energy of the prompt emission in units of 10^{52} erg, n_0 is the density of the ambient medium in cm^{-3} , η_γ is the efficiency of the shock in converting the energy of the ejecta into gamma radiation, and t_b is the break time in days. We set $n_0 = 1 \text{ cm}^{-3}$ and $\eta_\gamma = 0.2$. Assuming the observed break time at $t_b = 0.27 \pm 0.02$ days, as follows from the joint fit, with $E_{52} = 2.5_{-0.6}^{+3.1}$ (Butler et al. 2007) we get $\theta_{\text{jet}}^{\text{ISM}} = 2.37_{-0.10}^{+0.37}$ degrees. Changing η_γ to 1.0 does not increase $\theta_{\text{jet}}^{\text{ISM}}$ in a notable manner due to the weak dependence of it on η_γ . On the other hand, as already stated before (see Eq. 5.1), a very high gas density seems to be unlikely given that we do not see so much hydrogen at the redshift of the burst in the X-ray spectrum and in the optical spectrum as well. Assuming the above numbers, the corresponding beaming-corrected energy release in the gamma-ray band is $E_\gamma^{\text{corr}} = 2.14_{-0.52}^{+2.76} \times 10^{49}$ erg.

The mean value of the half-opening angle of the pre-*Swift* era GRBs is 4.39 degrees (Zeh et al. 2006) with a width of 0.13 dex. The beaming corrected energy is lognormal distributed characterised by a mean of $\sim 5 \times 10^{50}$ erg and a width of 0.5 dex. With respect to these values GRB 060605 is within 3σ in agreement.

As outlined by Panaitescu & Kumar (2000), assuming that the observed peak in the optical light curve signals the fireball deceleration timescale (which is $t_{\text{peak}}/(1+z)$), one can calculate the initial Lorentz factor, Γ_0 , of the outflow. Following Sari et al. (1999, Eq. 5.2), in the afterglow deceleration phase the time evolution of the Lorentz factor is given by

$$\Gamma(t) = 6 \left(\frac{E_{52}}{\eta_\gamma n_0} \right)^{1/8} \left(\frac{t}{1+z} \right)^{-3/8}. \quad (5.3)$$

Setting $E_{52} = 2.5$ (Butler et al. 2007), $\eta_\gamma = 0.2$, and $n_0 = 1 \text{ cm}^{-3}$, it follows $\Gamma(t = t_{\text{peak}}) = 116$, and hence $\Gamma_0 = 231 \pm 15$. Following the procedure outlined in Molinari et al. (2007) gives $\Gamma_0 = 366 \pm 23$.

5.1.6.2 The X-ray afterglow

The luminosity of the afterglow is given by (e.g., Nousek et al. 2006b)

$$L_X(t_{\text{host}}) = 4\pi d_L^2 (1+z)^{\beta-1} F_X(t_{\text{obs}}), \quad (5.4)$$

where $F_X(t_{\text{obs}})$ is the observed time-dependent flux in the X-ray band and d_L is the luminosity distance. Using $z=3.773$ and assuming $\beta = 1.06$ (Sect. 5.1.1) even at very early times, we get for the time evolution of the X-ray luminosity of the afterglow in the 0.3-10 keV energy

band (in units of erg s^{-1})

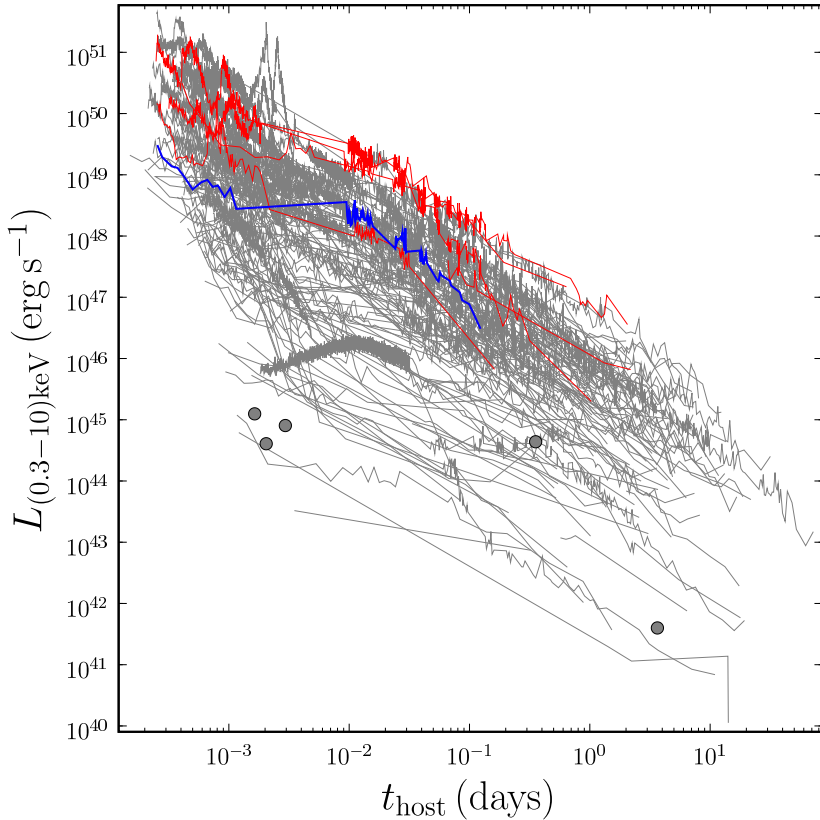
$$L_X(t) = 7.0 \times 10^{48} (t/t_1)^{-\alpha}, \quad \alpha = 0.32; \quad t_1 \leq t \leq t_2, \quad (5.5)$$

$$L_X(t) = 2.0 \times 10^{48} (t/t_2)^{-\alpha}, \quad \alpha = 1.54; \quad t_2 \leq t \leq t_3, \quad (5.6)$$

$$L_X(t) = 2.6 \times 10^{47} (t/t_3)^{-\alpha}, \quad \alpha = 2.56; \quad t \geq t_3, \quad (5.7)$$

where $t = t_{\text{host}}$ is measured in the GRB host frame and all the break times t_1 , t_2 and t_3 are also given in the host frame. For reasons of simplicity, a single power-law decay was assumed here, with $t_1 = 44$ s (0.0005 days), $t_2 = 1303$ s (0.015 days), and $t_3 = 4887$ (0.056 days). The isotropic energy release of the afterglow in the X-ray band was 4.1×10^{52} erg between 0.0005 and 0.015 days (which is 16% of E_γ ; Butler et al. 2007), 2.5×10^{51} erg between 0.015 and 0.056 days ($0.10 E_\gamma$), and 8.1×10^{50} erg thereafter ($0.03 E_\gamma$), assuming a constant decay.

Figure 5.9: X-ray afterglow of GRB 060605 (blue) in comparison to 132 Swift-era X-ray afterglows with known redshift since 2005. In addition, for comparison, in red are shown the GRBs with a redshift between $z = 3.59$ and $z = 3.97$, close to the redshift of 060605. All other bursts are colored in gray. GRB 060605 belongs to the more luminous subclass. At early times that afterglow is rather intrinsically faint compared to the others though due to the plateau phase it is more luminous at later times (for a more detailed discussion, see Schulze et al. 2008, in prep.).



Additionally, we compared the X-ray afterglow of GRB 060605 to the X-ray emission of 132 *Swift* era GRBs with known redshift (Fig. 5.9). The original data for all bursts were taken from the light curve repository by Evans et al. (2007). To compute the luminosities we followed Nousek et al. (2006b). This required a prior spectroscopic analysis of the data to obtain the spectral slope β . We obtained the spectral slope by fitting the spectrum with an absorbed power law. One absorption component represents the Galactic absorption, which was fixed to the value given by Kalberla et al. (2005), and the second one the extinction in the host frame. Compared to all 132 X-ray afterglows the one of GRB 060605 belongs to the

high luminosity subclass. At early times it is intrinsically fainter with respect to the rest of that subclass. At later times it is much more luminous due to the 0.01 days lasting plateau phase though.

5.1.6.3 The optical afterglow

Similar to the “Bronze Sample” of Kann et al. (2007), we can assume that the R_C -band afterglow of GRB 060605 is not affected by host galaxy extinction (which seems to be low at high redshifts anyway, Kann et al. 2007). This assumption is also supported by the observed SED of the afterglow at 0.43 days (Fig. 5.6). Furthermore, if the cooling break ν_c lies at wavelengths longer than the optical ones then $\beta_{\text{opt}} = \beta_X$. Therefore, assuming $A_V(\text{host})=0$, $\beta_{\text{opt}} = 1.06$, and using the method presented in Kann et al. (2006), we are able to derive a lower limit on the magnitude shift $dR_C \geq 3.61$ mag. This shift describes the magnitude change that appears when the afterglow light curve is corrected for extinction (which we are unable to do here, therefore we derive only a lower limit) and shifted to $z = 1$ (which also implies a temporal shift). Comparing the afterglow with the sample presented Kann et al. (2007), we find that it is among the brightest afterglows at early times, comparable to the afterglow of GRB 050820A (Fig. 5.10). At 43 s in the rest-frame ($z=1$ assumed), it has $R_C \leq 11.83 \pm 0.15$, which places it among the tight clustering found by Kann et al. (2007), although the afterglow is still rising. To derive a magnitude at one day after the GRB (if at $z=1$), we need to extrapolate the late steep decay. We find $R_C \leq 20.9 \pm 0.2$ ($M_B \leq -22.0 \pm 0.2$; assuming no host extinction), which is relatively faint. At a similar redshift, only the afterglow of GRB 050502A was fainter (Kann et al. 2007).

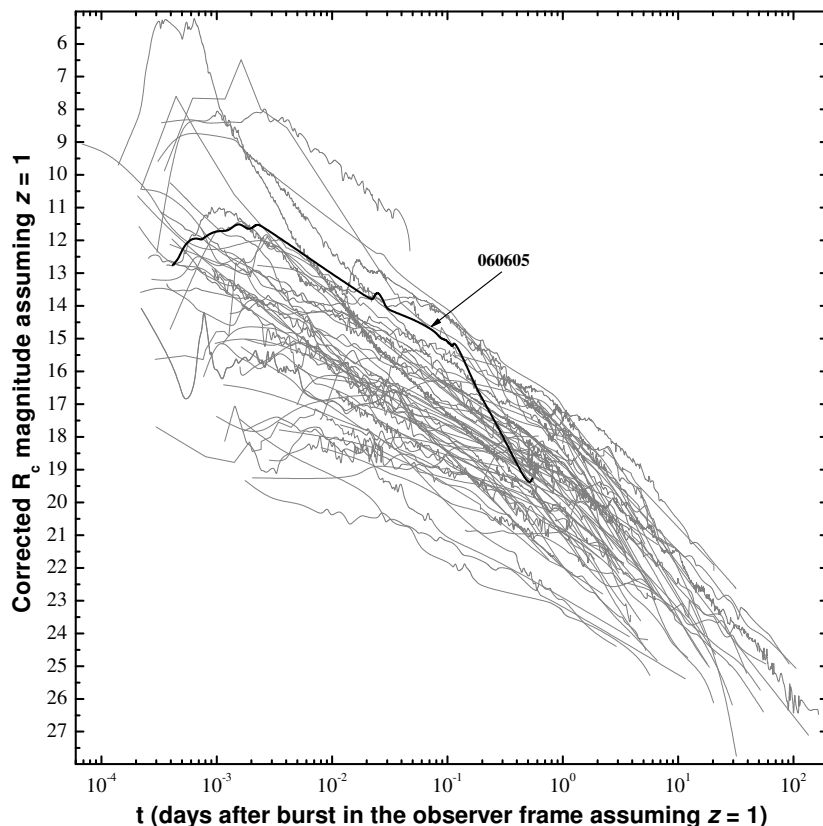


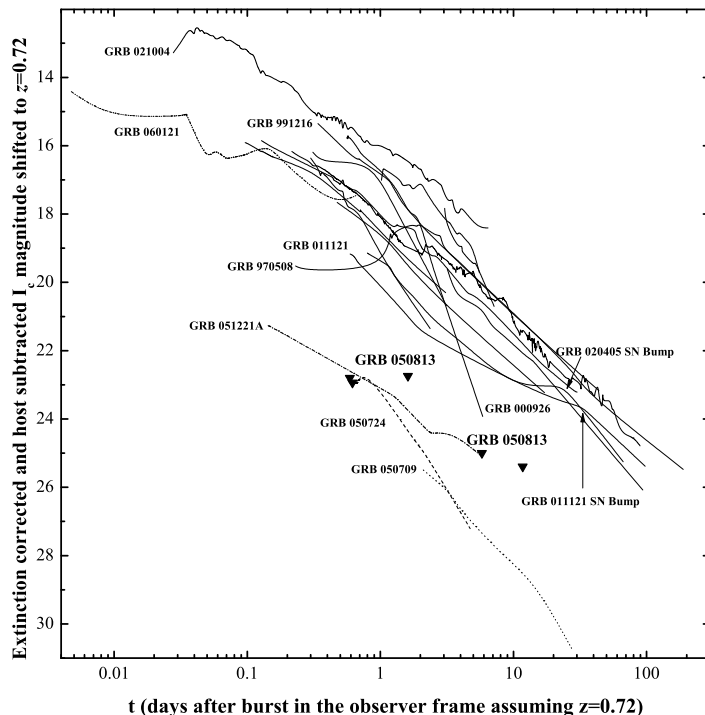
Figure 5.10: *The observed R_C -band light curve of the afterglow of GRB 060605 compared to the ensemble of optical afterglows known so far after shifting all light curves to a common redshift of $z=1$. All data are corrected for Galactic extinction. See Kann et al. (2006) for the method and Kann et al. (2007) for more details on other bursts.*

5.2 GRB 050813: searching for a fading optical afterglow component

Based on our deep FORS2 observing runs, we searched for a potential fading afterglow superimposed on the brightest extended sources (galaxies) in the field (Table 3.2). No evidence for variability due to an underlying transient source was found. Prochaska et al. (2006) identified object C and E as elliptical galaxies (Fig. 3.1), with C being the most likely host candidate based on its location relative to their revised elliptical error circle. In our images source E appears to have an irregular halo which does not support its classification as an elliptical. Image subtraction did not reveal any transient source superimposed on this galaxy.

In order to obtain an upper limit on a possible detection of an afterglow (or a SN) in the first (second) epoch FORS2 image superimposed source E, we artificially added point sources of different magnitudes to E and then performed an aperture photometry. These point sources were selected from the second epoch image. All pixels of the second epoch image were then set to zero except the pixels of the selected point source of known magnitude and the resulting image was then shifted and added to the first epoch image. This analysis showed that we would have been able to detect (at 3σ) a fading afterglow superimposed on this galaxy if its I -band magnitude had been 23.5 at the time of the first FORS2 observation.

Figure 5.11: *The I -band light curves of all afterglows from the “Golden Sample” of Kann et al. (2006) after correction for Galactic and for host extinction and after shifting them to a common redshift of $z=0.72$, the potential redshift of GRB 050813. Two long GRB supernova rebrightenings are indicated. Also shown are the I -band afterglows of the short bursts GRB 050709, 050724, 051221A and 060121 shifted in a similar way, and our upper limits on any afterglow or supernova from GRB 050813 (upside-down triangles). For GRB 060121 a redshift of $z = 4.6$ (de Ugarte Postigo et al. 2006) is assumed here.*



One of the main goals of our observing runs was the localization of the afterglow and hence the identification of the GRB host galaxy. Basically, the host cannot be identified with certainty and we have to consider other arguments that favor or disfavor any galaxy visible on the deep FORS2 I -band images of the XRT error circle as the potential host. GRB 050813 then joins the increasing list of short bursts with no detected optical afterglow, starting with GRB 050509B (Bloom et al. 2006; Castro-Tirado et al. 2005; Gehrels et al. 2005; Hjorth

et al. 2005a). Using the upper limits on the afterglow of GRB 050813 (Table 3.1) we can follow Kann et al. (2006) and place the properties of this afterglow in the context of other known GRB afterglows (Fig. 5.11). The long burst afterglows shown in Fig. 5.11 by solid lines are those from the “Golden Sample” of Kann et al. (2006), i.e., those that have sufficient I -band data. In addition, we analyzed the available afterglow data on the short bursts GRB 050709 (Hjorth et al. 2005b; Fox et al. 2005; Covino et al. 2006), GRB 050724 (Berger et al. 2005; Malesani et al. 2007), GRB 051221A (Soderberg et al. 2006a) and GRB 060121 (Levan et al. 2006; de Ugarte Postigo et al. 2006) in an analogous way and also included them in Fig. 5.11. As can be seen, short burst optical afterglows are intrinsically very faint, with the afterglows of GRB 050724 and GRB 051221A being about 3 magnitudes fainter than any long burst afterglow in the sample, and GRB 050709 being 4 magnitudes fainter at one day after the burst and assuming $z = 0.72$ (in agreement with the predictions for short burst afterglows; Panaitescu et al. 2001). They are also significantly fainter than intrinsically faint afterglows of some long GRBs, such as GRB 021211. Only the afterglow of GRB 060121 is comparable with the typical afterglows of long GRBs. The upper limits on the optical afterglow of GRB 050813 show that its luminosity was also far below typical luminosities of (extinction-corrected) afterglows of long bursts. On the other hand, it matches the luminosity region occupied so far by afterglows of the short bursts (with GRB 060121 being the only exception).

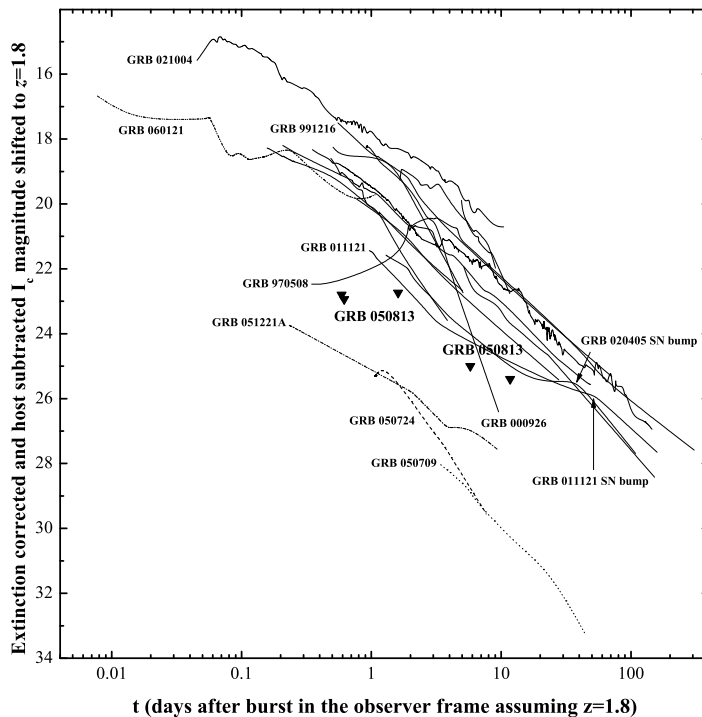


Figure 5.12: *The same as Fig. 5.11, but for a redshift of 1.8.*

Chapter 6

The host galaxies

GRB hosts are usually faint, blue, star-forming galaxies, dominated by a young stellar population. Luminosities are generally low, indicating low masses and low metallicities. Cosmological simulations suggest that hosts associated with long GRBs are representative of the whole galaxy population (Nuza et al. 2007). Given the extraordinary brightness of the afterglows in the optical bands, in many cases very detailed information about the ISM can be obtained even via high-resolution spectroscopy (e.g., Chen et al. 2005; Vreeswijk et al. 2001), and this concerns the gas as well as the properties of the dust.

Similar to the substantial differences of the three GRBs discussed here in the phenomenology of the appearing (non-appearing) afterglow and SN component, also the study of the corresponding host galaxies was of quite different quality. While for GRB 060218 the host galaxy was securely identified, in the case of 060605 it is only barely detected on deep VLT images, and finally only a host galaxy candidate could be provided by our data for the short burst 050813. On the other hand, interesting information on the chemical composition of the interstellar medium of the high-redshifted host of GRB 060605 could be obtained thanks to the bright GRB afterglow.

6.1 Searching for the host galaxy of GRB 050813

Given that we have only XRT error circles but no well-localized GRB afterglow, no host galaxy of the short burst 050813 can be identified with certainty. We can only provide host galaxy candidates.

Figure 3.1 shows that there are only two sources in the *Swift* XRT error ellipse (Prochaska et al. 2006), while there are at least three additional sources in the refined error circle (Moretti et al. 2006). The former might favor a burst related to the very faint sources #6 and #7 (source #6 appears point-like in our images) but it does not even exclude an event in the outer halo of source C, an elliptical galaxy at a redshift of 0.719 (Prochaska et al. 2006). The minimum distance between the border of the error ellipse and the center of this galaxy is 3.2 arcsec, corresponding to a projected distance of 23 kpc. This is less than the projected distance of the error circle of GRB 050509B from the center of its suspected host, an elliptical galaxy at a redshift of $z=0.225$ (Gehrels et al. 2005). In addition, the minimum angular distance between source E and the border of the error ellipse is 7.1 arcsec, corresponding to a projected distance of 51 kpc. Even this is within the range predicted by recent models of

merging compact objects (see Belczynski et al. 2002; Perna & Belczynski 2002). The error circle determined by Moretti et al. (2006) is much larger, and thus allows not only source C but also galaxy E at $z = 0.73 \pm 0.01$ (Prochaska et al. 2006) to be the potential host of GRB 050813. This galaxy was classified by Prochaska et al. (2006) as an elliptical galaxy, while our images show morphology that point either to a spiral or to an irregular galaxy. The nature of the fifth, point-like source in the refined error circle, #4, remains undetermined.

Another revised XRT error circle was reported by Butler (2007) with a radius of 3.8 arcsec and centered close to a faint edge-on galaxy. This galaxy (source #7, see Fig. 3.1) was only marginally detected during the first FORS observations. A comparison with the second FORS observations six days later does not provide convincing evidence for a photometric variability due to an underlying point source.

So, it remains open if this is indeed the GRB host. Its angular diameter as well as its apparent magnitude might be in agreement with a modest redshift of about 0.7, but we cannot prove this with certainty. Claims by Berger (2006) that this galaxy among others might be the member of a background cluster of galaxies have never been confirmed in the literature, so we do not trust this statement here. If source #7 is the host galaxy then the host of GRB 050813 was most likely not an elliptical; the shape of this galaxy is too much elongated. So, most likely it is a spiral galaxy seen nearly edge-on. If the burster was placed in the galactic plane of this galaxy then also interstellar extinction might have affected the visibility of its (non-detected) optical afterglow. Unfortunately, we do not have color information, so we cannot further characterize this galaxy. Getting additional color information might be difficult even with the VLT given the faintness of this source.

6.2 A compact host galaxy of GRB 060218

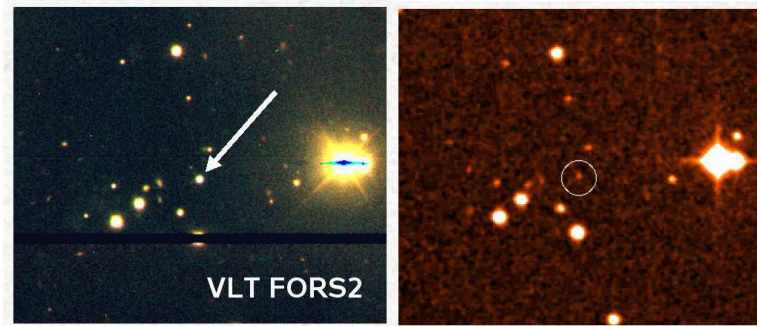
The host galaxy of GRB 060218/SN 2006aj (Fig. 6.1) was imaged pre-burst by the Sloan Digital Sky Survey (Cool et al. 2006). These images were used to obtain its magnitudes (see Sec. 3.2.4), as the SN brightness was hiding the host component, and to measure its diameter (~ 2 kpc, for $z=0.033$). The values used for the host galaxy in this work are $B = 20.57 \pm 0.07$, $V = 20.18 \pm 0.04$, $R = 20.03 \pm 0.03$ and $I = 19.58 \pm 0.06$, not corrected for Galactic extinction.

Given the world model used in this Thesis, for $z=0.033$ the luminosity distance is 0.14 Gpc and $m - M = 35.78$ mag. The absolute magnitudes of the host are therefore, neglecting minor corrections due to the (small) redshift, $M_B = -15.21 \pm 0.07$, $M_V = -15.6 \pm 0.04$, $M_R = -15.75 \pm 0.03$ and $M_I = -16.2 \pm 0.06$.

The VLT/UVES spectrum allowed a measurement of the total extinction toward SN 2006aj and it turned out that the main contribution is from our Galaxy ($E(B - V) = 0.127 \pm 0.005$), while $E(B - V)_{host}$ is only 0.044 ± 0.001 (Guenther et al. 2006). The latter is supported by the SED of the galaxy (see Fig. 6.2).

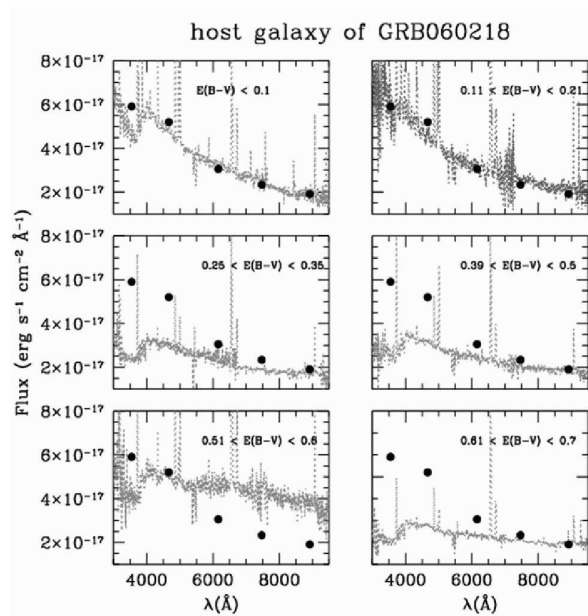
In addition, spectroscopic studies led to an estimate of the star formation rate $SFR \sim 0.07 M_\odot/year$ and of the metallicity $Z \sim 0.07 Z_\odot$ (Wiersema et al. 2007). Taking into account slit losses, the SFR might be underestimated by a factor 3. This would imply that the SN 2006aj host has a SFR comparable to that of the Milky Way, while its stellar mass is about 1000 times smaller ($M_{host} = 10^{7.2 \pm 0.3} M_\odot$) (Savaglio et al. 2008).

Figure 6.1: *Left: SN 2006aj/-GRB 060218 outshining its underlying host galaxy. Right: The host seen on archived DSS2 red images.*



We conclude, the host of GRB 060218 is a compact star-bursting galaxy, in agreement with the picture that the GRB progenitor was a massive star (see Sect. 4.1).

Figure 6.2: *The broad-band SED of the host galaxy of SN 2006aj (thick points) is compatible with a moderately absorbed galaxy starburst templates from (starburst templates from Kinney et al. 1996). The data have been corrected for galactic extinction. Adapted from Ferrero et al. (2007a).*



6.3 The high- z host galaxy of 060605

GRB 060605 is one of the bright examples that demonstrate in which way GRB research is a new tool to explore the high- z universe. Thanks to GRBs we get insight on the interstellar medium in remote galaxies that even with the VLT are barely detectable at all.

6.3.1 ISM signatures of the host galaxy

In Fig. 6.3 we show absorption lines identified in the PPAk spectrum of the afterglow (spectral resolution $\lambda/\Delta\lambda = 500$ at a wavelength of 5300 \AA). The highest redshifted Ly α is at $z = 3.773 \pm 0.001$, which we interpret as the redshift of the GRB (look-back time 11.98 Gyr). The HI column density is very uncertain, in the range $N_{\text{HI}} = 10^{18.5} - 10^{19.3} \text{ cm}^{-2}$, but certainly one of the lowest ever measured in a GRB afterglow at the redshift of the GRB (Savaglio 2006; Jakobsson et al. 2006; Chen et al. 2007a). We notice that the HI column densities measured for GRB 021004 and GRB 060607A are also low, $N_{\text{HI}} = 10^{19.5} \text{ cm}^{-2}$ and $10^{16.8} \text{ cm}^{-2}$, in the

former and latter, respectively. For GRB 030226, Shin et al. (2006) report $N_{\text{HI}} = 10^{20.5 \pm 0.3} \text{ cm}^{-2}$. Unfortunately, the low S/N of the spectrum does not allow us to measure column densities for metals. We also identify a strong Si IV absorption doublet at $z = 3.774 \pm 0.001$, $\Delta v = 120 \text{ km s}^{-1}$ redward of the Ly α , likely associated with the GRB-host system.

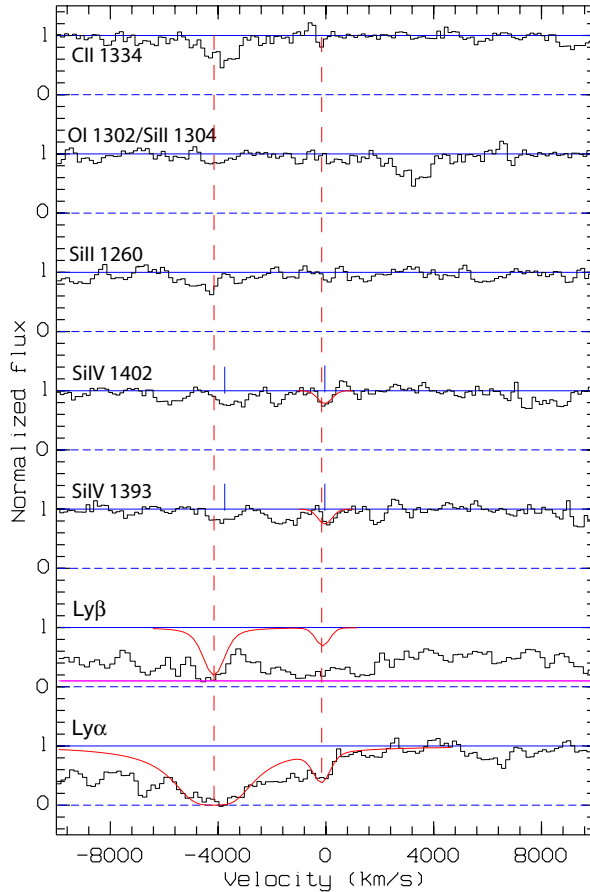


Figure 6.3: *The spectrum of the afterglow of GRB 060605 in velocity space, centered at a redshift of $z = 3.773$ ($v = 0 \text{ km s}^{-1}$). This is likely the redshift of the GRB, for which we detect Ly α and Si IV doublet absorptions. Offset by about -4000 km s^{-1} we also mark the strong absorption system (damped Lyman α) at $z = 3.709$ with Ly α , Ly β , O I and the Si IV doublet, likely associated with an intervening galaxy. For the method see Savaglio & Fall (2004).*

Blueward of the $z = 3.773$ we identify a strong Ly α absorber at $z = 3.709 \pm 0.003$ ($\Delta v = 4000 \text{ km s}^{-1}$ from the GRB redshift) likely associated with a Damped Ly α system (DLA), with an estimated HI column density of $N_{\text{HI}} = 10^{20.9} \text{ cm}^{-2}$. Redward of the Ly α , we detect the Si IV doublet at $z = 3.717 \pm 0.001$ ($\Delta v = 500 \text{ km s}^{-1}$ from the DLA). At approximately the redshift of the DLA, we identify absorption lines associated with C II 1334, Si II 1260, and O I 1302/ Si II 1304 (Fig. 6.3).

The separation between the two strong $z = 3.717$ and $z = 3.774$ Si IV absorbers $\Delta v = 3600 \text{ km s}^{-1}$ is comparable to that between the double C IV absorbers detected in the afterglows of GRB 021004 ($\Delta v = 2400 \text{ km s}^{-1}$; Savaglio et al. 2002; Fiore et al. 2005), GRB 030226 ($\Delta v = 2400 \text{ km s}^{-1}$; Klose et al. 2004), and GRB 060607A ($\Delta v = 1800 \text{ km s}^{-1}$; A. Smette et al. 2008, in preparation). The possibility that this is the effect of a stellar wind in Wolf-Rayet stars has been recently excluded by Chen et al. (2007b). The same authors suggested as a reason for this effect the presence of a foreground galaxies along the sight line of the GRBs.

In Fig. 6.4, the spectrum of a Lyman break galaxy (LBG) at a $z \sim 3$ (from Shapley et al. 2001) is overplotted on the spectrum of the GRB to show the typical absorption lines

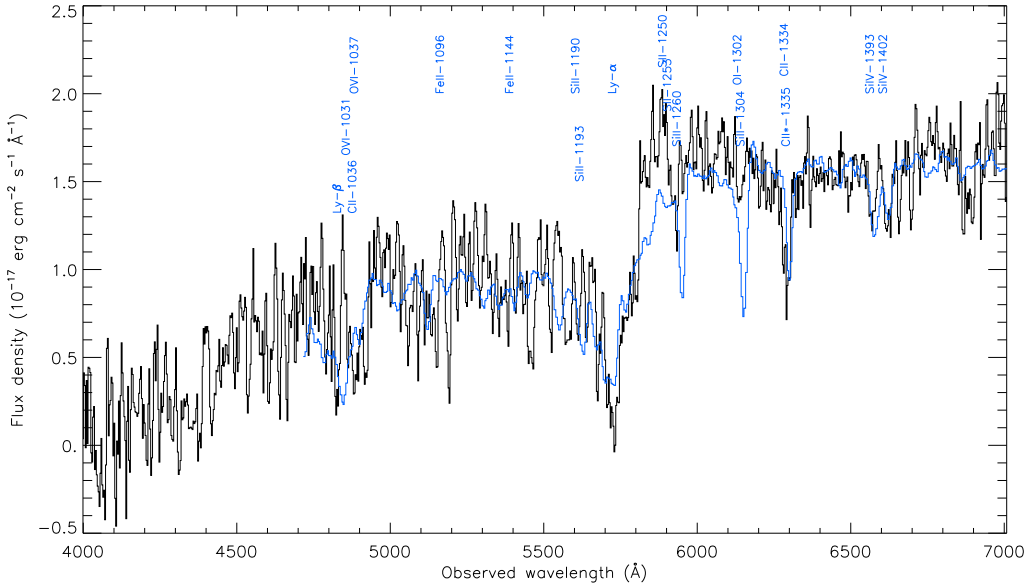


Figure 6.4: *Spectrum of the afterglow (black) of GRB 060605 obtained between 7.5 and 9.1 hours after the burst with PPAk mounted at the Calar Alto 3.5-m telescope, overplotted with the spectrum of a Lyman break galaxy (LBG) at the same redshift (from Shapley et al. 2001). The typical LBG lines are indicated in blue; only the strongest of them can also be found in the afterglow spectrum. The afterglow spectrum, calibrated in flux and wavelength, is a composition of six individual spectra of 15 min exposure time each. The spectral resolution is $\lambda/\Delta\lambda = 500$.*

observed in these galaxies at high redshifts and to help the comparison with our spectrum. The spectrum of the galaxy has been shifted in wavelength considering the redshift of the damped Lyman α absorption system at $z = 3.709$ and rescaled in flux for comparison.

6.3.2 Global parameters of the host galaxy

To search for the host galaxy of GRB 060605 and the potential foreground absorber detected in our optical spectrum (Fig. 6.3) we used VLT/FORS2 imaging data of the field obtained under the ESO Large Programme 177.A-0591 (PI: Jens Hjorth). Based on images obtained with the 3.5m Italian Telescopio Nazionale Galileo on La Palma (Malesani et al. 2006; J. Deng et al. 2008, in preparation) we were able to derive an improved astrometric position of the optical transient. Its refined position is R.A., Decl. (J2000) = $21^h 28^m 37.314$, $-06^\circ 3'30''.88$. On the deep VLT image the afterglow can be positioned with an accuracy of 0.1 arcsec. At this position a very faint extended source is visible (Fig. 6.5). Using the average zeropoint of FORS2 R_C -band images in the time period from July to September 2007 (28.404 ± 0.037), as it is provided on ESO's web pages, we derived a magnitude of $R_C = 26.4 \pm 0.3$ for this source (aperture diameter = 10 pixels). If this is the host galaxy, it implies that at its peak time the optical afterglow of GRB 060605 was approximately 11 mag brighter in R_C than its host. We note, however, that the detection is weak and we cannot claim that this object is the host of GRB 060605 as we have no information about its redshift. On the other hand, its position underlying the optical transient and its faint magnitude make a potential physical

association with GRB 060605 a reasonable assumption.

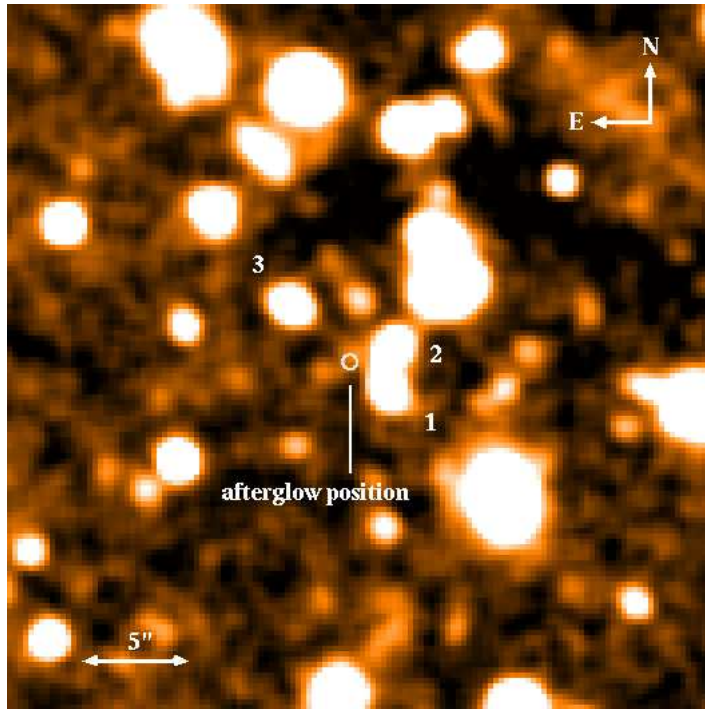


Figure 6.5: *The stellar field around the position of the afterglow of GRB 060605. The R_C -band image is the average of 8×500 s exposure time each, taken on 14 Sep 2006 and 18 Jun 2007 at VLT/FORS2, when the afterglow had faded away. The position of the optical transient is indicated. The faint extended source underlying the position of the optical transient is the suspected GRB host galaxy at $z=3.773$. The three bright galaxies next to it are indicated with numbers.*

Assuming for simplicity a power-law spectrum for this galaxy of the form $F_\nu \propto \nu^{-\beta_{\text{gal}}}$, its absolute R_C -band magnitude is $M_R = m_R - \mu - k$, where $\mu = 47.66$ mag is the distance modulus ($z = 3.773$) and k is the cosmological k -correction, $k = -2.5(1 - \beta_{\text{gal}}) \log(1 + z) = -1.70(1 - \beta_{\text{gal}})$. Hence, $M_R = -21.26 + 1.70(1 - \beta_{\text{gal}}) \pm 0.3$, which for $\beta_{\text{gal}}=1$ would place this galaxy approximately 1 mag away (more luminous) from M^* of the Schechter function describing the r -band luminosity function of galaxies in the Las Campanas redshift survey (Lin et al. 1996). A smaller β_{gal} would make the absolute magnitude correspondingly fainter.

We can also speculate if any of the other three bright, extended sources seen near the afterglow position on the VLT image could be the host galaxy of GRB 060605. In Fig. 6.5 these three galaxies are indicated with the numbers 1, 2, and 3. However, there are two arguments against this hypothesis. First, these galaxies have $R_C \sim 24.5$. For an assumed redshift of $z = 3.7$ this would place all of them at the very bright end of the Schechter luminosity function (cf. Lin et al. 1996). Second, the angular distance of the optical transient from the centers of these galaxies is $2''.12$, $2''.27$, and $3''.94$, respectively. For the considered world model at a redshift of $z = 3.773$ an angular distance of 1 arcsec corresponds to a projected distance of 7.26 kpc. The projected distance of the optical transient from the three galaxies is then 15.4, 16.5 and 28.6 kpc, respectively. Compared to the offset distribution of GRBs with respect to their host galaxies (in the pre-*Swift* era; Bloom et al. 2002) these large distances make it unlikely that one of these galaxies is the host. Finally, using basically the same arguments it is unlikely that one of them is the foreground absorber seen in the optical spectrum of the optical transient at $z=3.709$ (Sect. 6.3.1). On the other hand, the foreground absorber could be the faint object to the south-east of the possible host galaxy.

Chapter 7

Summary

Gamma-Ray Bursts in the prompt emission phase differ in various aspects, like in their morphology, luminosity, released energy and duration. Similarly, the observed phenomenology of their afterglows can be very different from each other. In this Thesis three very different GRBs have been analyzed in detail which demonstrate the richness in observational phenomena in several ways.

All bursts might have in common that they are signals of the formation of a compact stellar object, either a black hole or a neutron star. The plethora of phenomena which the observer can discover might depend on several physical parameters like (for long bursts) the mass, the angular momentum and the chemical composition of the collapsing star, or (for short bursts) the mass and nature (black hole-neutron star, neutron star-neutron star, black hole-white dwarf) of the merging stellar compact objects. All these properties might finally link to the energy released, the jet opening angles of the relativistic outflows, and the duration of the events in the gamma-ray band. In the optical bands, which are still the observational window where most information is obtained on the nature of the bursts and the physical processes related to them, additional parameters determine the observational phenomena like the extinction in the GRB host galaxy as well as the density and structure of the interstellar medium surrounding the burster into which the relativistic outflow (the fireball) expands. Microphysical parameters finally enter the theoretical description of the afterglow light, parameters which also might vary from burst to burst (which is indeed deduced from observational data but there is still no theoretical explanation for that). So, it is not surprising that follow-up observations of GRBs reveal a rich variety of light curves, luminosities and spectral energy distributions. This Thesis shows this variety in three special cases.

I have reported here on the detailed investigation of three bursts discovered by the *Swift* GRB satellite launched at the end of 2004. These bursts are very different from each other: a short burst (050813, duration about 0.6 seconds), a relatively normal long burst (060605, duration about 15 seconds) and a very long event (060218, duration about 2000 seconds) that finally turned out to be the signal of a very nearby GRB supernova. Two of these events were mainly followed by us with the ESO Very Large Telescope (050813 and 060218), while in the case of GRB 060605 the most important data were obtained with the 3.5m telescope on Calar Alto.

In the case of GRB 050813, we started our observing campaign with a deep imaging of the

Swift X-ray error circle with the VIMOS Integral Field Unit at the VLT but unfortunately had to discover that VIMOS suffered from mechanical problems at that time. Our additional deep follow-up observations with VLT/FORS2 allowed us, however, to set constraints on any fading afterglow and any rising supernova component following this burst. In particular, we conclude that if GRB 050813 was occurring in a cluster of galaxies at a redshift of $z=0.72$, as it might be indicated by the surrounding galaxy population, then its projected distance from its potential host galaxy could have been of the order of less than 4 to some dozen kpc, depending on the chosen potential host galaxy. The non-detection of the afterglow is well in accord with the faintness of optical afterglows following short bursts (Fig. 5.11). While the constraint we could set on the appearance of supernova light some days after the burst is not that strong, all our observational data support the interpretation that GRB 050813 was a *bona-fide* short burst.

The second event that was in detail studied in this Thesis was GRB 060218, which developed a bright supernova, now designated SN 2006aj. This GRB supernova was the fastest evolving and one of the least luminous GRB-SN discovered so far, being only about 70% as luminous as SN 1998bw. This places it at the faint end of the GRB-SN luminosity distribution which so far, after extinction correction, covers the range from about 0.6 to 2 times the luminosity of SN 1998bw. Placing SN 2006aj in the context of the luminosities of local Type Ic supernovae without detected GRB reveals, however, that SN 2006aj is still at the bright end of their luminosity distribution. SN 2006aj thus followed the general “rule” that GRB-SNe tend to be more luminous than (local) Type Ic SNe without detected GRB. Furthermore, GRBs 980425 and 060218 suggest that the prompt emission properties are not correlated with the optical properties of the associated SNe. GRB 980425 had a duration of 31 sec (Pian et al. 1999), while GRB 060218 lasted for more than 2000 sec (Campana et al. 2006), and the corresponding isotropic equivalent energy release in the gamma-ray band was different by a factor of 10. The corresponding SN luminosities, however, differ by only 30%. Assuming that differences in instrumental sensitivities (*BeppoSAX* versus *Swift*) do not play a role here, this supports the notion that the properties of the GRB and the associated SN are to a large extent independent of each other.

Finally, we obtained a lot of observational data on the afterglow of GRB 060605, which allowed us a detailed analysis of this event. In particular, we were able to derive its spectroscopic redshift and could in detail investigate its afterglow from the optical to the X-ray bands. Noteworthy, in the optical, at early times, the afterglow was among the most luminous ever detected. The afterglow spectrum revealed two absorption line systems at redshifts 3.773 and 3.709. We identified the former with the redshift of the burst, i.e., its host galaxy, with the latter possibly identified on deep VLT images. The smaller redshift could either be a signature from the stellar wind of the GRB progenitor or an imprinted signal from a foreground absorber. The measured HI column density for the host galaxy is unfortunately uncertain, ranging from $N_{\text{HI}} = 10^{18.5}$ to $10^{19.3}$ cm^{-2} . It is in any case one of the lowest ever detected in a GRB afterglow. From the X-ray/optical light curve we conclude that the most likely scenario is that the afterglow propagated into an ISM environment. The early jet break time we found (in the GRB host frame at about 4900 seconds after the burst) is the most remarkable property of this burst, implying a relatively small beaming angle of the

collimated outflow of about 2.4 degrees.

It should be stressed that many of the observational results we have obtained on these three events entered other studies of our group on more general terms of afterglow phenomenology (Kann et al. 2007, 2008). In addition, several other bursts, which were in detail investigated by our group (e.g., Greiner et al. 2008; Rossi et al. 2008), underlined further the richness of observational phenomena related to GRBs.

Appendix A

Integral Field Spectroscopy

Observations of the afterglow of GRB 060605 were performed using the Integral Field Unit (IFU) at the 3.5m telescope on Calar Alto, Spain. The original motivation for having such an approved observing proposal is explained below. While we were successful to get observing time for the very best IFUs available worldwide, we were finally faced with bad luck: (1) basically all the VIMOS data we got (for GRBs 061222B, 070129, 070306, 070411) turned out to be not useful because the limiting magnitude of VIMOS was found to be below its expectations, or technical problems hampered any data reduction (in the case of GRB 050813). (2) The Calar Alto proposal was only accepted twice and in these two semesters only three burst occurred that were observable from Calar Alto within hours. GRB 060526 was the first observed, but unfortunately due to its redshift (3.221, unknown at the moment of the trigger), the used set-up resulted to be the wrong one. The second was GRB 060605, whose afterglow was bright enough for PMAS/PPak. In case of GRB 070920, the first acquisition image was taken 11 minutes after the event, but in that case no OT was present and no IFU run was performed.

In the following the basic ideas and techniques of 3D data reduction are summarized.

A.1 Why using Integral Field Spectroscopy?

As explained in Chapters 1 and 2 the study and detection of the afterglows enable sub-arcsecond localization of the burst and unambiguous determination of its host galaxy and its redshift if the afterglow is bright enough. Besides this, the afterglow itself provides information about the physical processes that work and can reveal clues on the nature of the central engine and about the environmental properties of the progenitors. Most of these data can be derived only via a spectroscopic analysis of the optical and X-ray afterglow. The afterglows are usually identified as either new objects in comparison to archival images or by their fading behaviour.

Even though optical afterglows can be very bright at the beginning, the rapid fading of these transients makes the timing of observations crucial for the acquisition of spectroscopic data with a sufficient signal-to-noise (S/N) ratio. However, due to the time usually needed to identify the optical transient in a GRB X-ray error circle, rapid spectroscopic follow-up observations are a challenge. Indeed long-slit spectroscopy has to await the identification of the afterglow, or a best guess has to be made; i.e., if the error box is very small, one can

assume that the afterglow is the brightest object in the field. Integral field spectroscopy (IFS), on the other hand, using integral field units (IFUs), can start getting spectra of an entire error box as soon as an arcsecond X-ray location has been reported, usually in the case of the *Swift* satellite within minutes after the GRB trigger. In principle, once the afterglow has been identified by other means, IFS data could then be used to extract early spectra. This procedure would minimise an important bias, namely the pre-selection of afterglows for spectroscopic follow-up observations according to their apparent magnitude at the time of their discovery. Furthermore, in the *Swift* era, many optical afterglows are discovered first by the *Swift* UV/optical telescope which has only filters up to the v band precluding the rapid localization of $z \gtrsim 5$ or of highly extinguished afterglows (cf. Roming et al. 2006). Needing only *Swift* XRT localizations, IFS is basically not affected by this color-selection bias.

A.2 IFS vs. Long-Slit Spectroscopy

Traditional spectroscopy is based on dispersing the image of a slit (single or multiple) so that a spectrum is produced for whatever fraction of the light from the target of interest falls within the aperture defined by the slit. If the slit is extended in length beyond the confines of the target, then it is also possible to record the spectrum of the adjacent sky to subtract from that of the object – particularly important if the object is fainter than the sky, which is very frequently the case. While this is satisfactory for many applications, it makes poor use of the incident light when the object is extended, either intrinsically or due to poor seeing. In these cases, what is really required is the ability to record a spectrum from each part of an extended object.

This cannot be done with a long-slit except in one dimension defined by the length of the slit. However the long-slit can be stepped in position across the target by moving the telescope and recording separate exposures for each position. But this is time-consuming since the effective exposure time is multiplied by roughly the ratio of the object size to the width of the slit.

Other techniques are available such as Fabry-Perot scanning. This allows a large object to be surveyed in a single exposure but only at a single wavelength (which depends on position within the field) so that the required data volume with axes labeled by x -position, y -position and wavelength must be built up via a series of exposures. As with stepped long-slit spectroscopy, this is not a very efficient use of telescope time.

Techniques which record spectra from each part of an object simultaneously are termed Integral Field Spectroscopy. The terms two-dimensional spectroscopy or three-dimensional imaging are also used, although, strictly, they include non-simultaneous techniques as well.

Figure A.1 illustrates schematically a datacube resulting from a fully reduced 3D spectroscopy exposure. Depending on the specific application, one can analyse the dataset either in the picture of a of monochromatic images, or in the picture of single spectra, or groups of spectra, respectively.

A.3 Basic techniques

There are three main techniques (see Fig. A.2).

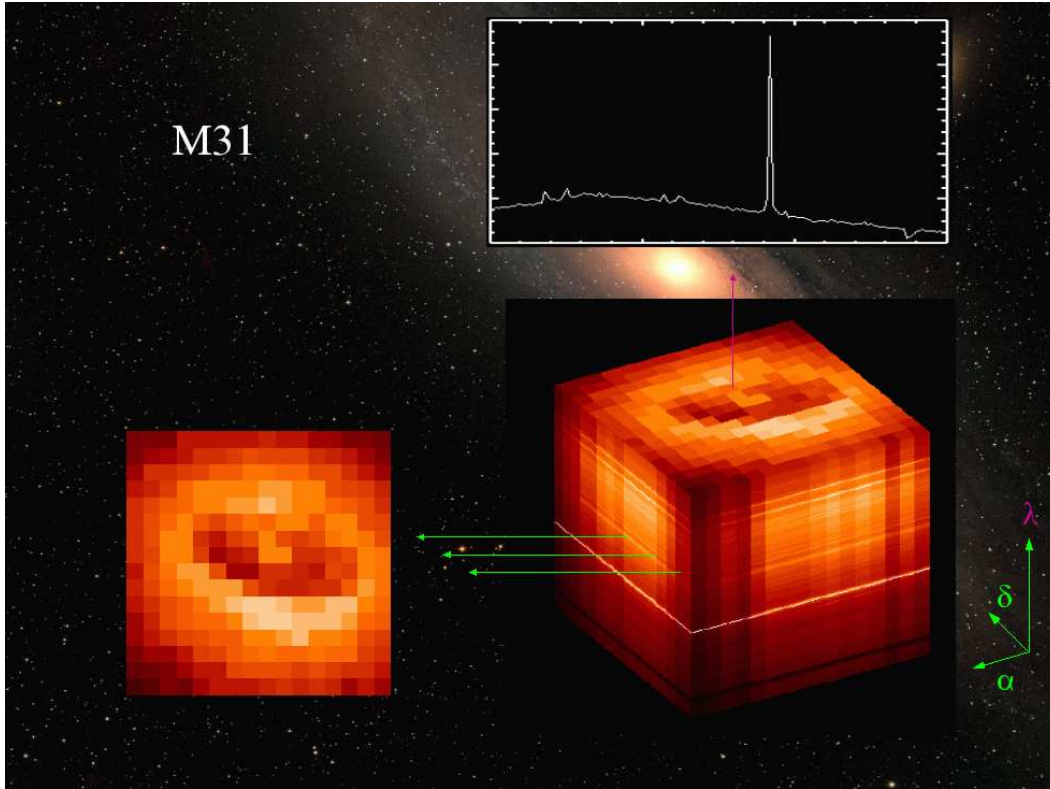


Figure A.1: *Datacube as obtained with 3D spectroscopy (adapted from M. M. Roth, power-point presentation, Garching, May 2004).*

Lenslet arrays: The input image is formed at the input surface of a microlens array (MLA). These form images of the telescope pupil which are then dispersed by the spectrograph. The pupil images are smaller than the aperture of each microlens so that light from each segment of the input image is concentrated into a dot. Because the dots are small, it is possible to tilt the MLA about the optical axis of the system so that the spectra do not fall on top of each other. This technique allows the input image to be sampled contiguously and is not subject to Focal Ratio Degradation (FRD)¹, so that the throughput and spectral resolution can be optimised, but the length of the spectrum that can be produced without overlapping is very small.

Fiber bundles: The input image is formed at the entrance to a bundle of fibers which transfer the light to the slit of the spectrograph. The flexibility of the fibres allows a round field of view to be reformatted into one (or more) slits so that the spectra are obtained without wavelength shifts between them. The disadvantages of this techniques are: (a) the sampling of the sky is not contiguous since there are gaps between the fibre cores and (b) all the fibres do not work in the same efficient way (causing FRD).

Image slicers: The input image is formed at segmented thin horizontal sections which are then sent in slightly different directions. A second segmented mirror is arranged to reformat

¹The Focal Ratio Degradation (FRD) is the decrease in focal ratio (decrease in effective F-number) in an optical fiber versus its length. Practically it depends on the ability of a fiber to preserve the angular distribution of the input beam from the telescope to the spectrometer.

the slices so that, instead of being above each other they are now laid out end to end to form the slit of the spectrograph (actually a virtual slit). The advantage of this technique is that FRD is avoided and the slicing arrangement gives contiguous coverage of the field. Because this system uses only mirrors, it is especially suitable for the infrared since it is inherently achromatic and can be cooled to cryogenic temperatures. Potential disadvantages are: (a) that the sampling along the slices is the same as that provided naturally by the telescope so there is reduced scope to optimise for use with a spectrograph that must also work in a normal slit-spectroscopy mode and (b) the optical system might be bulky and difficult to fabricate.

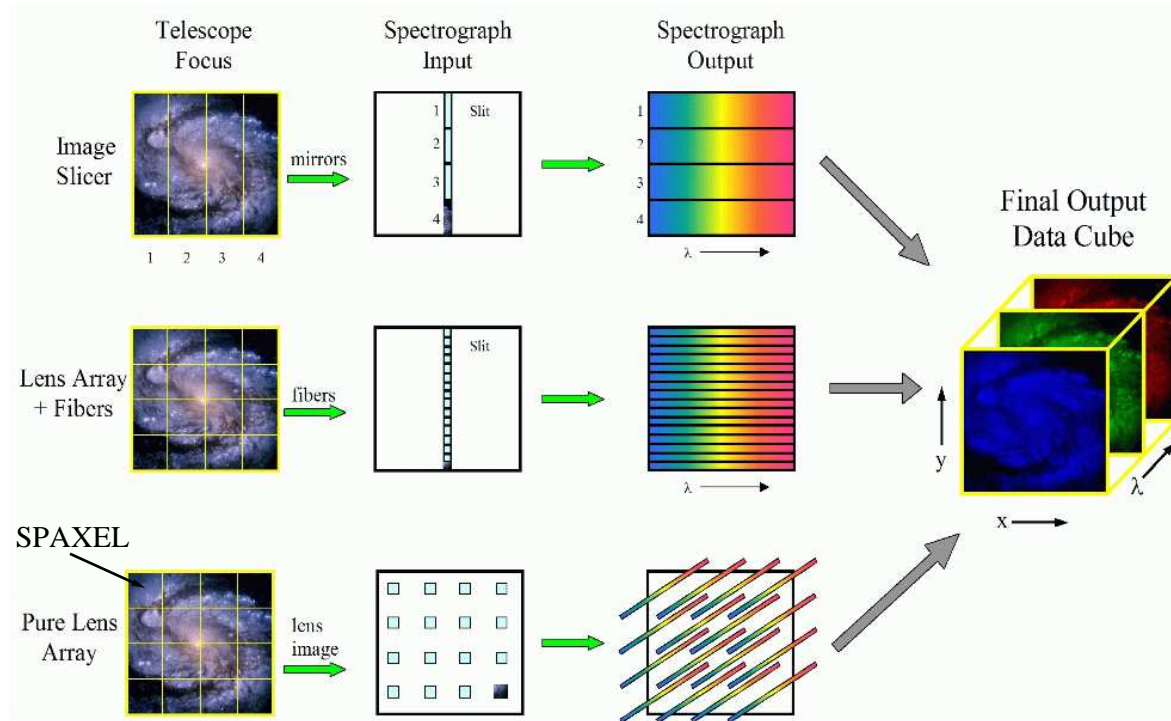


Figure A.2: A graphical representation of the three main techniques of the IFS (adapted from Richard McDermid's talk, IFU Neon School, May 2008, Potsdam).

A.4 Reduction and visualization of 3D data

The different implementations discussed in the previous paragraph have produced a set of instruments, which, while sharing the basics of the technique, produce very different representations of the spectra at the detectors. This apparent diversity has led to the development of reduction techniques and/or packages for each individual instrument (e.g., P3D: Becker 2002 and Roth et al. 2005; GEMINI, Turner et al. 2006). Together with the inherent complexity of this technique, this has reduced the use of IFS for decades to a handful of specialists, each usually working with a specific instrument.

IFS developers became aware of this handicap, and have started to produce standard techniques and tools valid for any integral field unit (IFU). In a recent effort, the Euro3D RTN (Walsh & Roth 2002) has created a standard data format (Kissler-Patig et al. 2004), a

coding platform (Pécontal-Rousset et al. 2004) and a visualization tool (E3D; Sánchez 2004), useful for any of the existing IFUs. All these tools are freely distributed to the community. However most of them are for working with reduced data, while the reduction itself has still not been addressed with a general approach.

A further step in this direction has been done by Sánchez & Cardiel (2005) and Sánchez (2006), who have tried to implement all of the main steps of the reduction progress in R3D, a reduction package coded in Perl able to reduce data from any fiber-fed IFU.

Bibliography

- Achterberg, A., Gallant, Y. A., Kirk, J. G., and Guthmann, A. W. 2001, *Mon. Not. R. Astron. Soc.*, 328, 393
- Adelman-McCarthy, J. K., Agüeros, M. A., Allam, S. S., Anderson, K. S. J., Anderson, S. F., Annis, J., Bahcall, N. A., Baldry, I. K., Barentine, J. C., Berlind, A., Bernardi, M., Blanton, M. R., Boroski, W. N., Brewington, H. J., Brinchmann, J., Brinkmann, J., Brunner, R. J., Budavári, T., Carey, L. N., Carr, M. A., Castander, F. J., Connolly, A. J., Csabai, I., Czarapata, P. C., Dalcanton, J. J., Doi, M., Dong, F., Eisenstein, D. J., Evans, M. L., Fan, X., Finkbeiner, D. P., Friedman, S. D., Frieman, J. A., Fukugita, M., Gillespie, B., Glazebrook, K., Gray, J., Grebel, E. K., Gunn, J. E., Gurbani, V. K., de Haas, E., Hall, P. B., Harris, F. H., Harvanek, M., Hawley, S. L., Hayes, J., Hendry, J. S., Hennessy, G. S., Hindsley, R. B., Hirata, C. M., Hogan, C. J., Hogg, D. W., Holmgren, D. J., Holtzman, J. A., Ichikawa, S.-i., Ivezić, Ž., Jester, S., Johnston, D. E., Jorgensen, A. M., Jurić, M., Kent, S. M., Kleinman, S. J., Knapp, G. R., Kniazev, A. Y., Kron, R. G., Krzesinski, J., Kuropatkin, N., Lamb, D. Q., Lampeitl, H., Lee, B. C., Leger, R. F., Lin, H., Long, D. C., Loveday, J., Lupton, R. H., Margon, B., Martínez-Delgado, D., Mandelbaum, R., Matsubara, T., McGehee, P. M., McKay, T. A., Meiksin, A., Munn, J. A., Nakajima, R., Nash, T., Neilsen, Jr., E. H., Newberg, H. J., Newman, P. R., Nichol, R. C., Nicinski, T., Nieto-Santisteban, M., Nitta, A., O'Mullane, W., Okamura, S., Owen, R., Padmanabhan, N., Pauls, G., Peoples, J. J., Pier, J. R., Pope, A. C., Pourbaix, D., Quinn, T. R., Richards, G. T., Richmond, M. W., Rockosi, C. M., Schlegel, D. J., Schneider, D. P., Schroeder, J., Scranton, R., Seljak, U., Sheldon, E., Shimasaku, K., Smith, J. A., Smolčić, V., Snedden, S. A., Stoughton, C., Strauss, M. A., SubbaRao, M., Szalay, A. S., Szapudi, I., Szkody, P., Tegmark, M., Thakar, A. R., Tucker, D. L., Uomoto, A., Vanden Berk, D. E., Vandenberg, J., Vogeley, M. S., Voges, W., Vogt, N. P., Walkowicz, L. M., Weinberg, D. H., West, A. A., White, S. D. M., Xu, Y., Yanny, B., Yocum, D. R., York, D. G., Zehavi, I., Zibetti, S., and Zucker, D. B. 2006, *Astroph. J. Suppl.*, 162, 38
- Akerlof, C., Balsano, R., Barthelmy, S., Bloch, J., Butterworth, P., Casperon, D., Cline, T., Fletcher, S., Frontera, F., Gisler, G., Heise, J., Hills, J., Kehoe, R., Lee, B., Marshall, S., McKay, T., Miller, R., Piro, L., Priedhorsky, W., Szymanski, J., and Wren, J. 1999, *Nature*, 398, 400
- Amati, L., Frontera, F., Guidorzi, C., and Montanari, E. 2006, *GCN Circ.*, 4846, 1
- Band, D., Matteson, J., Ford, L., Schaefer, B., Palmer, D., Teegarden, B., Cline, T., Briggs, M., Paciasas, W., Pendleton, G., Fishman, G., Kouveliotou, C., Meegan, C., Wilson, R., and Lestrade, P. 1993, *Astroph. J.*, 413, 281
- Barthelmy, S. D., Barbier, L. M., Cummings, J. R., Fenimore, E. E., Gehrels, N., Hullinger, D., Krimm, H. A., Markwardt, C. B., Palmer, D. M., Parsons, A., Sato, G., Suzuki, M., Takahashi, T., Tashiro, M., and Tueller, J. 2005, *Space Science Reviews*, 120, 143
- Becker, T. 2002, PhD thesis, University of Potsdam
- Belczynski, K., Bulik, T., and Kalogera, V. 2002, *Astroph. J.*, 571, L147
- Belczynski, K., Perna, R., Bulik, T., Kalogera, V., Ivanova, N., and Lamb, D. Q. 2006, *Astroph. J.*, 648, 1110

- Berger, E. 2005, GCN Circ., 3801
- Berger, E. 2006, in American Institute of Physics Conference Series, Vol. 836, Gamma-Ray Bursts in the Swift Era, ed. S. S. Holt, N. Gehrels, & J. A. Nousek, 33–42
- Berger, E. 2008, ArXiv e-prints, 0805.0306
- Berger, E., Fox, D. B., Price, P. A., Nakar, E., Gal-Yam, A., Holz, D. E., Schmidt, B. P., Cucchiara, A., Cenko, S. B., Kulkarni, S. R., Soderberg, A. M., Frail, D. A., Penprase, B. E., Rau, A., Ofek, E., Burnell, S. J. B., Cameron, P. B., Cowie, L. L., Dopita, M. A., Hook, I., Peterson, B. A., Podsiadlowski, P., Roth, K. C., Rutledge, R. E., Sheppard, S. S., and Songaila, A. 2007, *Astroph. J.*, 664, 1000
- Berger, E., Price, P. A., Cenko, S. B., Gal-Yam, A., Soderberg, A. M., Kasliwal, M., Leonard, D. C., Cameron, P. B., Frail, D. A., Kulkarni, S. R., Murphy, D. C., Krzeminski, W., Piran, T., Lee, B. L., Roth, K. C., Moon, D.-S., Fox, D. B., Harrison, F. A., Persson, S. E., Schmidt, B. P., Penprase, B. E., Rich, J., Peterson, B. A., and Cowie, L. L. 2005, *Nature*, 438, 988
- Bersier, D., Fruchter, A. S., Strolger, L.-G., Gorosabel, J., Levan, A., Burud, I., Rhoads, J. E., Becker, A. C., Cassan, A., Chornock, R., Covino, S., de Jong, R. S., Dominis, D., Filippenko, A. V., Hjorth, J., Holmberg, J., Malesani, D., Mobasher, B., Olsen, K. A. G., Stefanon, M., Castro Cerón, J. M., Fynbo, J. P. U., Holland, S. T., Kouveliotou, C., Pedersen, H., Tanvir, N. R., and Woosley, S. E. 2006, *Astroph. J.*, 643, 284
- Bessell, M. S. 1979, *Publ. Astron. Soc. Pacific*, 91, 589
- Bikmaev, I., Galeev, A., Sakhbullin, N., Burenin, R., Pavlinsky, M., Sunyaev, R., Aslan, Z., Khamitov, I., Kiziloglu, U., and Alpar, A. 2005, GCN Circ., 3797, 1
- Blackburn, J. K. 1995, in *Astronomical Society of the Pacific Conference Series*, Vol. 77, *Astronomical Data Analysis Software and Systems IV*, ed. R. A. Shaw, H. E. Payne, & J. J. E. Hayes, 367
- Blinnikov, S. I., Novikov, I. D., Perevodchikova, T. V., and Polnarev, A. G. 1984, *Soviet Astronomy Letters*, 10, 177
- Bloom, J. S., Frail, D. A., and Kulkarni, S. R. 2003, *Astroph. J.*, 594, 674
- Bloom, J. S., Kulkarni, S. R., and Djorgovski, S. G. 2002, *Astron. J.*, 123, 1111
- Bloom, J. S., Kulkarni, S. R., Djorgovski, S. G., Eichelberger, A. C., Côté, P., Blakeslee, J. P., Odewahn, S. C., Harrison, F. A., Frail, D. A., Filippenko, A. V., Leonard, D. C., Riess, A. G., Spinrad, H., Stern, D., Bunker, A., Dey, A., Grossan, B., Perlmutter, S., Knop, R. A., Hook, I. M., and Feroci, M. 1999, *Nature*, 401, 453
- Bloom, J. S. and Prochaska, J. X. 2006, in American Institute of Physics Conference Series, Vol. 836, Gamma-Ray Bursts in the Swift Era, ed. S. S. Holt, N. Gehrels, & J. A. Nousek, 473–482
- Bloom, J. S., Prochaska, J. X., Pooley, D., Blake, C. H., Foley, R. J., Jha, S., Ramirez-Ruiz, E., Granot, J., Filippenko, A. V., Sigurdsson, S., Barth, A. J., Chen, H.-W., Cooper, M. C., Falco, E. E., Gal, R. R., Gerke, B. F., Gladders, M. D., Greene, J. E., Hennanwi, J., Ho, L. C., Hurley, K., Koester, B. P., Li, W., Lubin, L., Newman, J., Perley, D. A., Squires, G. K., and Wood-Vasey, W. M. 2006, *Astroph. J.*, 638, 354
- Blustin, A. J., Band, D., Barthelmy, S., Boyd, P., Capalbi, M., Holland, S. T., Marshall, F. E., Mason, K. O., Perri, M., Poole, T., Roming, P., Rosen, S., Schady, P., Still, M., Zhang, B., Angelini, L., Barbier, L., Beardmore, A., Breeveld, A., Burrows, D. N., Cummings, J. R., Canizzo, J., Campana, S., Chester, M. M., Chincarini, G., Cominsky, L. R., Cucchiara, A., de Pasquale, M., Fenimore, E. E., Gehrels, N., Giommi, P., Goad, M., Gronwall, C., Grupe, D., Hill, J. E., Hinshaw, D., Hunsberger, S., Hurley, K. C., Ivanushkina, M., Kennea, J. A., Krimm, H. A., Kumar, P.,

- Landsman, W., La Parola, V., Markwardt, C. B., McGowan, K., Mészáros, P., Mineo, T., Moretti, A., Morgan, A., Nousek, J., O'Brien, P. T., Osborne, J. P., Page, K., Page, M. J., Palmer, D. M., Parsons, A. M., Rhoads, J., Romano, P., Sakamoto, T., Sato, G., Tagliaferri, G., Tueller, J., Wells, A. A., and White, N. E. 2006, *Astroph. J.*, 637, 901
- Blustin, A. J. and Page, M. J. 2006, *GCN Circ.*, 5228, 1
- Blustin, A. J., Retter, A., Page, M. J., Nousek, J., Voges, W., and Gehrels, N. 2005, *GCN Circ.*, 3791, 1
- Boella, G., Butler, R. C., Perola, G. C., Piro, L., Scarsi, L., and Bleeker, J. A. M. 1997a, *Astron. & Astroph. Suppl.*, 122, 299
- Boella, G., Chiappetti, L., Conti, G., Cusumano, G., del Sordo, S., La Rosa, G., Maccarone, M. C., Mineo, T., Molendi, S., Re, S., Sacco, B., and Tripiciano, M. 1997b, *Astron. & Astroph. Suppl.*, 122, 327
- Bromm, V. and Schaefer, B. E. 1999, *Astroph. J.*, 520, 661
- Burrows, D. N., Hill, J. E., Nousek, J. A., Kennea, J. A., Wells, A., Osborne, J. P., Abbey, A. F., Beardmore, A., Mukerjee, K., Short, A. D. T., Chincarini, G., Campana, S., Citterio, O., Moretti, A., Pagani, C., Tagliaferri, G., Giommi, P., Capalbi, M., Tamburelli, F., Angelini, L., Cusumano, G., Bräuninger, H. W., Burkert, W., and Hartner, G. D. 2005, *Space Science Reviews*, 120, 165
- Butler, N. R. 2007, *Astron. J.*, 133, 1027
- Butler, N. R., Kocevski, D., Bloom, J. S., and Curtis, J. L. 2007, *Astroph. J.*, 671, 656
- Campana, S., Mangano, V., Blustin, A. J., Brown, P., Burrows, D. N., Chincarini, G., Cummings, J. R., Cusumano, G., Della Valle, M., Malesani, D., Mészáros, P., Nousek, J. A., Page, M., Sakamoto, T., Waxman, E., Zhang, B., Dai, Z. G., Gehrels, N., Immler, S., Marshall, F. E., Mason, K. O., Moretti, A., O'Brien, P. T., Osborne, J. P., Page, K. L., Romano, P., Roming, P. W. A., Tagliaferri, G., Cominsky, L. R., Giommi, P., Godet, O., Kennea, J. A., Krimm, H., Angelini, L., Barthelmy, S. D., Boyd, P. T., Palmer, D. M., Wells, A. A., and White, N. E. 2006, *Nature*, 442, 1008
- Castro-Tirado, A. J., de Ugarte Postigo, A., Gorosabel, J., Fathkullin, T., Sokolov, V., Bremer, M., Márquez, I., Marín, A. J., Guziy, S., Jelínek, M., Kubánek, P., Hudec, R., Vitek, S., Mateo Sanguino, T. J., Eigenbrod, A., Pérez-Ramírez, M. D., Sota, A., Masegosa, J., Prada, F., and Moles, M. 2005, *Astron. & Astroph.*, 439, L15
- Chen, C. H., Patten, B. M., Werner, M. W., Dowell, C. D., Stapelfeldt, K. R., Song, I., Stauffer, J. R., Blaylock, M., Gordon, K. D., and Krause, V. 2005, *Astroph. J.*, 634, 1372
- Chen, H.-W., Prochaska, J. X., and Gnedin, N. Y. 2007a, *Astroph. J.*, 667, L125
- Chen, H.-W., Prochaska, J. X., Ramirez-Ruiz, E., Bloom, J. S., Dessauges-Zavadsky, M., and Foley, R. J. 2007b, *Astroph. J.*, 663, 420
- Chevalier, R. A. and Li, Z.-Y. 2000, *Astroph. J.*, 536, 195
- Christensen, L., Hjorth, J., and Gorosabel, J. 2004, *Astron. & Astroph.*, 425, 913
- Cobb, B. E., Bailyn, C. D., van Dokkum, P. G., and Natarajan, P. 2006, *Astroph. J.*, 645, L113
- Cool, R. J., Eisenstein, D. J., Hogg, D. W., Blanton, M. R., Schlegel, D. J., Brinkmann, J., Schneider, D. P., and vanden Berk, D. E. 2006, *GCN Circ.*, 4777, 1

- Costa, E., Frontera, F., Heise, J., Feroci, M., in't Zand, J., Fiore, F., Cinti, M. N., Dal Fiume, D., Nicastro, L., Orlandini, M., Palazzi, E., Rapisarda#, M., Zavattini, G., Jager, R., Parmar, A., Owens, A., Molendi, S., Cusumano, G., Maccarone, M. C., Giarrusso, S., Coletta, A., Antonelli, L. A., Giommi, P., Muller, J. M., Piro, L., and Butler, R. C. 1997, *Nature*, 387, 783
- Covino, S., Malesani, D., Israel, G. L., D'Avanzo, P., Antonelli, L. A., Chincarini, G., Fugazza, D., Conciatore, M. L., Della Valle, M., Fiore, F., Guetta, D., Hurley, K., Lazzati, D., Stella, L., Tagliaferri, G., Vietri, M., Campana, S., Burrows, D. N., D'Elia, V., Filliatre, P., Gehrels, N., Goldoni, P., Melandri, A., Mereghetti, S., Mirabel, I. F., Moretti, A., Nousek, J., O'Brien, P. T., Pellizza, L. J., Perna, R., Piranomonte, S., Romano, P., and Zerbi, F. M. 2006, *Astron. & Astroph.*, 447, L5
- Cusumano, G., Barthelmy, S., Gehrels, N., Hunsberger, S., Immler, S., Marshall, F., Palmer, D., and Sakamoto, T. 2006, *GCN Circ.*, 4775, 1
- de Ugarte Postigo, A. 2007, PhD thesis, Instituto de Astrofísica de Andalucía
- de Ugarte Postigo, A., Castro-Tirado, A. J., Guziy, S., Gorosabel, J., Jóhannesson, G., Aloy, M. A., McBreen, S., Lamb, D. Q., Benitez, N., Jelínek, M., Pandey, S. B., Coe, D., Pérez-Ramírez, M. D., Aceituno, F. J., Alises, M., Acosta-Pulido, J. A., Gómez, G., López, R., Donaghy, T. Q., Nakagawa, Y. E., Sakamoto, T., Ricker, G. R., Hearty, F. R., Bayliss, M., Gyuk, G., and York, D. G. 2006, *Astroph. J.*, 648, L83
- Della Valle, M., Chincarini, G., Panagia, N., Tagliaferri, G., Malesani, D., Testa, V., Fugazza, D., Campana, S., Covino, S., Mangano, V., Antonelli, L. A., D'Avanzo, P., Hurley, K., Mirabel, I. F., Pellizza, L. J., Piranomonte, S., and Stella, L. 2006a, *Nature*, 444, 1050
- Della Valle, M., Malesani, D., Bloom, J. S., Benetti, S., Chincarini, G., D'Avanzo, P., Foley, R. J., Covino, S., Melandri, A., Piranomonte, S., Tagliaferri, G., Stella, L., Gilmozzi, R., Antonelli, L. A., Campana, S., Chen, H.-W., Filliatre, P., Fiore, F., Fugazza, D., Gehrels, N., Hurley, K., Mirabel, I. F., Pellizza, L. J., Piro, L., and Prochaska, J. X. 2006b, *Astroph. J.*, 642, L103
- Deng, J., Tominaga, N., Mazzali, P. A., Maeda, K., and Nomoto, K. 2005, *Astroph. J.*, 624, 898
- Dickey, J. M. and Lockman, F. J. 1990, *Annu. Rev. Astro. Astroph.*, 28, 215
- Djorgovski, S. G., Frail, D. A., Kulkarni, S. R., Bloom, J. S., Odewahn, S. C., and Diercks, A. 2001, *Astroph. J.*, 562, 654
- Donaghy, T. Q., Lamb, D. Q., Sakamoto, T., Norris, J. P., Nakagawa, Y., Villasenor, J., Atteia, J. ., Vanderspek, R., Graziani, C., Kawai, N., Ricker, G. R., Crew, G. B., Doty, J., Prigozhin, G., Jernigan, J. G., Shirasaki, Y., Suzuki, M., Butler, N., Hurley, K., Tamagawa, T., Yoshida, A., Matsuoka, M., Fenimore, E. E., Galassi, M., Boer, M., Dezalay, J. ., Olive, J. ., Levine, A., Martel, F., Morgan, E., Sato, R., Woosley, S. E., Braga, J., Manchanda, R., Pizzichini, G., Takagishi, K., and Yamauchi, M. 2006, *ArXiv e-prints*, astro-ph/0605570
- Evans, P. A., Beardmore, A. P., Page, K. L., Tyler, L. G., Osborne, J. P., Goad, M. R., O'Brien, P. T., Vetere, L., Racusin, J., Morris, D., Burrows, D. N., Capalbi, M., Perri, M., Gehrels, N., and Romano, P. 2007, *Astron. & Astroph.*, 469, 379
- Ferrero, P., Kann, D. A., Zeh, A., Klose, S., Pian, E., Palazzi, E., Masetti, N., Hartmann, D. H., Sollerman, J., Deng, J., Filippenko, A. V., Greiner, J., Hughes, M. A., Mazzali, P., Li, W., Rol, E., Smith, R. J., and Tanvir, N. R. 2006, *Astron. & Astroph.*, 457, 857
- Ferrero, P., Palazzi, E., Pian, E., and Savaglio, S. 2007a, in *American Institute of Physics Conference Series*, Vol. 924, *The Multicolored Landscape of Compact Objects and Their Explosive Origins*, 120–125

- Ferrero, P., Sanchez, S. F., Kann, D. A., Klose, S., Greiner, J., Gorosabel, J., Hartmann, D. H., Henden, A. A., Møller, P., Palazzi, E., Rau, A., Stecklum, B., Castro-Tirado, A. J., Fynbo, J. P. U., Hjorth, J., Jakobsson, P., Kouveliotou, C., Masetti, N., Pian, E., Tanvir, N. R., and Wijers, R. A. M. J. 2007b, *Astron. J.*, 134, 2118
- Fiore, F., D'Elia, V., Lazzati, D., Perna, R., Sbordone, L., Stratta, G., Meurs, E. J. A., Ward, P., Antonelli, L. A., Chincarini, G., Covino, S., Di Paola, A., Fontana, A., Ghisellini, G., Israel, G., Frontera, F., Marconi, G., Stella, L., Vietri, M., and Zerbi, F. 2005, *Astroph. J.*, 624, 853
- Fishman, G. J., Meegan, C. A., Parnell, T. A., Wilson, R. B., Paciasas, W., Mateson, J. L., Cline, T. L., and Teegarden, B. J. 1985, in *International Cosmic Ray Conference*, Vol. 3, NASA. Goddard Space Flight Center 19th Intern. Cosmic Ray Conf., ed. F. C. Jones, 343–346
- Foley, R. J., Bloom, J. S., and Chen, H.-W. 2005, *GCN Circ.*, 3808, 1
- Ford, L. A., Band, D. L., Matteson, J. L., Briggs, M. S., Pendleton, G. N., Preece, R. D., Paciasas, W. S., Teegarden, B. J., Palmer, D. M., Schaefer, B. E., Cline, T. L., Fishman, G. J., Kouveliotou, C., Meegan, C. A., Wilson, R. B., and Lestrade, J. P. 1995, *Astroph. J.*, 439, 307
- Fox, D. B., Frail, D. A., Price, P. A., Kulkarni, S. R., Berger, E., Piran, T., Soderberg, A. M., Cenko, S. B., Cameron, P. B., Gal-Yam, A., Kasliwal, M. M., Moon, D.-S., Harrison, F. A., Nakar, E., Schmidt, B. P., Penprase, B., Chevalier, R. A., Kumar, P., Roth, K., Watson, D., Lee, B. L., Sheckman, S., Phillips, M. M., Roth, M., McCarthy, P. J., Rauch, M., Cowie, L., Peterson, B. A., Rich, J., Kawai, N., Aoki, K., Kosugi, G., Totani, T., Park, H.-S., MacFadyen, A., and Hurley, K. C. 2005, *Nature*, 437, 845
- Frail, D. A., Kulkarni, S. R., Nicastro, L., Feroci, M., and Taylor, G. B. 1997, *Nature*, 389, 261
- Frail, D. A., Kulkarni, S. R., Sari, R., Djorgovski, S. G., Bloom, J. S., Galama, T. J., Reichart, D. E., Berger, E., Harrison, F. A., Price, P. A., Yost, S. A., Diercks, A., Goodrich, R. W., and Chaffee, F. 2001, *Astroph. J.*, 562, L55
- Frontera, F., Costa, E., dal Fiume, D., Feroci, M., Nicastro, L., Orlandini, M., Palazzi, E., and Zavattini, G. 1997, *Astron. & Astroph. Suppl.*, 122, 357
- Fruchter, A. S., Levan, A. J., Strolger, L., Vreeswijk, P. M., Thorsett, S. E., Bersier, D., Burud, I., Castro Cerón, J. M., Castro-Tirado, A. J., Conselice, C., Dahlen, T., Ferguson, H. C., Fynbo, J. P. U., Garnavich, P. M., Gibbons, R. A., Gorosabel, J., Gull, T. R., Hjorth, J., Holland, S. T., Kouveliotou, C., Levay, Z., Livio, M., Metzger, M. R., Nugent, P. E., Petro, L., Pian, E., Rhoads, J. E., Riess, A. G., Sahu, K. C., Smette, A., Tanvir, N. R., Wijers, R. A. M. J., and Woosley, S. E. 2006, *Nature*, 441, 463
- Fynbo, J. P. U., Watson, D., Thöne, C. C., Sollerman, J., Bloom, J. S., Davis, T. M., Hjorth, J., Jakobsson, P., Jørgensen, U. G., Graham, J. F., Fruchter, A. S., Bersier, D., Kewley, L., Cassan, A., Cerón, J. M. C., Foley, S., Gorosabel, J., Hinse, T. C., Horne, K. D., Jensen, B. L., Klose, S., Kocevski, D., Marquette, J.-B., Perley, D., Ramirez-Ruiz, E., Stritzinger, M. D., Vreeswijk, P. M., Wijers, R. A. M., Woller, K. G., Xu, D., and Zub, M. 2006, *Nature*, 444, 1047
- Gal-Yam, A., Fox, D. B., Price, P. A., Ofek, E. O., Davis, M. R., Leonard, D. C., Soderberg, A. M., Schmidt, B. P., Lewis, K. M., Peterson, B. A., Kulkarni, S. R., Berger, E., Cenko, S. B., Sari, R., Sharon, K., Frail, D., Moon, D.-S., Brown, P. J., Cucchiara, A., Harrison, F., Piran, T., Persson, S. E., McCarthy, P. J., Penprase, B. E., Chevalier, R. A., and MacFadyen, A. I. 2006, *Nature*, 444, 1053
- Galama, T., Groot, P. J., Vanparadijs, J., Kouveliotou, C., Robinson, C. R., Fishman, G. J., Meegan, C. A., Sahu, K. C., Livio, M., Petro, L., Macchetto, F. D., Heise, J., Int Zand, J., Strom, R. G., Telting, J., Rutten, R. G. M., Pettini, M., Tanvir, N., and Bloom, J. 1997, *Nature*, 387, 479

- Galama, T. J., Vreeswijk, P. M., van Paradijs, J., Kouveliotou, C., Augusteijn, T., Bönhardt, H., Brewer, J. P., Doublier, V., Gonzalez, J.-F., Leibundgut, B., Lidman, C., Hainaut, O. R., Patat, F., Heise, J., in't Zand, J., Hurley, K., Groot, P. J., Strom, R. G., Mazzali, P. A., Iwamoto, K., Nomoto, K., Umeda, H., Nakamura, T., Young, T. R., Suzuki, T., Shigeyama, T., Koshut, T., Kippen, M., Robinson, C., de Wildt, P., Wijers, R. A. M. J., Tanvir, N., Greiner, J., Pian, E., Palazzi, E., Frontera, F., Masetti, N., Nicastro, L., Feroci, M., Costa, E., Piro, L., Peterson, B. A., Tinney, C., Boyle, B., Cannon, R., Stathakis, R., Sadler, E., Begam, M. C., and Ianna, P. 1998, *Nature*, 395, 670
- Gehrels, N. 2006, *GCN Circ.*, 4787, 1
- Gehrels, N., Chincarini, G., Giommi, P., Mason, K. O., Nousek, J. A., Wells, A. A., White, N. E., Barthelmy, S. D., Burrows, D. N., Cominsky, L. R., Hurley, K. C., Marshall, F. E., Mészáros, P., Roming, P. W. A., Angelini, L., Barbier, L. M., Belloni, T., Campana, S., Caraveo, P. A., Chester, M. M., Citterio, O., Cline, T. L., Cropper, M. S., Cummings, J. R., Dean, A. J., Feigelson, E. D., Fenimore, E. E., Frail, D. A., Fruchter, A. S., Garmire, G. P., Gendreau, K., Ghisellini, G., Greiner, J., Hill, J. E., Hunsberger, S. D., Krimm, H. A., Kulkarni, S. R., Kumar, P., Lebrun, F., Lloyd-Ronning, N. M., Markwardt, C. B., Mattson, B. J., Mushotzky, R. F., Norris, J. P., Osborne, J., Paczynski, B., Palmer, D. M., Park, H.-S., Parsons, A. M., Paul, J., Rees, M. J., Reynolds, C. S., Rhoads, J. E., Sasseen, T. P., Schaefer, B. E., Short, A. T., Smale, A. P., Smith, I. A., Stella, L., Tagliaferri, G., Takahashi, T., Tashiro, M., Townsley, L. K., Tueller, J., Turner, M. J. L., Vietri, M., Voges, W., Ward, M. J., Willingale, R., Zerbi, F. M., and Zhang, W. W. 2004, *Astroph. J.*, 611, 1005
- Gehrels, N., Norris, J. P., Barthelmy, S. D., Granot, J., Kaneko, Y., Kouveliotou, C., Markwardt, C. B., Mészáros, P., Nakar, E., Nousek, J. A., O'Brien, P. T., Page, M., Palmer, D. M., Parsons, A. M., Roming, P. W. A., Sakamoto, T., Sarazin, C. L., Schady, P., Stamatikos, M., and Woosley, S. E. 2006, *Nature*, 444, 1044
- Gehrels, N., Sarazin, C. L., O'Brien, P. T., Zhang, B., Barbier, L., Barthelmy, S. D., Blustin, A., Burrows, D. N., Cannizzo, J., Cummings, J. R., Goad, M., Holland, S. T., Hurkett, C. P., Kennea, J. A., Levan, A., Markwardt, C. B., Mason, K. O., Meszaros, P., Page, M., Palmer, D. M., Rol, E., Sakamoto, T., Willingale, R., Angelini, L., Beardmore, A., Boyd, P. T., Breeveld, A., Campana, S., Chester, M. M., Chincarini, G., Cominsky, L. R., Cusumano, G., de Pasquale, M., Fenimore, E. E., Giommi, P., Gronwall, C., Grupe, D., Hill, J. E., Hinshaw, D., Hjorth, J., Hullinger, D., Hurley, K. C., Klose, S., Kobayashi, S., Kouveliotou, C., Krimm, H. A., Mangano, V., Marshall, F. E., McGowan, K., Moretti, A., Mushotzky, R. F., Nakazawa, K., Norris, J. P., Nousek, J. A., Osborne, J. P., Page, K., Parsons, A. M., Patel, S., Perri, M., Poole, T., Romano, P., Roming, P. W. A., Rosen, S., Sato, G., Schady, P., Smale, A. P., Sollerman, J., Starling, R., Still, M., Suzuki, M., Tagliaferri, G., Takahashi, T., Tashiro, M., Tueller, J., Wells, A. A., White, N. E., and Wijers, R. A. M. J. 2005, *Nature*, 437, 851
- Ghisellini, G. 2001, in *Proceedings of the 25th Johns Hopkins Workshop: "2001: A Relativistic Spacetime Odyssey. Experiments and Theoretical Viewpoints on General Relativity and Quantum Gravity"*, Florence, Sep. 2001
- Gladders, M., Berger, E., Morrell, N., and Roth, M. 2005, *GCN Circ.*, 3798, 1
- Godet, O., Page, K. L., Rol, E., Beardmore, A. P., and Page, M. J. 2006, *GCN Circ.*, 5227, 1
- Goodman, J. 1986, *Astroph. J.*, 308, L47
- Gorosabel, J., Castro-Tirado, A. J., Guziy, S., de Ugarte Postigo, A., Reverte, D., Antonelli, A., Covino, S., Malesani, D., Martín-Gordón, D., Melandri, A., Jelínek, M., Elias de La Rosa, N., Bogdanov, O., and Castro Cerón, J. M. 2006, *Astron. & Astroph.*, 450, 87
- Gorosabel, J., Guziy, S., Sota, A., Castro-Tirado, A. J., de Ugarte Postigo, A., and Jelinek, M. 2005, *GCN Circ.*, 3796, 1

- Granot, J., Piran, T., and Sari, R. 2000, *Astroph. J.*, 534, L163
- Greiner, J., Klose, S., Salvato, M., Zeh, A., Schwarz, R., Hartmann, D. H., Masetti, N., Stecklum, B., Lamer, G., Lodieu, N., Scholz, R. D., Sterken, C., Gorosabel, J., Burud, I., Rhoads, J., Mitrofanov, I., Litvak, M., Sanin, A., Grinkov, V., Andersen, M. I., Castro Cerón, J. M., Castro-Tirado, A. J., Fruchter, A., Fynbo, J. U., Hjorth, J., Kaper, L., Kouveliotou, C., Palazzi, E., Pian, E., Rol, E., Tanvir, N. R., Vreeswijk, P. M., Wijers, R. A. M. J., and van den Heuvel, E. 2003, *Astroph. J.*, 599, 1223
- Greiner, J., Kruehler, T., Fynbo, J. P. U., Rossi, A., Schwarz, R., Klose, S., Savaglio, S., Tanvir, N. R., McBreen, S., Totani, T., Zhang, B. B., Wu, X. F., Watson, D., Barthelmy, S. D., Beardmore, A. P., Ferrero, P., Gehrels, N., Kann, D. A., Kawai, N., Kuepcue Yoldas, A., Meszaros, P., Milvang-Jensen, B., Oates, S. R., Pierini, D., Schady, P., Toma, K., Vreeswijk, P. M., Yoldas, A., Zhang, B., Afonso, P., Aoki, K., Burrows, D. N., Clemens, C., Filgas, R., Haiman, Z., Hartmann, D. H., Hasinger, G., Hjorth, J., Jehin, E., Levan, A. J., Liang, E. W., Malesani, D., Pyo, T. ., Schulze, S., Szokoly, G., Terada, H., and Wiersema, K. 2008, *ArXiv e-prints*, 0810.2314
- Grupe, D., Gronwall, C., Wang, X.-Y., Roming, P. W. A., Cummings, J., Zhang, B., Mészáros, P., Trigo, M. D., O'Brien, P. T., Page, K. L., Beardmore, A., Godet, O., vanden Berk, D. E., Brown, P. J., Koch, S., Morris, D., Stroh, M., Burrows, D. N., Nousek, J. A., McMath Chester, M., Immler, S., Mangano, V., Romano, P., Chincarini, G., Osborne, J., Sakamoto, T., and Gehrels, N. 2007a, *Astroph. J.*, 662, 443
- Grupe, D., Nousek, J. A., vanden Berk, D. E., Roming, P. W. A., Burrows, D. N., Godet, O., Osborne, J., and Gehrels, N. 2007b, *Astron. J.*, 133, 2216
- Guenther, E. W., Klose, S., Vreeswijk, P., Pian, E., and Greiner, J. 2006, *GCN Circ.*, 4863, 1
- Heise, J., in't Zand, J., Kippen, R. M., and Woods, P. M. 2001, in *Gamma-Ray Bursts in the Afterglow Era: Proceedings of the International Workshop Held in Rome, Italy, 17-20 October 2000*, ed. E. Costa, F. Frontera, & J. Hjorth, *ESO ASTROPHYSICS SYMPOSIA* (Springer-Verlag), 16
- Hicken, M., Modjaz, M., Challis, P., Kirshner, R., Prieto, J. L., Stanek, K., and Cool, R. 2006, *GCN Circ.*, 4898, 1
- Hjorth, J., Sollerman, J., Gorosabel, J., Granot, J., Klose, S., Kouveliotou, C., Melinder, J., Ramirez-Ruiz, E., Starling, R., Thomsen, B., Andersen, M. I., Fynbo, J. P. U., Jensen, B. L., Vreeswijk, P. M., Castro Cerón, J. M., Jakobsson, P., Levan, A., Pedersen, K., Rhoads, J. E., Tanvir, N. R., Watson, D., and Wijers, R. A. M. J. 2005a, *Astroph. J.*, 630, L117
- Hjorth, J., Sollerman, J., Møller, P., Fynbo, J. P. U., Woosley, S. E., Kouveliotou, C., Tanvir, N. R., Greiner, J., Andersen, M. I., Castro-Tirado, A. J., Castro Cerón, J. M., Fruchter, A. S., Gorosabel, J., Jakobsson, P., Kaper, L., Klose, S., Masetti, N., Pedersen, H., Pedersen, K., Pian, E., Palazzi, E., Rhoads, J. E., Rol, E., van den Heuvel, E. P. J., Vreeswijk, P. M., Watson, D., and Wijers, R. A. M. J. 2003, *Nature*, 423, 847
- Hjorth, J., Watson, D., Fynbo, J. P. U., Price, P. A., Jensen, B. L., Jørgensen, U. G., Kubas, D., Gorosabel, J., Jakobsson, P., Sollerman, J., Pedersen, K., and Kouveliotou, C. 2005b, *Nature*, 437, 859
- Horváth, I. 1998, *Astroph. J.*, 508, 757
- Horváth, I., Balázs, L. G., Bagoly, Z., Ryde, F., and Mészáros, A. 2006, *Astron. & Astroph.*, 447, 23
- Hu, E. M., Cowie, L. L., McMahon, R. G., Capak, P., Iwamuro, F., Kneib, J.-P., Maihara, T., and Motohara, K. 2002, *Astroph. J.*, 568, L75
- Jager, R., Mels, W. A., Brinkman, A. C., Galama, M. Y., Goulooze, H., Heise, J., Lowes, P., Muller, J. M., Naber, A., Rook, A., Schuurhof, R., Schuurmans, J. J., and Wiersma, G. 1997, *Astron. & Astroph. Suppl.*, 125, 557

- Jakobsson, P., Fynbo, J. P. U., Ledoux, C., Vreeswijk, P., Kann, D. A., Hjorth, J., Priddey, R. S., Tanvir, N. R., Reichart, D., Gorosabel, J., Klose, S., Watson, D., Sollerman, J., Fruchter, A. S., de Ugarte Postigo, A., Wiersema, K., Björnsson, G., Chapman, R., Thöne, C. C., Pedersen, K., and Jensen, B. L. 2006, *Astron. & Astroph.*, 460, L13
- Jakobsson, P., Hjorth, J., Fynbo, J. P. U., Watson, D., Pedersen, K., Björnsson, G., and Gorosabel, J. 2004, *Astroph. J.*, 617, L21
- Jin, Z. P. and Fan, Y. Z. 2007, *Mon. Not. R. Astron. Soc.*, 378, 1043
- Kalberla, P. M. W., Burton, W. B., Hartmann, D., Arnal, E. M., Bajaja, E., Morras, R., and Pöppel, W. G. L. 2005, *Astron. & Astroph.*, 440, 775
- Kann, D. A., Klose, S., and Zeh, A. 2006, *Astroph. J.*, 641, 993
- Kann, D. A., Klose, S., Zhang, B., Malesani, D., Nakar, E., Wilson, A. C., Butler, N. R., Antonelli, L. A., Chincarini, G., Cobb, B. E., Covino, S., D'Avanzo, P., D'Elia, V., Della Valle, M., Ferrero, P., Fugazza, D., Gorosabel, J., Israel, G. L., Mannucci, F., Piranomonte, S., Schulze, S., Stella, L., Tagliaferri, G., and Wiersema, K. 2007, *ArXiv e-prints*, 712
- Kann, D. A., Klose, S., Zhang, B., Wilson, A. C., Butler, N. R., Malesani, D., Nakar, E., Antonelli, L. A., Chincarini, G., Cobb, B. E., Covino, S., D'Avanzo, P., D'Elia, V., Della Valle, M., Ferrero, P., Fugazza, D., Gorosabel, J., Israel, G. L., Mannucci, F., Piranomonte, S., Schulze, S., Stella, L., Tagliaferri, G., and Wiersema, K. 2008, *ArXiv e-prints*, 0804.1959
- Karska, A. and Garnavich, P. 2006, *GCN Circ.*, 5260, 1
- Kawai, N., Kosugi, G., Aoki, K., Yamada, T., Totani, T., Ohta, K., Iye, M., Hattori, T., Aoki, W., Furusawa, H., Hurley, K., Kawabata, K. S., Kobayashi, N., Komiyama, Y., Mizumoto, Y., Nomoto, K., Noumaru, J., Ogasawara, R., Sato, R., Sekiguchi, K., Shirasaki, Y., Suzuki, M., Takata, T., Tamagawa, T., Terada, H., Watanabe, J., Yatsu, Y., and Yoshida, A. 2006, *Nature*, 440, 184
- Kelz, A., Verheijen, M. A. W., Roth, M. M., Bauer, S. M., Becker, T., Paschke, J., Popow, E., Sánchez, S. F., and Laux, U. 2006, *Publ. Astron. Soc. Pacific*, 118, 129
- Kennea, J. A., Burrows, D. N., Cusumano, G., and Tagliaferri, G. 2006, *GCN Circ.*, 4776, 1
- Khamitov, I., Saygac, A. T., Aslan, Z., Kiziloglu, U., Gogus, E., Alis, S., Onal, O., Burenin, R., Pavlinsky, M., Sunyaev, R., Bikmaev, I., and Sakhbullin, N. 2006a, *GCN Circ.*, 5224, 1
- Khamitov, I., Saygac, A. T., Aslan, Z., Kiziloglu, U., Gogus, E., Alis, S., Onal, O., Burenin, R., Pavlinsky, M., Sunyaev, R., Bikmaev, I., and Sakhbullin, N. 2006b, *GCN Circ.*, 5235, 1
- Kinney, A. L., Calzetti, D., Bohlin, R. C., McQuade, K., Storchi-Bergmann, T., and Schmitt, H. R. 1996, *Astroph. J.*, 467, 38
- Kirk, J. G., Guthmann, A. W., Gallant, Y. A., and Achterberg, A. 2000, *Astroph. J.*, 542, 235
- Kissler-Patig, M., Copin, Y., Ferruit, P., Pécontal-Rousset, A., and Roth, M. M. 2004, *Astronomische Nachrichten*, 325, 159
- Klebesadel, R. W., Strong, I. B., and Olson, R. A. 1973, *Astroph. J.*, 182, L85
- Klose, S., Greiner, J., Rau, A., Henden, A. A., Hartmann, D. H., Zeh, A., Ries, C., Masetti, N., Malesani, D., Guenther, E., Gorosabel, J., Stecklum, B., Antonelli, L. A., Brinkworth, C., Castro Cerón, J. M., Castro-Tirado, A. J., Covino, S., Fruchter, A., Fynbo, J. P. U., Ghisellini, G., Hjorth, J., Hudec, R., Jelínek, M., Kaper, L., Kouveliotou, C., Lindsay, K., Maiorano, E., Mannucci, F., Nysewander, M., Palazzi, E., Pedersen, K., Pian, E., Reichart, D. E., Rhoads, J., Rol, E., Smail, I., Tanvir, N. R., de Ugarte Postigo, A., Vreeswijk, P. M., Wijers, R. A. M. J., and van den Heuvel, E. P. J. 2004, *Astron. J.*, 128, 1942

- Kommers, J. M., Lewin, W. H. G., Kouveliotou, C., van Paradijs, J., Pendleton, G. N., Meegan, C. A., and Fishman, G. J. 2000, *Astroph. J.*, 533, 696
- Kouveliotou, C., Meegan, C. A., Fishman, G. J., Bhat, N. P., Briggs, M. S., Koshut, T. M., Paciesas, W. S., and Pendleton, G. N. 1993, *Astroph. J.*, 413, L101
- Krimm, H., Barbier, L., Barthelmy, S., Cummings, J., Fenimore, E., Gehrels, N., Hullinger, D., Koss, M., Markwardt, C., Palmer, D., Parsons, A., Sakamoto, T., Sato, G., Schady, P., Stamatikos, M., and Tueller, J. 2006, *GCN Circ.*, 5704, 1
- Krisciunas, K., Suntzeff, N. B., Candia, P., Arenas, J., Espinoza, J., Gonzalez, D., Gonzalez, S., Höflich, P. A., Landolt, A. U., Phillips, M. M., and Pizarro, S. 2003, *Astron. J.*, 125, 166
- Kulkarni, S. R. 2005, *ArXiv Astrophysics e-prints*
- Kulkarni, S. R., Frail, D. A., Sari, R., Moriarty-Schieven, G. H., Shepherd, D. S., Udomprasert, P., Readhead, A. C. S., Bloom, J. S., Feroci, M., and Costa, E. 1999, *Astroph. J.*, 522, L97
- Lamb, D. Q. and Reichart, D. E. 2000, *Astroph. J.*, 536, 1
- Landolt, A. U. 1992, *Astron. J.*, 104, 340
- Levan, A. J., Tanvir, N. R., Fruchter, A. S., Rol, E., Fynbo, J. P. U., Hjorth, J., Williams, G., Bergeron, E., Bersier, D., Bremer, M., Grav, T., Jakobsson, P., Nilsson, K., Olszewski, E., Priddey, R. S., Rafferty, D., and Rhoads, J. 2006, *Astroph. J.*, 648, L9
- Li, L.-X. and Paczyński, B. 1998, *Astroph. J.*, 507, L59
- Li, W. 2005, *GCN Circ.*, 3794, 1
- Li, W., Filippenko, A. V., Chornock, R., and Jha, S. 2003, *Publ. Astron. Soc. Pacific*, 115, 844
- Li, Z.-Y. and Chevalier, R. A. 2001, *Astroph. J.*, 551, 940
- Liang, E.-W. and Kargatis, V. 1996, *Nature*, 381, 49
- Liang, E.-W., Racusin, J. L., Zhang, B., Zhang, B.-B., and Burrows, D. N. 2008, *Astroph. J.*, 675, 528
- Liang, E.-W., Zhang, B.-B., and Zhang, B. 2006, *Astroph. J.*, 646, 351
- Liang, E.-W., Zhang, B.-B., and Zhang, B. 2007, *Astroph. J.*, 670, 565
- Lin, H., Kirshner, R. P., Sheckman, S. A., Landy, S. D., Oemler, A., Tucker, D. L., and Schechter, P. L. 1996, *Astroph. J.*, 464, 60
- Lithwick, Y. and Sari, R. 2001, *Astroph. J.*, 555, 540
- Malesani, D., Covino, S., D'Avanzo, P., D'Elia, V., Fugazza, D., Piranomonte, S., Ballo, L., Campana, S., Stella, L., Tagliaferri, G., Antonelli, L. A., Chincarini, G., Della Valle, M., Goldoni, P., Guidorzi, C., Israel, G. L., Lazzati, D., Melandri, A., Pellizza, L. J., Romano, P., Stratta, G., and Vergani, S. D. 2007, *Astron. & Astroph.*, 473, 77
- Malesani, D., Fiore, F., Masetti, N., Pedani, M., and Mainella, G. 2006, *GCN Circ.*, 5225, 1
- Malesani, D., Tagliaferri, G., Chincarini, G., Covino, S., Della Valle, M., Fugazza, D., Mazzali, P. A., Zerbi, F. M., D'Avanzo, P., Kalogerakos, S., Simoncelli, A., Antonelli, L. A., Burderi, L., Campana, S., Cucchiara, A., Fiore, F., Ghirlanda, G., Goldoni, P., Götz, D., Mereghetti, S., Mirabel, I. F., Romano, P., Stella, L., Minezaki, T., Yoshii, Y., and Nomoto, K. 2004, *Astroph. J.*, 609, L5

- Manzo, G., Giarrusso, S., Santangelo, A., Ciralli, F., Fazio, G., Piraino, S., and Segreto, A. 1997, *Astron. & Astroph. Suppl.*, 122, 341
- Marshall, F., Immler, S., and Cusumano, G. 2006, *GCN Circ.*, 4779, 1
- Masetti, N., Palazzi, E., Pian, E., and Patat, F. 2006, *GCN Circ.*, 4803, 1
- Mazzali, P. A., Deng, J., Nomoto, K., Sauer, D. N., Pian, E., Tominaga, N., Tanaka, M., Maeda, K., and Filippenko, A. V. 2006a, *Nature*, 442, 1018
- Mazzali, P. A., Deng, J., Pian, E., Malesani, D., Tominaga, N., Maeda, K., Nomoto, K., Chincarini, G., Covino, S., Della Valle, M., Fugazza, D., Tagliaferri, G., and Gal-Yam, A. 2006b, *Astroph. J.*, 645, 1323
- McEney, J. and GLAST Mission Team. 2006, in *American Institute of Physics Conference Series*, Vol. 836, *GAMMA-RAY BURSTS IN THE SWIFT ERA: Sixteenth Maryland Astrophysics Conference*, ed. S. S. Holt, N. Gehrels, & J. A. Nousek, 660–663
- Meegan, C. A., Fishman, G. J., Wilson, R. B., Horack, J. M., Brock, M. N., Paciesas, W. S., Pendleton, G. N., and Kouveliotou, C. 1992, *Nature*, 355, 143
- Mereghetti, S., Tavani, M., Argan, A., Chen, A., Caraveo, P., Perotti, F., Vercellone, S., Barbiellini, G., Prest, M., Vallazza, E., di Cocco, G., Labanti, C., Trifoglio, M., Costa, E., Feroci, M., Lapshov, I., Rubini, A., Soffitta, P., Picozza, P., Morselli, A., Cocco, V., Pittori, C., Zanello, D., Lipari, P., and Longo, F. 2001, in *Astrophysics and Space Science Library*, Vol. 267, *The Nature of Unidentified Galactic High-Energy Gamma-Ray Sources. Proceedings of the Workshop held at Tonantzintla, Puebla, México, 9-11 October 2000.*, ed. A. Carramiñana, O. Reimer, & D. J. Thompson (Kluwer Academic Publishers Dordrecht), 331–338
- Mészáros, P. 2006, *Rept. Prog. Phys.*, 69, 2259
- Metzger, M. R., Cohen, J. L., Chaffee, F. H., and Blandford, R. D. 1997a, *IAU Circ.*, 6676, 3
- Metzger, M. R., Djorgovski, S. G., Kulkarni, S. R., Steidel, C. C., Adelberger, K. L., Frail, D. A., Costa, E., and Frontera, F. 1997b, *Nature*, 387, 878
- Mirabal, N. and Halpern, J. P. 2006, *GCN Circ.*, 4792, 1
- Mirabal, N., Halpern, J. P., An, D., Thorstensen, J. R., and Terndrup, D. M. 2006, *Astroph. J.*, 643, L99
- Modjaz, M., Stanek, K. Z., Garnavich, P. M., Berlind, P., Blondin, S., Brown, W., Calkins, M., Challis, P., Diamond-Stanic, A. M., Hao, H., Hicken, M., Kirshner, R. P., and Prieto, J. L. 2006, *Astroph. J.*, 645, L21
- Molinari, E., Vergani, S. D., Malesani, D., Covino, S., D’Avanzo, P., Chincarini, G., Zerbi, F. M., Antonelli, L. A., Conconi, P., Testa, V., Tosti, G., Vitali, F., D’Alessio, F., Malaspina, G., Nicastro, L., Palazzi, E., Guetta, D., Campana, S., Goldoni, P., Masetti, N., Meurs, E. J. A., Monfardini, A., Norci, L., Pian, E., Piranomonte, S., Rizzuto, D., Stefanon, M., Stella, L., Tagliaferri, G., Ward, P. A., Ihle, G., Gonzalez, L., Pizarro, A., Sinclair, P., and Valenzuela, J. 2007, *Astron. & Astroph.*, 469, L13
- Moretti, A., Perri, M., Capalbi, M., Angelini, L., Hill, J. E., Campana, S., Burrows, D. N., Osborne, J. P., Tagliaferri, G., Cusumano, G., Giommi, P., Romano, P., Mineo, T., Kennea, J., Morris, D., Nousek, J., Pagani, C., Racusin, J., Abbey, A. F., Beardmore, A. P., Godet, O., Goad, M. R., Page, K. L., Wells, A. A., and Chincarini, G. 2006, *Astron. & Astroph.*, 448, L9
- Morris, D. C., Burrows, D. N., Kennea, J. A., Racusin, J. L., Cucchiara, N., Retter, A., and Gehrels, N. . 2005, *GCN Circ.*, 3790, 1

- Mukherjee, S., Feigelson, E. D., Jogesh Babu, G., Murtagh, F., Fraley, C., and Raftery, A. 1998, *Astroph. J.*, 508, 314
- Nakar, E. 2007, *Physics Reports*, 442, 166
- Nardini, M., Ghisellini, G., and Ghirlanda, G. 2008, *Mon. Not. R. Astron. Soc.*, 386, L87
- Nemiroff, R. J. 1994, *Comments on Astrophysics*, 17, 189
- Norris, J. P. and Bonnell, J. T. 2006, *Astroph. J.*, 643, 266
- Norris, J. P., Share, G. H., Messina, D. C., Dennis, B. R., Desai, U. D., Cline, T. L., Matz, S. M., and Chupp, E. L. 1986, *Astroph. J.*, 301, 213
- Nousek, J., Cusumano, G., Moretti, A., Tagliaferri, G., Campana, S., Kennea, J., Burrows, D., Roming, P., vanden Berk, D., Brown, P., Gehrels, N., Barthelmy, S., Marshall, F., Boyd, P., Sakamoto, T., Osborne, J., O'Brien, P., Chincarini, G., Zhang, B., and de Pasquale, M. 2006a, *GCN Circ.*, 4805, 1
- Nousek, J. A., Kouveliotou, C., Grupe, D., Page, K. L., Granot, J., Ramirez-Ruiz, E., Patel, S. K., Burrows, D. N., Mangano, V., Barthelmy, S., Beardmore, A. P., Campana, S., Capalbi, M., Chincarini, G., Cusumano, G., Falcone, A. D., Gehrels, N., Giommi, P., Goad, M. R., Godet, O., Hurkett, C. P., Kennea, J. A., Moretti, A., O'Brien, P. T., Osborne, J. P., Romano, P., Tagliaferri, G., and Wells, A. A. 2006b, *Astroph. J.*, 642, 389
- Nuza, S. E., Tissera, P. B., Pellizza, L. J., Lambas, D. G., Scannapieco, C., and de Rossi, M. E. 2007, *Mon. Not. R. Astron. Soc.*, 375, 665
- Oke, J. B. 1990, *Astron. J.*, 99, 1621
- Paczyński, B. 1986, *Astroph. J.*, 308, L43
- Page, M. J., Blustin, A. J., Brown, P. J., Godet, O., Holland, S. T., Kennea, J. A., Krimm, H. A., Pagani, C., Parsons, A. M., Sato, G., and Stamatikos, M. 2006, *GCN Circ.*, 5221, 1
- Panaitescu, A. 2007, *Mon. Not. R. Astron. Soc.*, 380, 374
- Panaitescu, A. and Kumar, P. 2000, *Astroph. J.*, 543, 66
- Panaitescu, A. and Kumar, P. 2001, *Astroph. J.*, 554, 667
- Panaitescu, A. and Kumar, P. 2002, *Astroph. J.*, 571, 779
- Panaitescu, A., Kumar, P., and Narayan, R. 2001, *Astroph. J.*, 561, L171
- Parmar, A. N., Martin, D. D. E., Bavdaz, M., Favata, F., Kuulkers, E., Vacanti, G., Lammers, U., Peacock, A., and Taylor, B. G. 1997, *Astron. & Astroph. Suppl.*, 122, 309
- Patat, F., Cappellaro, E., Danziger, J., Mazzali, P. A., Sollerman, J., Augusteijn, T., Brewer, J., Doublier, V., Gonzalez, J. F., Hainaut, O., Lidman, C., Leibundgut, B., Nomoto, K., Nakamura, T., Spyromilio, J., Rizzi, L., Turatto, M., Walsh, J., Galama, T. J., van Paradijs, J., Kouveliotou, C., Vreeswijk, P. M., Frontera, F., Masetti, N., Palazzi, E., and Pian, E. 2001, *Astroph. J.*, 555, 900
- Pécontal-Rousset, A., Copin, Y., and Ferruit, P. 2004, *Astronomische Nachrichten*, 325, 163
- Perna, R. and Belczynski, K. 2002, *Astroph. J.*, 570, 252
- Peterson, B. and Schmidt, B. 2006, *GCN Circ.*, 5223, 1

- Pian, E., Amati, L., Antonelli, L. A., Butler, R. C., Costa, E., Cusumano, G., Danziger, J., Feroci, M., Fiore, F., Frontera, F., Giommi, P., Masetti, N., Muller, J. M., Oosterbroek, T., Owens, A., Palazzi, E., Piro, L., Castro-Tirado, A., Coletta, A., dal Fiume, D., del Sordo, S., Heise, J., Nicastro, L., Orlandini, M., Parmar, A., Soffitta, P., Torroni, V., and in 't Zand, J. J. M. 1999, *Astron. & Astroph. Suppl.*, 138, 463
- Pian, E., Mazzali, P. A., Masetti, N., Ferrero, P., Klose, S., Palazzi, E., Ramirez-Ruiz, E., Woosley, S. E., Kouveliotou, C., Deng, J., Filippenko, A. V., Foley, R. J., Fynbo, J. P. U., Kann, D. A., Li, W., Hjorth, J., Nomoto, K., Patat, F., Sauer, D. N., Sollerman, J., Vreeswijk, P. M., Guenther, E. W., Levan, A., O'Brien, P., Tanvir, N. R., Wijers, R. A. M. J., Dumas, C., Hainaut, O., Wong, D. S., Baade, D., Wang, L., Amati, L., Cappellaro, E., Castro-Tirado, A. J., Ellison, S., Frontera, F., Fruchter, A. S., Greiner, J., Kawabata, K., Ledoux, C., Maeda, K., Møller, P., Nicastro, L., Rol, E., and Starling, R. 2006, *Nature*, 442, 1011
- Piran, T. 1997, in *Unsolved Problems in Astrophysics*, ed. J. Bahcall & J. Ostriker (Princeton University Press), 343–377
- Piran, T. 2000, *Physics Reports*, 333, 529
- Piran, T. 2005, *Rev. Mod. Phys.*, 76, 1143
- Poole, T. S., Breeveld, A. A., Page, M. J., Landsman, W., Holland, S. T., Roming, P., Kuin, N. P. M., Brown, P. J., Gronwall, C., Hunsberger, S., Koch, S., Mason, K. O., Schady, P., vanden Berk, D., Blustin, A. J., Boyd, P., Broos, P., Carter, M., Chester, M. M., Cucchiara, A., Hancock, B., Huckle, H., Immler, S., Ivanushkina, M., Kennedy, T., Marshall, F., Morgan, A., Pandey, S. B., de Pasquale, M., Smith, P. J., and Still, M. 2008, *Mon. Not. R. Astron. Soc.*, 383, 627
- Preece, R. D., Briggs, M. S., Mallozzi, R. S., Pendleton, G. N., Paciasas, W. S., and Band, D. L. 2000, *Astroph. J. Suppl.*, 126, 19
- Prochaska, J. X., Bloom, J. S., Chen, H.-W., Foley, R. J., Perley, D. A., Ramirez-Ruiz, E., Granot, J., Lee, W. H., Pooley, D., Alatalo, K., Hurley, K., Cooper, M. C., Dupree, A. K., Gerke, B. F., Hansen, B. M. S., Kalirai, J. S., Newman, J. A., Rich, R. M., Richer, H., Stanford, S. A., Stern, D., and van Breugel, W. J. M. 2006, *Astroph. J.*, 642, 989
- Rees, M. J. and Mészáros, P. 1992, *Mon. Not. R. Astron. Soc.*, 258, 41P
- Retter, A., Barbier, L., Barthelmy, S., Blustin, A., Burrows, D., Cucchiara, A., Gehrels, N., Godet, O., Kennea, J., Markwardt, C., Morris, D., Palmer, D., Racusin, J., and Roming, P. 2005, *GCN Circ.*, 3788, 1
- Rhoads, J. E. 1997, *Astroph. J.*, 487, L1
- Rhoads, J. E. 1999, *Astroph. J.*, 525, 737
- Richardson, D., Branch, D., and Baron, E. 2006, *Astron. J.*, 131, 2233
- Richardson, D., Branch, D., Casebeer, D., Millard, J., Thomas, R. C., and Baron, E. 2002, *Astron. J.*, 123, 745
- Rol, E., Wijers, R. A. M. J., Kouveliotou, C., Kaper, L., and Kaneko, Y. 2005, *Astroph. J.*, 624, 868
- Roming, P. W. A., Kennedy, T. E. and Mason, K. O., Nousek, J. A., Ahr, L., Bingham, R. E., Broos, P. S., Carter, M. J., Hancock, B. K., Huckle, H. E., Hunsberger, S. D., Kawakami, H., Killough, R., Koch, T. S., McLelland, M. K., Smith, K., Smith, P. J., Soto, J. C., Boyd, P. T., Breeveld, A. A., Holland, S. T., Ivanushkina, M., Pryzby, M. S., Still, M. D., and Stock, J. 2005, *Space Sci. Mod. Rev.*, 120, 95

- Roming, P. W. A., Schady, P., Fox, D. B., Zhang, B., Liang, E., Mason, K. O., Rol, E., Burrows, D. N., Blustin, A. J., Boyd, P. T., Brown, P., Holland, S. T., McGowan, K., Landsman, W. B., Page, K. L., Rhoads, J. E., Rosen, S. R., Vanden Berk, D., Barthelmy, S. D., Breeveld, A. A., Cucchiara, A., De Pasquale, M., Fenimore, E. E., Gehrels, N., Gronwall, C., Grupe, D., Goad, M. R., Ivanushkina, M., James, C., Kennea, J. A., Kobayashi, S., Mangano, V., Mészáros, P., Morgan, A. N., Nousek, J. A., Osborne, J. P., Palmer, D. M., Poole, T., Still, M. D., Tagliaferri, G., and Zane, S. 2006, *Astroph. J.*, 652, 1416
- Rossi, A., Greiner, J., Kruehler, T., Yoldas, A., Klose, S., and Yoldas, A. K. 2008, *GCN Circ.*, 8218, 1
- Rossi, E., Lazzati, D., and Rees, M. J. 2002, *Mon. Not. R. Astron. Soc.*, 332, 945
- Roth, M. M., Kelz, A., Fechner, T., Hahn, T., Bauer, S.-M., Becker, T., Böhm, P., Christensen, L., Dionies, F., Paschke, J., Popow, E., Wolter, D., Schmoll, J., Laux, U., and Altmann, W. 2005, *Publ. Astron. Soc. Pacific*, 117, 620
- Rykoff, E. S. and Schaefer, B. E. 2006, *GCN Circ.*, 5220, 1
- Sakamoto, T., Lamb, D. Q., Graziani, C., Donaghy, T. Q., Suzuki, M., Ricker, G., Atteia, J.-L., Kawai, N., Yoshida, A., Shirasaki, Y., Tamagawa, T., Torii, K., Matsuoka, M., Fenimore, E. E., Galassi, M., Tavenner, T., Doty, J., Vanderspek, R., Crew, G. B., Villasenor, J., Butler, N., Prigozhin, G., Jernigan, J. G., Barraud, C., Boer, M., Dezalay, J.-P., Olive, J.-F., Hurley, K., Levine, A., Monnelly, G., Martel, F., Morgan, E., Woosley, S. E., Cline, T., Braga, J., Manchanda, R., Pizzichini, G., Takagishi, K., and Yamauchi, M. 2004, *Astroph. J.*, 602, 875
- Sánchez, S. F. 2004, *Astron. Nachr.*, 325, 167
- Sánchez, S. F. 2006, *Astron. Nachr.*, 327, 850
- Sánchez, S. F. and Cardiel, N. 2005, *Calar Alto Newsletter*, num. 100
- Sari, R. 1997, *Astroph. J.*, 489, L37
- Sari, R., Piran, T., and Halpern, J. P. 1999, *Astroph. J.*, 519, L17
- Sari, R., Piran, T., and Narayan, R. 1998, *Astroph. J.*, 497, L17
- Sato, G., Angelini, L., Barbier, L., Barthelmy, S., Cummings, J., Fenimore, E., Gehrels, N., Grenier, J., Hullinger, D., Krimm, H., Markwardt, C., Mitani, T., Palmer, D., Parsons, A., Sakamoto, T., Suzuki, M., and Tueller, J. 2005, *GCN Circ.*, 3793, 1
- Sato, G., Barbier, L., Barthelmy, S., Cummings, J., Fenimore, E., Gehrels, N., Hullinger, D., Krimm, H., Koss, M., Markwardt, C., Palmer, D., Parsons, A., Sakamoto, T., Stamatikos, M., and Tueller, J. 2006, *GCN Circ.*, 5231, 1
- Savaglio, S. 2006, *New J. Phys.*, 8, 195
- Savaglio, S. and Fall, S. M. 2004, *Astroph. J.*, 614, 293
- Savaglio, S., Fiore, F., Israel, G., Marconi, G., Antonelli, L. A., Fontana, A., Stella, L., di, A. P., Stratta, G., Covino, S., Chincarini, G., Ghisellini, G., Saracco, P., Zerbi, F., Lazzati, D., Perna, R., Vietri, M., Frontera, F., Mereghetti, S., Meurs, E. J. A., and Kawai, N. 2002, *GCN Circ.*, 1633, 1
- Savaglio, S., Glazebrook, K., and Le Borgne, D. 2006, in *American Institute of Physics Conference Series*, Vol. 836, *Gamma-Ray Bursts in the Swift Era*, ed. S. S. Holt, N. Gehrels, & J. A. Nousek, 540–545
- Savaglio, S., Glazebrook, K., and Le Borgne, D. 2008, *ArXiv e-prints*, 803

- Schaefer, B. E., Rykoff, E. S., Smith, D. A., and Quimby, R. 2006, *GCN Circ.*, 5222, 1
- Schechter, P. 1976, *Astroph. J.*, 203, 297
- Schlegel, D. J., Finkbeiner, D. P., and Davis, M. 1998, *Astroph. J.*, 500, 525
- Shapley, A. E., Steidel, C. C., Adelberger, K. L., Dickinson, M., Giavalisco, M., and Pettini, M. 2001, *Astroph. J.*, 562, 95
- Sharapov, D., Augusteijn, T., and Pozanenko, A. 2006, *GCN Circ.*, 5263, 1
- Sharapov, D., Ibrahimov, M., Pozanenko, A., and Rumyantsev, V. 2005, *GCN Circ.*, 3857, 1
- Shin, M.-S., Berger, E., Penprase, B. E., Fox, D. B., Price, P. A., Kulkarni, S. R., Soderberg, A. M., West, M. J., Cote, P., and Jordan, A. 2006, *ArXiv Astrophysics e-prints*
- Soderberg, A. M., Berger, E., Fox, D. B., Cucchiara, A., Rau, A., Ofek, E., Kasliwal, M., and Cenko, S. B. 2008, *GCN Circ.*, 7165, 1
- Soderberg, A. M., Berger, E., Kasliwal, M., Frail, D. A., Price, P. A., Schmidt, B. P., Kulkarni, S. R., Fox, D. B., Cenko, S. B., Gal-Yam, A., Nakar, E., and Roth, K. C. 2006a, *Astroph. J.*, 650, 261
- Soderberg, A. M., Kulkarni, S. R., Nakar, E., Berger, E., Cameron, P. B., Fox, D. B., Frail, D., Gal-Yam, A., Sari, R., Cenko, S. B., Kasliwal, M., Chevalier, R. A., Piran, T., Price, P. A., Schmidt, B. P., Pooley, G., Moon, D.-S., Penprase, B. E., Ofek, E., Rau, A., Gehrels, N., Nousek, J. A., Burrows, D. N., Persson, S. E., and McCarthy, P. J. 2006b, *Nature*, 442, 1014
- Soderberg, A. M., Kulkarni, S. R., Price, P. A., Fox, D. B., Berger, E., Moon, D.-S., Cenko, S. B., Gal-Yam, A., Frail, D. A., Chevalier, R. A., Cowie, L., Da Costa, G. S., MacFadyen, A., McCarthy, P. J., Noel, N., Park, H. S., Peterson, B. A., Phillips, M. M., Rauch, M., Rest, A., Rich, J., Roth, K., Roth, M., Schmidt, B. P., Smith, R. C., and Wood, P. R. 2006c, *Astroph. J.*, 636, 391
- Sollerman, J., Jaunsen, A. O., Fynbo, J. P. U., Hjorth, J., Jakobsson, P., Stritzinger, M., Féron, C., Laursen, P., Ovaldsen, J.-E., Selj, J., Thöne, C. C., Xu, D., Davis, T., Gorosabel, J., Watson, D., Duro, R., Ilyin, I., Jensen, B. L., Lysfjord, N., Marquart, T., Nielsen, T. B., Näränen, J., Schwarz, H. E., Walch, S., Wold, M., and Östlin, G. 2006, *Astron. & Astroph.*, 454, 503
- Stanek, K. Z., Garnavich, P. M., Nutzman, P. A., Hartman, J. D., Garg, A., Adelberger, K., Berlind, P., Bonanos, A. Z., Calkins, M. L., Challis, P., Gaudi, B. S., Holman, M. J., Kirshner, R. P., McLeod, B. A., Osip, D., Pimenova, T., Reiprich, T. H., Romanishin, W., Spahr, T., Tegler, S. C., and Zhao, X. 2005, *Astroph. J.*, 626, L5
- Stanek, K. Z., Matheson, T., Garnavich, P. M., Martini, P., Berlind, P., Caldwell, N., Challis, P., Brown, W. R., Schild, R., Krisciunas, K., Calkins, M. L., Lee, J. C., Hathi, N., Jansen, R. A., Windhorst, R., Echevarria, L., Eisenstein, D. J., Pindor, B., Olszewski, E. W., Harding, P., Holland, S. T., and Bersier, D. 2003, *Astroph. J.*, 591, L17
- Starling, R. L. C., van der Horst, A. J., Rol, E., Wijers, R. A. M. J., Kouveliotou, C., Wiersema, K., Curran, P. A., and Weltevrede, P. 2008, *Astroph. J.*, 672, 433
- Steele, I. A., Smith, R. J., Rees, P. C., Baker, I. P., Bates, S. D., Bode, M. F., Bowman, M. K., Carter, D., Etherton, J., Ford, M. J., Fraser, S. N., Gomboc, A., Lett, R. D. J., Mansfield, A. G., Marchant, J. M., Medrano-Cerda, G. A., Mottram, C. J., Raback, D., Scott, A. B., Tomlinson, M. D., and Zamanov, R. 2004, in *Ground-based Telescopes. Proceedings of the SPIE.*, ed. J. M. Oschmann, Jr., Vol. 5489, 679–692
- Stetson, P. B. 1987, *Publ. Astron. Soc. Pacific*, 99, 191
- Still, A., Kniazev, M., Romero-Colmenero, E., Hashimoto, Y., Loaring, N., Vaisanen, P., Buckley, D., Charles, P., O'Donoghue, D., Nordsieck, K., Burgh, E., and Reichart, D. 2006, *GCN Circ.*, 5226, 1

- Stratta, G., Fiore, F., Antonelli, L. A., Piro, L., and De Pasquale, M. 2004, *Astroph. J.*, 608, 846
- Thöne, C. C., Fynbo, J. P. U., Östlin, G., Milvang-Jensen, B., Wiersema, K., Malesani, D., Della Monica Ferreira, D., Gorosabel, J., Kann, D. A., Watson, D., Michałowski, M. J., Fruchter, A. S., Levan, A. J., Hjorth, J., and Sollerman, J. 2008, *Astroph. J.*, 676, 1151
- Turner, J. E. H., Miller, B. W., Beck, T. L., Song, I., Cooke, A. J., Seaman, R. L., and Valdés, F. G. 2006, *New Astronomy Review*, 49, 655
- van Paradijs, J., Groot, P. J., Galama, T., Kouveliotou, C., Strom, R. G., Telting, J., Rutten, R. G. M., Fishman, G. J., Meegan, C. A., Pettini, M., Tanvir, N., Bloom, J., Pedersen, H., Nørdgaard-Nielsen, H. U., Linden-Vørnle, M., Melnick, J., van der Steene, G., Bremer, M., Naber, R., Heise, J., in't Zand, J., Costa, E., Feroci, M., Piro, L., Frontera, F., Zavattini, G., Nicastro, L., Palazzi, E., Bennet, K., Hanlon, L., and Parmar, A. 1997, *Nature*, 386, 686
- Vanderspek, R., Villaseñor, J., Doty, J., Jernigan, J. G., Levine, A., Monnelly, G., and Ricker, G. R. 1999, *Astron. & Astroph. Suppl.*, 138, 565
- Vaughan, S., Goad, M. R., Beardmore, A. P., O'Brien, P. T., Osborne, J. P., Page, K. L., Barthelmy, S. D., Burrows, D. N., Campana, S., Cannizzo, J. K., Capalbi, M., Chincarini, G., Cummings, J. R., Cusumano, G., Giommi, P., Godet, O., Hill, J. E., Kobayashi, S., Kumar, P., La Parola, V., Levan, A., Mangano, V., Mészáros, P., Moretti, A., Morris, D. C., Nousek, J. A., Pagani, C., Palmer, D. M., Racusin, J. L., Romano, P., Tagliaferri, G., Zhang, B., and Gehrels, N. 2006, *Astroph. J.*, 638, 920
- Verheijen, M. A. W., Bershad, M. A., Andersen, D. R., Swaters, R. A., Westfall, K., Kelz, A., and Roth, M. M. 2004, *Astron. Nachr.*, 325, 151
- Vreeswijk, P. M., Fruchter, A., Kaper, L., Rol, E., Galama, T. J., van Paradijs, J., Kouveliotou, C., Wijers, R. A. M. J., Pian, E., Palazzi, E., Masetti, N., Frontera, F., Savaglio, S., Reinsch, K., Hessman, F. V., Beuermann, K., Nicklas, H., and van den Heuvel, E. P. J. 2001, *Astroph. J.*, 546, 672
- Walsh, J. R. and Roth, M. M. 2002, *The Messenger*, 109, 54
- Wang, X. Y., Dai, Z. G., and Lu, T. 2000, *Mon. Not. R. Astron. Soc.*, 317, 170
- Watson, D., Hjorth, J., Fynbo, J. P. U., Jakobsson, P., Foley, S., Sollerman, J., and Wijers, R. A. M. J. 2007, *Astroph. J.*, 660, L101
- Wiersema, K., Savaglio, S., Vreeswijk, P. M., Ellison, S. L., Ledoux, C., Yoon, S.-C., Møller, P., Sollerman, J., Fynbo, J. P. U., Pian, E., Starling, R. L. C., and Wijers, R. A. M. J. 2007, *Astron. & Astroph.*, 464, 529
- Winkler, C., Courvoisier, T. J.-L., Di Cocco, G., Gehrels, N., Giménez, A., Grebenev, S., Hermsen, W., Mas-Hesse, J. M., Lebrun, F., Lund, N., Palumbo, G. G. C., Paul, J., Roques, J.-P., Schnopper, H., Schönfelder, V., Sunyaev, R., Teegarden, B., Ubertini, P., Vedrenne, G., and Dean, A. J. 2003, *Astron. & Astroph.*, 411, L1
- Woosley, S. E. 1993, *Astroph. J.*, 405, 273
- Woosley, S. E. and Bloom, J. S. 2006, *Annu. Rev. Astro. Astroph.*, 44, 507
- Yost, S. A., Harrison, F. A., Sari, R., and Frail, D. A. 2003, *Astroph. J.*, 597, 459
- Zeh, A., Kann, D. A., Klose, S., and Hartmann, D. H. 2005, *Nuovo Cimento C Geophysics Space Physics C*, 28, 617
- Zeh, A., Klose, S., and Hartmann, D. H. 2004, *Astroph. J.*, 609, 952

Zeh, A., Klose, S., and Kann, D. A. 2006, *Astroph. J.*, 637, 889

Zhai, M., Qiu, Y. L., Wei, J. Y., Hu, J. Y., Deng, J. S., and Zheng, W. K. 2006, *GCN Circ.*, 5230, 1

Zhang, B. 2006, *Nature*, 444, 1010

Zhang, B. 2007, *Chin. J. Astron. Astroph.*, 7, 1

Zhang, B., Fan, Y. Z., Dyks, J., Kobayashi, S., Mészáros, P., Burrows, D. N., Nousek, J. A., and Gehrels, N. 2006, *Astroph. J.*, 642, 354

Zhang, B. and Mészáros, P. 2004, *International Journal of Modern Physics A*, 19, 2385

Acknowledgements

First of all, I would like to express all my gratitude to Dr. Sylvio Klose, the supervisor of my Ph.D. work. Without his help and support this Thesis would probably not exist. These three years and a half have been really fruitful under his guide. I have also to thank him for all the occasions he helped me to solve daily life problems. I will never be able to find all the words to thank him.

Many thanks also to Prof. Artie Hatzes to support this work at University and to the Thüringer Landessternwarte Tautenburg, which gave me a grant in these last months, after the expiration of my DFG contract.

I want to thank all the observatory staff, in particular the components of the GRB group: Alex, Steve, Andrea, Andreas and Robert. It has been a pleasure to collaborate with them.

Thanks to the “Tautenburg Italian Community”: Alessio, Felice, Rebeca, Andrea and Davide. Staying here with them has been a special thing and it has made the daily life easier and funnier.

Thanks to Steve and Dr. Holger Lehmann for the German translation of the abstract of this Thesis.

I want also to thank all our collaborators, in particular: Elisabetta Maiorano, Eliana Palazzi, Elena Pian, Nicola Masetti and Daniele Malesani for their advice and useful discussions.

Many thanks go to all my friends in Italy and in Jena for their friendship.

Special thanks go to Massimiliano, for his presence and support and for all the nice things we share, including our lives. To meet him has been the most precious event of my staying here.

Thanks to my parents Valter and Margherita and to my sister Anna, for their love and encouragement: without them I would be completely lost.

Finally thanks to “all my angels”, i.e. all those many people that at the very last moment gave me very useful advice in many situations.

This work is dedicated to the memory of my grandfather Angelo (1915-1991), who was a prisoner in the concentration camp of Buchenwald, some kilometers far away from here. Only after a while I was here, I realized that I was near the place I heard him speaking about, when I was a young girl. My grandfather, during all his life, expressed the desire to visit again these places as a free man. He didn't, but I will do for him.

Ehrenwörtliche Erklärung

Ich erkläre hiermit ehrenwörtlich, dass ich die vorliegende Arbeit selbständig, ohne unzulässige Hilfe Dritter und ohne Benutzung anderer als der angegebenen Hilfsmittel und Literatur angefertigt habe. Die aus anderen Quellen direkt oder indirekt übernommenen Daten und Konzepte sind unter Angabe der Quelle gekennzeichnet.

Bei der Auswahl und Auswertung folgenden Materials haben mir die nachstehend aufgeführten Personen in der jeweils beschriebenen Weise unentgeltlich geholfen:

1. Dr. habil. Sylvio Klose: Betreuung der vorliegenden Arbeit
2. Dipl.-Phys. David Alexander Kann half bei der Erstellung und Analyse der optischen Lichtkurven und der Gestaltung der zugehörigen Abbildungen.
3. Dipl.-Phys. Steve Schulze half bei der Analyse der Röntgendaten und erstellte die Abbildungen der Röntgenlichtkurven.
4. Dr. Andreas Zeh half bei der statistischen Analyse der Supernova-Daten.

Weitere Personen waren an der inhaltlich-materiellen Erstellung der vorliegenden Arbeit nicht beteiligt. Insbesondere habe ich hierfür nicht die entgeltliche Hilfe von Vermittlungs bzw. Beratungsdiensten (Promotionsberater oder andere Personen) in Anspruch genommen. Niemand hat von mir unmittelbar oder mittelbar geldwerte Leistungen für Arbeiten erhalten, die in Zusammenhang mit dem Inhalt der vorgelegten Dissertation stehen.

Die Arbeit wurde bisher weder im In- noch im Ausland in gleicher oder ähnlicher Form einer anderen Prüfungsbehörde vorgelegt.

Die geltende Promotionsordnung der Physikalisch-Astronomischen Fakultät ist mir bekannt.

Ich versichere ehrenwörtlich, dass ich nach bestem Wissen die reine Wahrheit gesagt und nichts verschwiegen habe.

Lebenslauf

Zur Person:

Name: Ferrero

Vorname: Patrizia

Geburtsdatum: 29.06.1975

Geburtsort: Asti (Italien)

Werdegang:

- seit Sep. 2005: Doktorandin an der Thüringer Landessternwarte Tautenburg
Betreuer: Dr. habil. Sylvio Klose
Titel: The variety of progenitors and afterglows: analysis of three *Swift* Gamma-Ray Bursts
- Mär. 2003 - Mär. 2005 Wissenschaftliche Mitarbeiterin am INAF/IASF Bologna (Italien)
Betreuer: Dr. Graziella Pizzichini
Wissenschaftliche Arbeit mit Daten des HETE-2-Satelliten
- Okt. 1994 - Dez. 2002 Astronomie-Studium an der Universität Bologna (Italien)
und Diplomarbeit am Osservatorio di Bologna
Betreuer: Prof. Corrado Bartolini
Titel: Studio del buco nero XTEJ1118+480
Abschluß: Dott.ssa Magistrale in Astronomia
- Sep. 1989 - Jul. 1994 Liceo Scientifico "F. Vercelli"- Asti (Italien)
Abschluß: Maturità Scientifica (Hochschulzugangsberechtigung)
- Sep. 1986 - Jun. 1989 Scuola Media - Montiglio (Italien)
- Sep. 1981 - Jun. 1986 Scuola Elementare - Montechiaro d'Asti (Italien)

Jena, den 09. Dezember 2008

Patrizia Ferrero

Publications on International Refereed Journals

1. J. Gorosabel, A. de Ugarte Postigo, A. J. Castro-Tirado, I. Agudo, M. Jelínek, S. Leon, T. Augusteijn, J. P. U. Fynbo, J. Hjorth, M. J. Michalowski, D. Xu, **P. Ferrero**, D. A. Kann, S. Klose, A. Rossi, J. P. Madrid, A. LLorente, M. Bremer, J.-M. Winters, *Simultaneous polarization monitoring of SN2007uy and the axisymmetric SN2008D/XRF080109: isolating geometry from dust*, submitted to The Astrophysical Journal Letters, arXiv:0810.4333;
2. J. Greiner, T. Kruehler, J. P. U. Fynbo, A. Rossi, R. Schwarz, S. Klose, S. Savaglio, N. R. Tanvir, S. McBreen, T. Totani, B. B. Zhang, X. F. Wu, D. Watson, S. D. Barthelmy, A. P. Beardmore, **P. Ferrero**, N. Gehrels, D. A. Kann, N. Kawai, A. Küpcü Yoldaş, P. Meszaros, B. Milvang-Jensen, S. R. Oates, D. Pierini, P. Schady, K. Toma, P. M. Vreeswijk, A. Yoldaş, B. Zhang, P. Afonso, K. Aoki, D. N. Burrows, C. Clemens, R. Filgas, Z. Haiman, D. H. Hartmann, G. Hasinger, J. Hjorth, E. Jehin, A. J. Levan, E. W. Liang, D. Malesani, T.-S. Pyo, S. Schulze, G. Szokoly, H. Terada, K. Wiersema, *GRB 080913 at redshift 6.7*, The Astrophysical Journal, in press, arXiv:0810.2314;
3. A. Rossi, A. de Ugarte Postigo, **P. Ferrero**, D. A. Kann, S. Klose, S. Schulze, J. Greiner, P. Schady, R. Filgas, E. E. Gonsalves, A. Küpcü Yoldaş, T. Krühler, G. Szokoly, A. Yoldaş, P. M. J. Afonso, C. Clemens, J. S. Bloom, D. A. Perley, J. P. U. Fynbo, A. J. Castro-Tirado, J. Gorosabel, P. Kubánek, A. C. Updike, D. H. Hartmann, A. Giuliani, S. T. Holland, L. Hanlon, M. Bremer, A. García-Hernández, *A photometric redshift of $z = 1.8^{+0.4}_{-0.3}$ for the Agile GRB 080514B*, 2008, Astronomy & Astrophysics, 491, L29 , arXiv:0808.0151;
4. D. A. Kann, S. Klose, B. Zhang, A. C. Wilson, N. R. Butler, D. Malesani, E. Nakar, L. A. Antonelli, G. Chincarini, B. E. Cobb, S. Covino, P. D'Avanzo, V. D'Elia, M. Della Valle, **P. Ferrero**, D. Fugazza, J. Gorosabel, G. L. Israel, F. Mannucci, S. Piranomonte, S. Schulze, L. Stella, G. Tagliaferri, K. Wiersema, *The Afterglows of Swift-era Gamma-Ray Bursts. II. Short/Hard (Type I) vs. Long/Soft (Type II) Optical Afterglows*, submitted to The Astrophysical Journal, arXiv:0804.1959;
5. J. Castro-Tirado, A. de Ugarte Postigo, J. Gorosabel, T. A. Fatkhullin, V. V. Sokolov, M. Jelínek, **P. Ferrero**, D. A. Kann, S. Klose, D. Sluse, M. Bremer, J. M. Winters, D. Nuernberger, D. Pérez-Ramírez, M. A. Guerrero, J. French, G. Melady, L. Hanlon, B. McBreen, F. J. Aceituno, R. Cunniffe1, P. Kubánek, S. Vitek, S. Schulze, A. C. Wilson, R. Hudec, J.M. González-Pérez, T. Shahbaz, S. Guziy, L. Pavlenko, E. Sonbas, S. Trushkin, N. Bursov, N. A. Nizhelskij and L. Sabau-Graziati, *Flares from a candidate Galactic magnetar suggest a missing link to dim isolated neutron stars*, 2008, Nature, 455, 506;
6. **Patrizia Ferrero**, Sylvio Klose, David Alexander Kann, Sandra Savaglio, Eliana Palazzi, Elisabetta Maiorano, Petra Böhm, Dirk Grupe, Samantha R. Oates, Sebastián Sánchez, Steve Schulze, Lorenzo Amati, Jochen Greiner, Jens Hjorth, Daniele Malesani, Scott D. Barthelmy, Javier Gorosabel, Nicola Masetti, and Martin M. Roth, *Analysing afterglows using Integral Field Spectroscopy: GRB 060605, the first practical example*, submitted to Astronomy & Astrophysics, arXiv:0804.2457;
7. D. A. Kann, S. Klose, B. Zhang, D. Malesani, E. Nakar, A. C. Wilson, N. R. Butler, L. A. Antonelli, G. Chincarini, B. E. Cobb, S. Covino, P. D'Avanzo, V. D'Elia, M. Della Valle, **P. Ferrero**, D. Fugazza, J. Gorosabel, G. L. Israel, F. Mannucci, S. Piranomonte, S. Schulze, L. Stella, G. Tagliaferri, K. Wiersema, *The Afterglows of Swift-era Gamma-Ray Bursts. I. Comparing pre-Swift and Swift era Long/Soft (Type II) GRB Optical Afterglows*, submitted to The Astrophysical Journal, arXiv:0712.2186;
8. **P. Ferrero**, S. F. Sánche, D. A. Kann, S. Klose, J. Greiner, J. Gorosabel, D. H. Hartmann, A. A. Henden, P. Møller, E. Palazzi, A. Rau, B. Stecklum, A. J. Castro-Tirado, J. P. U. Fynbo, J. Hjorth, P. Jakobsson, C. Kouveliotou, N. Masetti, E. Pian, N. R. Tanvir and R. A. M. J. Wijers, *Constraints on an optical afterglow and on supernova light following the short burst GRB 050813*, 2007, The Astronomical Journal, 134, 2118, arXiv:astro-ph/0610255;

9. J. Castro-Tirado, M. Jelínek, S. B. Pandey, S. McBreen, J. de Jong, D. K. Sahu, **P. Ferrero**, J. A. Caballaro, J. Gorosabel, D. A. Kann, S. Klose, A. de Ugarte Postigo, G. C. Anupama, C. Gry, S. Guziy, S. Srividya, L. Valdivielso, S. Vanniarajan and A. A. Henden, *GRB 051028: an intrinsically faint gamma-ray burst at high redshift?*, 2006, *Astronomy & Astrophysics*, 459, 763, arXiv:astro-ph/0609654;
10. J. Hjorth, A. Levan, N. Tanvir, R. Starling, S. Klose, C. Kouveliotou, C. Féron, **P. Ferrero**, A. Fruchter, J. Fynbo, J. Gorosabel, P. Jakobsson, D. A. Kann, K. Pedersen, E. Ramirez-Ruiz, J. Sollerman, C. Thöne, D. Watson, K. Wiersema, D. Xu, *The Short Gamma-Ray Burst Revolution*, 2006, *The Messenger*, 126, 16
11. **P. Ferrero**, D. A. Kann, A. Zeh, S. Klose, E. Pian, E. Palazzi, N. Masetti, D. H. Hartmann, J. Sollerman, J. Deng, A. V. Filippenko, J. Greiner, M. A. Hughes, P. Mazzali, W. Li, E. Rol, R. J. Smith and N. R. Tanvir, *The GRB 060218/ SN 2006aj event in the context of other gamma-ray burst supernovae*, 2006, *Astronomy & Astrophysics*, 457, 857, arXiv:astro-ph/0605058;
12. E. Pian, P. Mazzali, N. Masetti, **P. Ferrero**, S. Klose, E. Palazzi, E. Ramirez-Ruiz, S. E. Woosley, C. Kouveliotou, J. Deng, A. V. Filippenko, R. Foley, J. P. U. Fynbo, A. Kann, J. Hjorth, K. Nomoto, F. Patat, D.N. Sauer, J. Sollerman, P. M. Vreeswijk, E. W. Guenther, A. Levan, P. O'Brien, N. R. Tanvir, R. A. M. J. Wijers, C. Dumas, O. Hainaut, D. S. Wong, D. Baade, L. Wang, L. Amati, E. Cappellaro, A. J. Castro-Tirado, S. Ellison, F. Frontera, A. S. Fruchter, J. Greiner, K. Kawabata, C. Ledoux, K. Maeda, P. Møller, L. Nicastro, E. Rol and R. Starling, *An optical supernova associated with the X-ray flash XRF 060218*, 2006, *Nature*, 442, 1011, arXiv:astro-ph/0603530.

Publications on Refereed Conference Proceedings

1. P. A. Curran, D. A. Kann, **P. Ferrero**, E. Rol and R. A. M. J. Wijers, *The prompt emission & peculiar break of GRB 060124*, 2007, *Nuovo Cimento B*, Volume 121, Issue 12, pp 1461-1462, Proceedings of the conference "SWIFT and GRBs: Unveiling the Relativistic Universe", held on June 5-9, 2006 in Venice, Italy, arXiv:astro-ph/0610067;
2. G. Pizzichini, *P. Ferrero*, M. Genghini, F. Gianotti and M. Topinka, *The $E_{peak}^{rest} - E_{rad}$ correlation in GRBs in the BATSE catalog*, 2006, *Advances in Space Research*, Vol. 38, Issue 7, Proceedings of the 35th Cospar Scientific Assembly, held on July 18-25, 2004 in Paris, France, pp. 1338-1341, arXiv:astro-ph/0503264;
3. G. Pizzichini, *P. Ferrero*, M. Genghini, F. Gianotti and M. Topinka, *Towards the $E_{peak}^{rest} - E_{iso}$ correlation in GRBs in the BATSE catalog: a progress report*, 2005, *Nuovo Cimento C*, Vol. 28, Issue 3, Proceedings of the 4th Workshop Gamma-Ray Burst in the Afterglow Era, held on October 18-22, 2004 in Rome, Italy. Edited by L. Piro, L. Amati, S. Covino and B. Gendre, pp. 319-322.

Publications on non-refereed Conference Proceedings

1. J. Gorosabel, A. de Ugarte Postigo, A.J. Castro-Tirado, M. Jelínek, V. Larionov, S. Guziy, T. Augusteijn, J. P. U. Fynbo, J. Hjorth, D. Malesani, D. Xu, **P. Ferrero**, A. Kann, S. Klose, A. Rossi, A. Llorente, J.P. Madrid, *Optical linear polarization in the case of two supernovae associated to XRFs: XRF060218/SN2006aj and XRF080109/SN2008D*, 2009, in *Astronomical Polarimetry 2008: Science from Small to Large Telescopes*, ASP Conference Series, Vol. 4**, pp XX-XX. Conference held on July 6-11, 2008, Fairmont Le Manoir Richelieu, La Malbaie (Quebec, Canada), submitted;
2. De Ugarte Postigo, A. J. Castro-Tirado, J. Gorosabel, T. A. Fatkhullin, V. V. Sokolov, M. Jelínek, D. Sluse, **P. Ferrero**, D. A. Kann, S. Klose, M. Bremer, J. M. Winters, D. Nurenberger, D. Pérez-Ramírez, M. A. Guerrero, J. French, G. Melady, L. Hanlon, B. McBreen, F. J. Aceituno, R. Cunniffe, P. Kubánek, S. Vitek, S. Schulze, A. C. Wilson, R. Hudec, J. M. González-Pérez, T. Shahbaz, S. Guziy, L. Pavlenko, E. Sonbas, S. Trushki, N. Bursov, N. A. Nizhelskij, L. Sabau-Graziati, *GRB 070610: Flares from a peculiar Galactic source*, 2008, in

- GAMMA-RAY BURSTS 2007: Proceedings of the Santa Fe Conference, AIP Conference Proceedings, Volume 1000, pp. 337-341. Conference held on November 5-9, 2007, Santa Fe (New Mexico);
3. Andrea Rossi, David Alexander Kann, Steve Schulze, **Patrizia Ferrero**, Robert Filgas, Sylvio Klose, Christian Clemens, Aybüke Küpcü Yoldaş, Thomas Krühler, Abdullah Yoldaş, Jochen Greiner, *Dark bursts in the Swift era*, 2008, in GAMMA-RAY BURSTS 2007: Proceedings of the Santa Fe Conference, AIP Conference Proceedings, Volume 1000, pp. 327-330. Conference held on November 5-9, 2007, Santa Fe (New Mexico);
 4. **P. Ferrero**, D. A. Kann, S. Klose, J. Greiner, E. S. Rykoff (on behalf of the ROTSE collaboration), H. Mikuž, B. Dintinjana, J. Skvarč, D. Malesani, S. Schulze, R. Filgas, A. Rossi, *A rapid response to GRB 070411*, 2008, in GAMMA-RAY BURSTS 2007: Proceedings of the Santa Fe Conference, AIP Conference Proceedings, Volume 1000, pp. 257-260. Conference held on November 5-9, 2007, Santa Fe (New Mexico);
 5. **Patrizia Ferrero**, Eliana Palazzi, Elena Pian, Sandra Savaglio, *Optical observations of GRB 060218/SN 2006aj and its host galaxy*, 2007, in The multicoloured landscape of compact objects and their explosive origins, AIP Conference Proceedings, Volume 924, pp. 120-125. Conference held on June 11-18, 2006, Cefal, Sicily (Italy), arXiv:astro-ph/0610417v1;
 6. J. Castro-Tirado, S. McBreen, M. Jelínek, S. B. Pandey, M. Bremer, A. de Ugarte Postigo, J. Gorosabel, S. Guziy, G. Bihain, J. A. Caballero, **P. Ferrero**, J. de Jong, K. Misra, D. K. Sahu, *The latest two GRB detected by Hete-2: GRB 051022 and GRB 051028*, 2006, AIP Conference Proceedings, Vol. 836 Gamma-Ray Bursts in the Swift Era, Sixteenth Maryland Astrophysics Conference, held on November 29- December 2, 2005 in Washington, DC. Edited by S.S. Holt, N. Gehrels, and J.A.Nousek. Melville, NY: American Institute of Physics, pp.79-84;
 7. G. Pizzichini, **P. Ferrero**, F. Gianotti, E. Morelli and the HETE Science Team, *GRB 030329 and GRB 021211 detected by HETE-2*, 2005, 1604-2004 Supernovae as Cosmological Lighthouses, ASP Conference Series, Vol. 342, Proceedings of the conference held on June 15-19, 2004 in Padua, Italy. Edited by M. Turatto, S. Benetti, L. Zampieri and W. Shea. San Francisco: Astronomical Society of the Pacific, 2005, p. 326;
 8. G. Pizzichini, **P. Ferrero**, F. Gianotti, E. Morelli and the HETE Science Team, *The HETE-2 satellite: detection of Gamma-Ray Bursts and other transient phenomena*, 2004, Memorie Societ Astronomica Italiana Supplement, Vol. 5, 48th Annual Meeting of the Italian Astronomical Society: I Colori dell'Universo - Astronomia Italiana dalla Terra e dallo Spazio, Proceedings of the conference held on April 19-23, 2004 in Milan, Italy. Edited by A. Wolter, G. Israel and F. Bacciotti, pp. 166-171;
 9. C. Bartolini, A. Guarnieri, A. Piccioni, **P. Ferrero** and G. Pizzichini, *Observations of GRB optical afterglows from Loiano*, 2004, AIP Conference Proceedings, Vol. 727, Gamma-Ray Bursts: 30 Years of Discovery, Gamma-Ray Burst Symposium, Santa Fe (New Mexico), held on September 8-12 , 2003. Edited by E. E. Fenimore and M. Galassi. Melville, NY: American Institute of Physics, pp. 471-474;
 10. G. Pizzichini, **P. Ferrero**, C. Bartolini, A. Guarnieri and A. Piccioni, *Prompt Comparison of Data for Optical Transients of Gamma-Ray Bursts*, 2004, AIP Conference Proceedings, Vol. 727, Gamma-Ray Bursts: 30 Years of Discovery, Gamma-Ray Burst Symposium, Santa Fe (New Mexico), held on September 8-12, 2003. Edited by E. E. Fenimore and M. Galassi. Melville, NY: American Institute of Physics, pp. 77-80.

GCN Circulars

1. **P. Ferrero**, S. Klose, D. A. Kann, S. Schulze, *GRB 070411: deep VLT detection*, 2007, GCN Circ. 6319;
2. S. Savaglio, E. Palazzi, **P. Ferrero**, S. Klose, *GRB 060605 new redshift*, 2007, GCN Circ. 6166;

3. **P. Ferrero**, S. Klose, D. A. Kann, P. Boehm, M. M. Roth, S. F. Sanchez, J. Greiner, S. Savaglio, N. Masetti, *GRB 060605, observations using an integral field unit*, 2006, GCN Circ. 5489;
4. D. A. Kann, S. Klose and **P. Ferrero**, *Short GRB 060502B: Tautenburg observation*, 2006, GCN Circ. 5062;
5. D. A. Kann, **P. Ferrero**, B. Stecklum and S. Klose, *GRB 051008 Tautenburg supernova search*, 2005, GCN Circ. 4246;
6. S. Klose, **P. Ferrero**, D. A. Kann, B. Stecklum and U. Laux, *GRB 051103, optical observations*, 2005, GCN Circ. 4207;
7. S. Klose, **P. Ferrero**, D. A. Kann, U. Laux and B. Stecklum, *GRB 051105A, 2nd epoch optical observations*, 2005, GCN Circ. 4203;
8. **P. Ferrero**, D. A. Kann, S. Klose and C. Hoegner, *GRB051028: optical observations*, 2005, GCN Circ. 4178;
9. **P. Ferrero**, S. Klose, D. A. Kann, A. Zeh and B. Stecklum, *GRB 051008 - a low redshift low-luminosity burst?*, 2005, GCN Circ. 4085;
10. **P. Ferrero** and S. Klose, *GRB051008: r-band upper limit*, 2005, GCN Circ. 4076;
11. G. Greco, C. Bartolini, A. Guarnieri, A. Piccioni, **P. Ferrero**, G. Pizzichini and I. Bruni, *GRB 050319: optical observations*, 2005, GCN Circ. 3142;
12. **P. Ferrero**, G. Pizzichini, G. Greco, C. Bartolini, A. Guarnieri, A. Piccioni and R. Gualandi, *GRB 041218: optical observations*, 2004, GCN Circ. 2897;
13. G. Greco, C. Bartolini, A. Guarnieri, A. Piccioni, **P. Ferrero**, G. Pizzichini, E. Mazzotti Epifani and R. Gualandi, *GRB 041218: optical observations*, 2004, GCN Circ. 2863;
14. G. Greco, C. Bartolini, A. Guarnieri, A. Piccioni, **P. Ferrero**, G. Pizzichini and R. Gualandi, *GRB 041006 R observations in Loiano*, 2004, GCN Circ. 2804;
15. **P. Ferrero**, C. Bartolini, G. Greco, A. Guarnieri, A. Piccioni, E. Mazzotti Epifani, R. Gualandi and G. Pizzichini, *GRB041006(=HETE3570): optical observations*, 2004, GCN Circ. 2777;
16. Piccioni, C. Bartolini, A. Guarnieri, G. Greco, **P. Ferrero**, G. Pizzichini, F. Giovannelli and R. Gualandi, *GRB040825A: optical observations*, 2004, GCN Circ. 2664;
17. Piccioni, C. Bartolini, A. Guarnieri, G. Greco, **P. Ferrero**, G. Pizzichini, F. Giovannelli and R. Gualandi, *GRB040825B: optical observations*, 2004, GCN Circ. 2663;
18. Piccioni, C. Bartolini, A. Guarnieri, **P. Ferrero**, G. Pizzichini and S. Bernabei, *GRB040624: optical observations*, 2004, GCN Circ. 2623;
19. Piccioni, C. Bartolini, A. Guarnieri, **P. Ferrero**, G. Pizzichini and I. Bruni, *GRB040422: optical observations at Loiano*, 2004, GCN Circ. 2578;
20. Piccioni, C. Bartolini, A. Guarnieri, **P. Ferrero**, G. Pizzichini and J. Casares, *GRB031111, optical observations*, 2004, GCN Circ. 2524;
21. **P. Ferrero**, G. Pizzichini, C. Bartolini, A. Guarnieri, A. Piccioni and A. De Blasi, *GRB030418: R optical observations*, 2003, GCN Circ. 2284;
22. G. Pizzichini, **P. Ferrero**, C. Bartolini, A. Guarnieri, A. Piccioni, A. Righini and I. Bruni, *GRB030329, correction to Rc observations in Loiano*, 2003, GCN Circ. 2228;
23. G. Pizzichini, **P. Ferrero**, C. Bartolini, A. Guarnieri, A. Piccioni, A. Righini and I. Bruni, *GRB030329 Rc observations*, 2003, GCN Circ. 2136;
24. C. Bartolini, A. Guarnieri, A. Piccioni, G. Gavazzi, R. Gualandi, G. Pizzichini and **P. Ferrero**, *GRB030329: R and B observations*, 2003, GCN Circ. 2030;
25. Guarnieri, L. Cortese, C. Bartolini, A. Piccioni, R. Gualandi, S. Bernabei, G. Pizzichini and **P. Ferrero**, *GRB030226, addendum to GCN 1892*, 2003, GCN Circ. 1940.

Talks

I presented the following talks:

1. March 6, 2008, at the Dark Cosmology Centre (Denmark), Analysing afterglows using Integral Field Spectroscopy: GRB 060605, the first practical example;
2. February 25, 2008, at the Thüringer Landessternwarte Tautenburg (Germany), during the Beirats visit, First steps toward a rapid 3D spectroscopy of arcsec-sized Gamma-Ray burst error boxes;
3. February 1, 2008, at the Dr. Remeis-Sternwarte Bamberg (Germany), Integral Field Spectroscopy: A new tool to study Gamma-ray Burst;
4. October 17, 2007, at INAF/IASF Sezione di Bologna (Italy), 3D Spectroscopy: An overview;
5. June 22, 2006, at Brera Astronomical Observatory Merate (Italy), Gamma-Ray Burst supernovae and GRB/SN 2006aj;
6. June 21, 2006, at INAF/IASF Sezione di Bologna (Italy), Gamma-Ray Burst supernovae and GRB/SN 2006aj;
7. June 2, 2005, at the Thüringer Landessternwarte Tautenburg (Germany), GRB events: a glance at their optical afterglows;
8. November 1-3, 2004, oral contribution to IBWS 2004 - 3rd Integral Bart Workshop, Chocerady (Czech Republic), Fast dissemination of GRB afterglow information;
9. November 1-3, 2004, oral contribution to IBWS 2004 - 3rd Integral Bart Workshop, Chocerady (Czech Republic), GRB ToO observations in Loiano;
10. September 20-25, 2004, oral contribution to XC Annual Meeting of the Italian Society of Physics (SIF), Brescia (Italy), La diffusione veloce dei dati su osservazioni ottiche dei Lampi Gamma, 2004;
11. September 20-25, 2004, oral contribution to XC Annual Meeting of the Italian Society of Physics (SIF), Brescia (Italy), Osservazioni di transienti ottici di Lampi Gamma all'Osservatorio di Loiano.